Screening triterpenoid compounds with potential to treat retinal diseases

Zhengqi Cheng

A thesis submitted in fulfilment of the requirements for the degree of Doctor of Philosophy

School of Pharmacy

Faculty of Medicine and Health

The University of Sydney

2020

Statement of Originality

This thesis is submitted to the School of Pharmacy, Faculty of Medicine and Health, The University of Sydney, in fulfilment of the requirement for the degree of Doctor of Philosophy. This is to certify that to the best of my knowledge, the content of this thesis is my own work. This thesis has not been submitted for any degree or other purposes.

I certify that the intellectual content of this thesis is the product of my own work and that all the assistance received in preparing this thesis and sources have been acknowledged.

Zhengqi Cheng
January 2020

Contents

Acknowledgements

First of all, I'd like to express my deepest gratitude to my supervisor A/Prof. Fanfan Zhou, for her patient and generous guidance throughout three years of my PhD life. As a supervisor, she is always eager to help me with difficulties in research, and often inspires me with novel ideas and encourages me to think independently to be a real researcher. She is also a brilliant guide and a kind friend to me, it is never easy to do a PhD, but Fanfan comforted me a lot and supported me to weather the tough period in my research. Therefore I'm sincerely grateful to Fanfan, her knowledge and rigorous attitude to science strengthened my belief in scientific research, her optimism and enthusiasm shaped me into a person of courage and independence.

Next, I would like to thank all the collaborators and Pharmacy Support Team for their kind contribution for this thesis and help in my PhD study: Mrs. Priyanka Tharkar and A/Prof. Wojciech Chrzanowski for their help in liposome preparation and characterization; Dr. Ling Zhu and Dr. Ting Zhang from Save Sight Institute, for their help in primary cell culture and reagents; Dr. Donna Lai and Dr. Sheng Hua from Bosch, for their guidance in flow cytometry, liposome size, particle concentration and zeta potential measurement; Mrs. Padmaja Dhanvate (Paddy), Dr. Kaiser Hamid and Mrs. Jiamin You, for their lab trainings and support in my UPLC experiment.

I also wish to thank members in my group, including Yue Li, Youmna Ali and previous summer scholar and Honours students Jessica Nguyen, Yulu Wang and Chelsea Siu-wai Chun, who kindly helped with my experiments. Especially, I want to thank visiting scholars in our lab, A/Prof. Wenjuan Yao and Dr. Wenying Shu, who not only provided me with advice in experiments and research, but also motivated me to move forward during my PhD journey.

Besides, I want to say a big thank you to all my friends who bring me a lot of happiness, especially Huiping (Ophelia) Huang, Qingyu (Sarah) Lei, Mengyu Li, Yiqun (Amy) Qu, Quanqing (Helen) Gao, Amjad Alrosan and Tingyue Yang, who are good listeners and understand me a lot. They are always there when I'm depressed and want someone to talk with, their company makes my life colorful and gives me tremendous emotional support.

Last but not least, I would like to appreciate my parents and grandparents, their endless love empowers me all the time, and they financially supported me to finish my PhD, so that I was able to pursue my dream and career bravely.

List of Publications

Publications in support of this thesis:

Cheng Z, Yao W, Zheng J, Ding W, Wang Y, Zhang T, Zhu L, Zhou F. A derivative of betulinic acid protects human Retinal Pigment Epithelial (RPE) cells from cobalt chloride-induced acute hypoxic stress. *Exp Eye Res*. 2019 Mar 1;180:92-101. **(Chapter 2)**

Cheng Z, Zhang T, Zheng J, Ding W, Wang Y, Li Y, Zhu L, Murray M, Zhou F. Betulinic acid derivatives can protect human Müller cells from glutamate-induced oxidative stress. *Exp Cell Res*. 2019 Oct 1;383(1):111509. **(Chapter 3)**

Other publications during candidature:

Lu X, Chan T, **Cheng Z**, Shams T, Zhu L, Murray M, Zhou F. The 5′-AMP-Activated Protein Kinase Regulates the Function and Expression of Human Organic Anion Transporting Polypeptide 1A2. *Mol Pharmacol.* 2018 Dec 1;94(6):1412-20.

Moussa YE, Ong YQ, Perry JD, **Cheng Z**, Kayser V, Cruz E, Kim RR, Sciortino N, Wheate NJ. Demonstration of in vitro host-guest complex formation and safety of para-sulfonatocalix [8] arene as a delivery vehicle for two antibiotic drugs. *J Pharm Sci.* 2018 Dec 1;107(12):3105-11.

Ali Y, Shams T, Wang K, **Cheng Z**, Li Y, Shu W, Bao X, Zhu L, Murray M, Zhou F. The involvement of human Organic Anion Transporting Polypeptides (OATPs) in drug-herb/food interactions. *Chin Med.* (Accepted)

Ali Y, Shams T, **Cheng Z**, Li Y, Chun CS., Shu W, Bao X, Zhu L, Murray M, Zhou F. The clinical Wnt inhibitor PRI-724 regulates transport activity by human renal Organic Anion Transporters (OATs) and Organic Anion Transporting Polypeptides (OATPs). *J Pharm Sci.* (Revision submitted)

Li Y, **Cheng Z**, Wang K, Zhu X, Ali Y, Shu W, Bao X, Zhu L, Fan X, Murray M, Zhou F. Procyanidin B2 and rutin protect human Retinal Pigment Epithelial (RPE) cells from oxidative stress by modulating Nrf2 and Erk1/2 signalling. *Eur J Pharm Sci.* (In review)

Cheng Z, Li Y, Zhu X, Wang K, Ali Y, Shu W, Zhang T, Zhu L, Murray M, Zhou F. The potential application of pentacyclic triterpenoids in the prevention and treatment of retinal diseases. *Eur J Pharm Biopharm.* (In review)

List of Abbreviations

11β-HSD1	11β-Hydroxysteroid dehydrogenase type 1
AA	Asiatic acid
AKBA	Acetyl-11-keto-b-boswellic acid
AMD	Age-related macular degeneration
ATCC	American type culture collection
BA	Betulinic acid
BAC	Benzalkonium chloride
BARD	Bardoxolone methyl
BBB	Blood brain barrier
BDNF	Brain-derived neurotrophic factor
BE	Betulin
BRB	Brain retina barrier
CA	Corosolic acid
CBX	Carbenoxolone
CNV	Choroidal neovascularization
COHT	Chronic ocular hypertension
CVI	Chronic venous insufficiency
DES	Dry eye syndrome
DMEM	Dulbecco's modified eagle medium
DMSO	Dimethyl sulfoxide
DR	Diabetic retinopathy
EE	Encapsulation efficiency
ER	Endoplasmic reticulum
Erk	Extracellular signal-regulated kinases
FBS	Fetal bovine serum

GA	Glycyrrhizic acid
GCLC	Glutamate-cysteine ligase catalytic subunit
GCLM	Glutamate-cysteine ligase regulatory subunit
GFAP	Glial fibrillary acidic protein
GL	Glycyrrhizin
GRX1	Glutaredoxin-1
GST	Glutathione S-transferase
HIF-1α	Hypoxia-inducible factors
HMGB1	High-mobility group box protein 1
HO-1 (or HMOX1)	Heme oxygenase-1
HRMECs	Human retinal microvascular endothelial cells
Hsp70	70 kilodalton heat shock proteins
HUVECs	Human umbilical vein endothelial cells
I/R	Ischemia-reperfusion
ICAM-1 (or CD54)	Intercellular adhesion molecule 1
IOP	Intraocular pressure
JNK	c-jun N-termnal kinase
KBA	11-keto-β-boswellic acid
Keap1	Kelch like-ECH-associated protein 1
LPS	Lipopolysaccharide
MA	Madecassic acid
MAPK	Mitogen-activated protein kinase
MCP-1 (or Ccl2)	Monocyte chemoattractant protein 1
mGluR5	Major metabotropic glutamate receptor 5
MTT	Thiazolyl blue tetrazolium bromide
NLCs	Nanostructured lipid carriers
NMDA	N-methyl-D-aspartic acid
NQO1	NAD(P)H quinone oxidoreductase 1
Nrf2	Nuclear factor erythroid-2 related factor 2
OA	Oleanolic acid

OH	Ocular hypertension
OIR	Oxygen-induced retinopathy
ONC	Optic nerve crush
ONL	Outer nuclear layer
P-gp	P-glycoprotein
PARP-1	Poly (ADP-ribose) polymerase 1
PBS	Phosphate-buffered saline
PDI	Polydispersity index
PDR	Proliferative diabetic retinopathy
PI	Propidium iodide
PI3K	Phosphoinositide-3 kinase
PLGA	Poly(dl-lactide-coglycolide) acid
PTs	Pentacyclic triterpenoids
RECs	Human retinal endothelial cells
ROP	Retinopathy of prematurity
ROS	Reactive oxygen species
RP	Retinitis pigmentosa
RPE	Retinal pigment epithelium
SHP-1	Src homology region 2 domain-containing phosphatase-1
SI	Sodium iodate
SLMs	Solid lipid microparticles
SLNs	Solid lipid nanoparticles
SQSTM1	Sequestosome-1
SRXN1	Sulfiredoxin 1
STAT3	Signal transducer and activator of transcription 3
TA	Triamcinolone acetonide
tBHP	tert-Butyl hydroperoxide
TNFα	Tumor necrosis factor-α
TRX1	Thioredoxin-1
TXNRD1	Thioredoxin reductase 1

UA	Ursolic acid
UPLC	Ultra-high performance liquid chromatography
VEGF	Vascular endothelial growth factor
ZO-1	Tight junction protein-1

List of Tables

List of Figures

Thesis Abstract

Retinal degeneration is a leading cause of impaired vision or even blindness all around the world, unfortunately, most retinal diseases are irreversible, and there is no ideal treatment to cure the diseases, therefore it is important to protect retina from disease progression. In the recent years, natural compounds have shown great pharmacological potentials. Pentacyclic triterpenoids (PTs) are a group of compounds widely existing in nature, they have shown diverse pharmacological effects *in vitro* and *in vivo*. In this thesis, we evaluated the antioxidative effect of betulin, betulinic acid and their 18 derivatives (groups were modified at C3 and C28 positions of betulinic acid skeleton) in human retinal pigment epithelium (RPE) and human Müller cells.

RPE is a monolayer of cells between the outer neural layer of photoreceptors and choroid, responsible for mediating visual cycle and nourishing photoreceptors. Hypoxia in RPE cells is likely to cause retinal diseases such as the age-related macular degeneration (AMD), which is the leading cause of blindness in old people worldwide. In Chapter 2, we established the hypoxia model in ARPE-19 cells with $CoCl_2$, which induced a dramatic reduced cell viability, increased reactive oxygen species (ROS) level, induced apoptosis and necrosis. H7 pretreatment could significantly reversed the above damage. In addition, H7 could inhibit the activation of Akt, Erk1/2 and JNK pathways stimulated by $CoCl_2$. We also verified the same signaling pathways in human primary RPE cells.

Müller cells are predominant neuron-supporting glial cells, they play important roles in maintaining the retinal homeostasis, releasing trophic factors and supporting other retinal cells. One of the key functions is to uptake the neurotransmitter glutamate and convert it into glutamine, therefore high concentrations of glutamate will lead to pathological changes of Müller cells, which may promote progressions of some retinal degenerations like diabetic retinopathy (DR) and glaucoma. In Chapter 3, we tested the antioxidative effect of betulinic derivatives in MIO-M1 cells against glutamate-induced excitotoxicity. The betulinic derivatives H3, H5, H7 and H11 could significantly increase cell survival and reduce necrosis level after glutamate treatment. H3, H5 and H7 could effectively inhibit ROS production. H5 and H7 showed the effects by inhibit the activation of Akt, Erk1/2 and JNK pathways induced by glutamate, while H3 only inhibited Erk1/2 phosphorylation. Studies in Chapter 2 and Chapter 3 indicate that these

betulinic derivatives protected RPE and Müller cells by deactivating Akt, Erk1/2 and JNK.

However, the effective concentrations of betulinic derivatives in Chapter 2 and Chapter 3 are hard to reach in the retina by systematic administration. Liposome is a widely-used approach to increase drug delivery efficacy and therapeutic effects, therefore we encapsulated the active betulinic derivatives (H3, H5 and H7) into Compritol 888 ATO or Compritol HD5 ATO liposomes and evaluated the cytoprotective effect of each liposome-based formulations in ARPE-19 and MIO-M1 cells. We found that H3 and H5 Compritol 888 ATO liposomes, as well as H5 Compritol HD5 ATO liposomes increased cell viability in glutamate-treated MIO-M1 cells. H5 Compritol 888ATO liposome, and Compritol HD5 ATO liposomes with H3, H5, H7 significantly attenuated ROS production caused by $CoCl_2$. Furthermore, Compritol 888 ATO liposomes particularly enabled encapsulated compounds to release sustainably. Studies in this Chapter indicated that liposomes are a promising drug delivery carrier for betulinic acid derivatives to achieve an improved cellular protective effect against oxidative stress in human RPE and Müller cells.

Chapter 1 Literature review

Abstract

Retinal diseases are a leading cause of impaired vision and blindness but some lack effective treatments. New therapies are required urgently to better manage retinal diseases. Natural pentacyclic triterpenoids (PTs) and their derivatives have shown a wide range of activities in the retina, such as anti-oxidative, anti-inflammatory, cytoprotective, neuroprotective and anti-angiogenic properties. A variety of chemically modified PTs have shown enhanced activities compared to their parental compounds, therefore group modification is a promising approach to increase their pharmacological activities. The retina-protective effects of PTs are often mediated through signaling pathways, including Nrf2, HMGB1, 11β-HSD1 and SHP-1. This review summarizes recent *in vitro* and *in vivo* evidence of the pharmacological potential of natural and chemically modified PTs in the prevention and treatment of retinal diseases.

1.1 Background

The retina is a light-sensitive layer at the rear of the eye that converts light into neuronal impulses to obtain vision. *Ramony Cajal* discovered the cellular connections in the retina (1). He identified the retinal pigment epithelium (RPE), photoreceptor cells, horizontal cells, bipolar cells, amacrine cells, ganglion cells and Müller cells and illustrated the major circuitry and connections in the tissue (1). The retina is one of the most metabolically active tissues in the body and requires appropriate levels of nutrients and oxygen for normal function (2). Disruption to the blood flow or oxygen consumption are leading causes of impaired energy production in the retina and may also promote inflammation, neovascularization and even retinal cell death, other factors like hypertension, high blood sugar level, heredity will also contribute to disease progression. Common retinal diseases include Age-related Macular Degeneration, Diabetic Retinopathy (DR), glaucoma, retinal detachment and Retinitis Pigmentosa (RP). Patients suffering from these diseases have blurred or distorted vision, and their lives can be seriously affected. However, effective treatments are few and current

interventions are limited to intravitreal injections of anti-Vascular Endothelial Growth Factor (anti-VEGF) or corticosteroids, surgery and laser, these treatments are miserable and not friendly to patients, therefore new mild therapies are urgently needed to prevent/treat the initiation and progression of disease.

Natural compounds are the subject of intensive research interest for their potential in managing a range of diseases. This review focuses on recent advances in the potential application of natural compounds, particularly pentacyclic triterpenoids (PTs) and their derivatives, in the prevention and treatment of retinal disease.

1.2 Biosynthesis of Triterpenoids

The terpenoids are a large and diverse group of natural products. The biosynthesis of terpenoids begins with condensation of the five-carbon isoprenoid subunits dimethylallylpyrophosphate and its isomer isopentenyl pyrophosphate to produce the C10 monoterpenoids (3). Condensation with additional isoprenoid subunits produces the sesquiterpenoids (C15), diterpenoids (C20), sesterpenoids (C25), triterpenoids (C30), and tetraterpenoids (C40) (4). As the number of component isoprenoid subunits increases, the potential for structural complexity increases.

The linear triterpenoid squalene is the precursor of a wide range of triterpenoids. Thus, squalene is cyclised to lanosterol and then to cholesterol (3), which is the precursor to important molecules, such as the steroids, bile acids and vitamin D that act via a series of nuclear receptors to activate target genes and regulate mammalian homeostasis.

Over 30,000 triterpenoids exist in nature; most of which are distributed in plants (5). Many triterpenoids are present as the aglycones (free hydroxyl or carboxylate moieties), while others are glycosylated (the saponins) or carry other types of conjugates (6).

PTs have received considerable attention due to their potent biological and pharmacological properties (4, 5). Different PTs exhibit anti-tumor, antiviral, antimicrobial, antiparasitic, anti-diabetic and anti-inflammatory actions, and also mediate cardio-, hepato- and gastro-protection (4, 6). Important PTs that have found clinical application include glycyrrhizin (GL), celastrol, carbenoxolone (CBX), acetyl-11-keto-β-boswellic acid (AKBA), escin, ursolic acid (UA) and oleanolic acid (OA; Fig. 1). These molecules have attracted attention for their potential in treating a range of human pathologies, including recent interest in the treatment of retinal diseases.

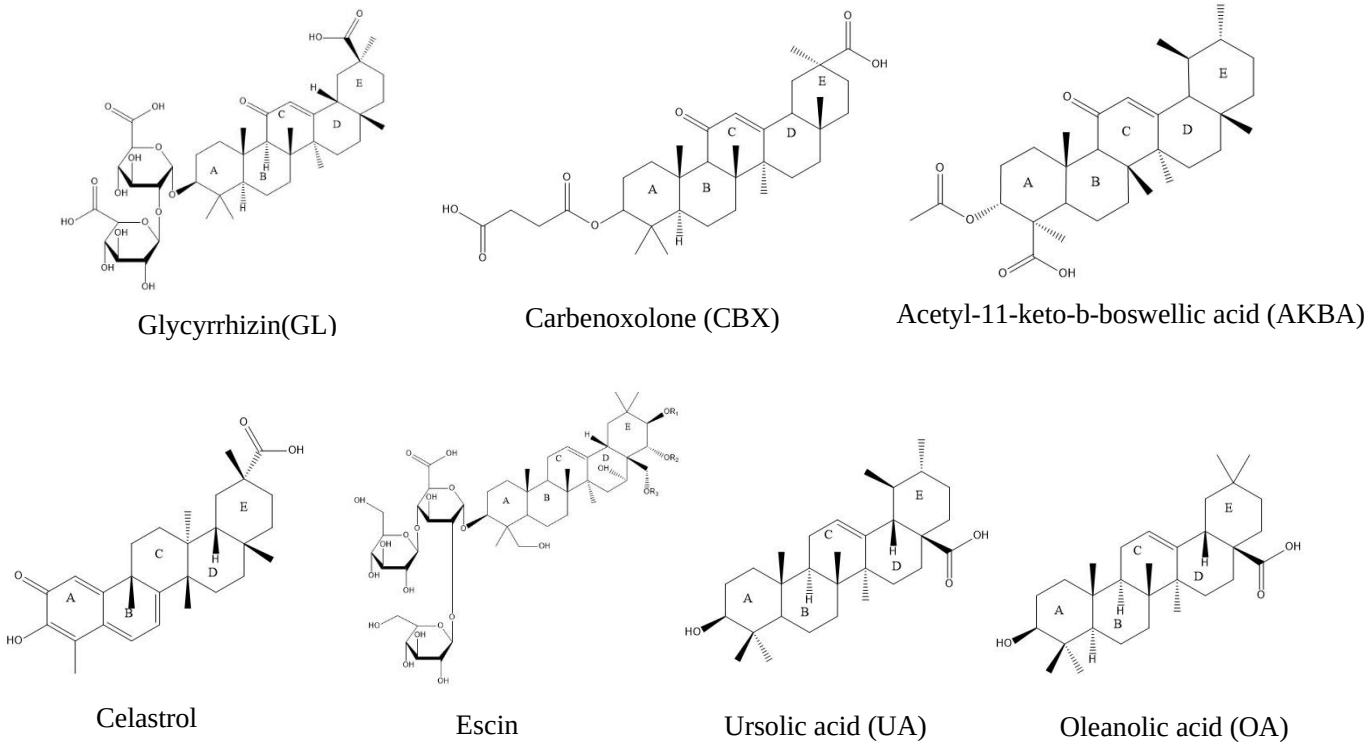

Figure 1.1 Structures of common PTs

1.3 Naturally occurring PTs

1.3.1 Glycyrrhizin

Glycyrrhizin (GL; 20β-Carboxy-11-oxo-30-norolean-12-en-3β-yl-2-O-β-D-glucopyranuronosyl-α-D-glucopyranosiduronic Acid), also known as glycyrrhizic acid or glycyrrhizinic acid, is a saponin glycoside from the root of the medicinal herb *Glycyrrhiza glabra* (liquorice) (7). GL has been used in China and Japan for over 20 years to treat chronic hepatitis (7). There is evidence that GL also has anti-inflammatory, anti-viral and anti-microbial, and anti-cancer actions (8). GL has been approved by the FDA as a dietary sweetener (9) and was previously approved in Canada (9). There are 29 clinical investigation records of GL, mainly for the treatment of liver diseases and cancers. According to clinical data, GL showed linear pharmacokinetics profile below orally 200 mg 6 times/week (10), drug accumulation was seen with consecutive administration (10), the threshold GL plasma concentration for sufficient effect is close

to 5 mg/mL with chronic hepatitis (11).

The protective actions of GL in the retina include maintenance of the structure and metabolic activities of retinal cells *in vitro* and *in vivo* in disease models. For example, *He et al.* (12) reported that GL significantly decreased the production of reactive oxygen species (ROS) induced by sodium iodate (SI) and prevented apoptosis in human ARPE-19 cells. GL was also found to promote the activation of nuclear factor erythroid-2 related factor 2 (Nrf2) and heme oxygenase-1 (HO-1, HMOX1) expression by increasing the phosphorylation and activation of the pro-survival Akt cascade. These findings are in broad agreement with another study that also reported that GL protected the retina by attenuating ROS production, increasing the Poly [ADP-ribose] polymerase 1 (PARP-1) DNA-repair enzyme and decreasing cell death mediated by caspase-3 (13).

In mice, GL (10mg/kg by i.p. injection) administered prior to and following ischemia-reperfusion (I/R) injury, protected the retina from neuronal and vascular damage (14). In addition, *Song et al.* (15) reported that GL suppressed ocular hypertension induced by triamcinolone acetonide, improved electrophysiological parameters and compensated for triamcinolone acetonide -induced changes in ocular metabolism.

GL also inhibits high-mobility group box protein 1 (HMGB1), which is a ubiquitous nuclear protein that is released from damaged cells and induces proinflammatory responses (16). The intravitreal injection of HMGB1 upregulated the pro-inflammatory intercellular adhesion molecule-1 (ICAM-1) in the rat retina, which was attenuated after oral administration of GL (17). Accordingly, GL has the potential to inhibit pro-inflammatory processes mediated by HMGB1.

Detailed studies by *Mohammad's* group (18) and others have established a role for HMGB1 in pathogenic mechanisms that are activated in DR. HMGB1 is proangiogenic (19) and has been shown to increase retinal proliferation in patients with DR (20). By suppressing the increase in HMGB1 expression and the activation of NF-κB in DR, GL attenuated pro-angiogenic signaling (21). GL also prevented the diabetes-induced loss of brain-derived neurotrophic factor (BDNF) in rats (22), decreased excitotoxicity by high glutamate concentrations in the central nervous system (23) and restored retinal occludin (18). In addition, GL prevented the activation of Toll-like receptor 4 (TRL4) and tumor necrosis factor α (TNFα) in primary retinal endothelial cells that were cultured in high glucose medium. This modulated the decrease in phosphorylated-Akt under the culture conditions and decreased caspase-3 cleavage to promote cell survival (14).

There has been no study reporting side-effects of GL's application in the retina, but multiple studies have observed GL has induction or inhibition effects on PK

performances of other drugs or chemicals, such as Midazolam (24), Paeoniflorin (25), Ribavirin (26), Puerarin (27), Glibenclamide (28), Omeprazole (29, 30), Aconitine (31), Talinolol (32), and even other PTs like Asiatic acid (33) and Celastrol (34) in systematic administration, this effect may due to impact on CYP450 enzymes and P-glycoprotein (P-gp) activity.

1.3.2 Carbenoxolone

Carbenoxolone (CBX; 3-O-(β-carboxypropionyl)-11-oxo-18β-olean-12-en-30-oic acid) is a derivative of GL and is also found in licorice root. CBX has been used in the treatment of ulcers of the stomach and digestive tract (35), but this has decreased because of adverse effects, such as electrolyte disturbance and hypertension (15).

CBX is a non-selective inhibitor of 11β-hydroxysteroid dehydrogenase type 1 (11β-HSD1) (15) that regulates the biosynthesis of ligands for glucocorticoid and mineralocorticoid receptors (36). *Na et al.* (37) reported that CBX prevented dry eye syndrome in the rat by inhibiting the expression and activity of 11β-HSD1.

Pan et al.(38) found that CBX was a partially reversible inhibitor of gap junction channels, which are specialized membrane domains between adjacent cells that regulate the transfer of cytoplasmic components (39). CBX is now used as an experimental reagent in *in vitro* and *in vivo* retinal models to decrease membrane potential, to study the role of connexins in gap junctions (40), and to investigate a range of retinal processes (41-44). As an irreversible inhibitor of voltage-dependent calcium channels, CBX has been used to evaluate the role of these channels in the retina (45-47). However, the clinical usage of CBX is limited by its toxicity that leads to retinal opacity, swelling (38) and thinning (48). CBX also decreases the responses of photoreceptors to light (49, 50) and photoreceptor-to-horizontal cell synaptic transmission (51).

1.3.3 Acetyl-11-keto-β-boswellic acid

Boswellic acids are PTs present in resin of *Boswellia* species (52). Boswellic acids have reported anti-inflammatory (52, 53), anti-microbial (52, 53), anti-parasitic (52), anti-cancer (54), anti-arthritic (53) and immunomodulatory (53) actions. Three clinical trials have evaluated boswellic acids in relapsing remitting multiple sclerosis, osteoarthritis of the knee, and in pain, stiffness and impaired function in joints; another trial of the efficacy of boswellic acids in the treatment of renal stones is scheduled, but recruitment has not yet started. Although more than 12 different boswellic acids have

been identified in resin extracts, 11-keto-β-boswellic acid and acetyl-11-keto-β-boswellic acid (AKBA) appear to have the greatest pharmacological significance (52).

The Src homology region 2 domain-containing phosphatase-1 (SHP-1, also known as tyrosine-protein phosphatase non-receptor type 6) regulates growth, mitosis, differentiation, and oncogenic transformation in a range of cell types, including retinal cells. Indeed, SHP-1-deficient mice exhibit progressive retinal degeneration (55), while the activation of SHP-1 in retinal pericytes promotes apoptosis in DR (56).

AKBA has been reported to increase SHP-1 expression and activity in normoxic mouse retina explants (57), which modulates signaling by STAT3. This prevents the activation of hypoxia-inducible factor-1α and VEGF in the oxygen-induced mouse model of retinopathy (OIR) (57). As a result of neovascularization in the OIR mouse retina was decreased by AKBA by suppressing STAT3 phosphorylation and VEGF expression. AKBA also inhibited cell proliferation and tube formation in this model. Similarly, AKBA prevented the increase in p-STAT3 in VEGF-treated human retinal microvascular endothelial cells (HRMECs) (58). The anti-angiogenic actions of AKBA are of potential value in studying the role of neovascularization in the pathogenesis of retinal disease (58).

The fed/fasted condition has a huge impact on PK performance of AKBA, the C_{max} and absorbance increased around four folds after a high-fat meal in healthy volunteers receiving single oral dose of *Boswellia* extract (AKBA 20-30 mg) (C_{max}: 6 ng/mL (fasted) vs. 28.8 ng/mL (fed)) (59, 60). In repeated oral administration (*Boswellia* extract 800 mg, three times daily, 4 weeks), the steady-state concentration was 0.04 μM/L (~20.5 ng/mL) (61), low absorption and/or extensive metabolism may be the reason for the poor bioavailability of AKBA (62).

1.3.4 Celastrol

Celastrol is a major constituent of the medicinal plant *Tripterygium wilfordii* Hook F. Its reported pharmacological activities are broad and include anti-inflammatory, cardioprotective and neuroprotective actions, as well as anti-cancer, anti-obesity and anti-diabetic effects (63). The anti-inflammatory actions of celastrol in the retina are attributed to its capacity to modulate multiple inflammatory mediators, including the cytokines IL-1β, CCL2 and TNFα, heat shock protein-70 (Hsp70) and cyclooxygenase-2 (COX2)(63-67). *Bian et al*. demonstrated the efficacy of celastrol against light-induced retinal inflammation at low concentrations (64). Pre-treatment of ARPE-19 cells with 0.1–1.5 μM celastrol inhibited the phosphorylation and activation of the NF-

κB p65 subunit on Ser536 and decreased IL-6 secretion following the application of lipopolysaccharide (LPS).

Celastrol protected rat retinal ganglion cells (RGCs) from damage due to ocular hypertension (65). The intraperitoneal injection of celastrol (1mg/kg for 14 days) promoted RGC survival in the rat optic nerve crush model (66). Celastrol also preserved the outer nuclear layer structure and thickness in mouse retina after damage by bright light, attenuated light-induced photoreceptor apoptosis and increased the amplitudes of scotopic a- and b-waves (64).

Most studies report that the intraperitoneal administration of celastrol *in vivo* decreases body weight in experimental animals (66, 68, 69). Thus, to retain the pharmacological benefits of celastrol, alternate delivery routes have been tested. Intravitreal administration of celastrol (1 mg/kg) was effective, but less so than daily intraperitoneal administration, and multiple applications may be required for optimal benefit. Detailed studies are now warranted to evaluate this possibility.

1.3.5 Escin

Escin is a mixture of triterpenoid saponins from the horse chestnut tree, *Aesculus hippocastanum*. Earlier studies reported anti-inflammatory, anti-edematous and anti-cancer properties of escin (70, 71), which has potential application in chronic venous insufficiency, haemorrhoids and post-operative edema (70, 71). It has been reported that escin functions by activating Akt-Nrf2 signaling (72).

In the ARPE-19 model the combination of escin and triamcinolone acetonide prevented the disruption of the brain-retinal barrier due to VEGF treatment, and increased the expression of occludin and the ZO-1 protein that maintains tight junctions(73). Similar effects were also produced by the combination *in vivo* and decreased retinal leakage in the rat following ischemia and that was associated with loss of the integrity of the brain-retinal barrier (74).

Clinical studies by *Wu* (75) reported the C_{max} of escin Ia and escin Ib to be 0.77±0.64 ng/mL and 0.38±0.26 ng/mL in healthy volunteers after oral administration of 60 mg escin saposin tablets (escin Ia 18.6 mg, escin Ib 11.4 mg), both compounds reached T_{max} at around 2 h.

1.3.6 Oleanolic acid

Oleanoic acid (OA; 3-hydroxyolean-12-en-28-oic acid) is one of the best-known PTs

and is found in the bark, leaves and fruits of over 1,600 plant species as both the free acid and the glycosylated saponin (76). OA is most abundant in members of the *Oleaceae* family such as the principal commercial source olive (*Olea europaea*), *Lantana camara* and *Lisgustrum lucidum* (76-80)

OA has been used clinically in China as a hepatoprotective adjuvant agent for decades (76, 77, 79) and has also been reported to have antitumor, anti-diabetic, antimicrobial, anti-parasitic and anti-hypertensive actions, as well as antioxidant and anti-inflammatory properties (79). Studies in Chinese healthy volunteers showed plasma concentration of 12.12±6.84 ng/mL after single oral dose of 40 mg (81). The highest used oral dose in rats can be 50 mg/kg with C_{max} of 132.0±122.0 ng/mL (82).

OA suppresses VEGF induced activation of VEGF-receptor 2 and its downstream protein Erk1/2 in human umbilical vein endothelial cells (HUVECs). However, the anti-angiogenic actions of OA in mouse retina *in vivo* requires higher doses (up to 125mg/kg), which may be due to its short half-life and low oral bioavailability (only ~0.7%), most likely due to poor absorption (83).

1.3.7 Ursolic acid

Ursolic acid (UA; 3β-hydroxy-urs-12-ene-28-oic acid) is a secondary plant metabolite that is structurally similar to OA. UA is present in the bark, leaves, peel and wax layers of many edible fruits (84). UA reportedly has diverse pharmacological properties, including anticancer (84, 85), anti-microbial (84), anti-virus (84), anti-inflammatory (85), and antidiabetic activities (85). Clinical trials of UA have provided some evidence that it may have value in preventing muscle atrophy and sarcopenia (NCT02401113; study completed). However, the application of UA in the treatment of the metabolic syndrome (NCT02337933; study completed, but results not reported) and primary sclerosing cholangitis (NCT03216876; study withdrawn due to lack of feasibility) didn't result in a satisfactory outcome.UA is rapidly absorbed (t_{max} ≤1 h) (86, 87), but the bioavailability is low, with C_{max} reached 294.8 ng/mL by orally taking 80 mg/kg UA extract in Wistar rats (86), and 68.26 ng/mL in SD rats by taking 10 mg/kg pure UA (87).

The photoprotective activity of UA in RPE cells has been assessed. UA was found to mitigate damage elicited by UV light by inhibiting the NF-κB pathway (88, 89), but also produced an increase in ROS (88). However, the bioavailability of UA is low and both medicinal chemistry and formulation strategies have been undertaken to improve its activity. *Alvarado et al.* (90) designed and tested UA-loaded PLGA (poly(dl-lactide-

coglycolide) acid) nanoparticles that exhibited potent anti-inflammatory activity in the rabbit eye without producing toxicity. Such approaches may be valuable in optimising the clinical application of PTs, especially those with poor pharmacokinetic properties.

1.3.8 Other PTs

There are several other PTs with pharmacological potential in the treatment of retinal injury (Table 1.1). The intravitreal injection of asiatic acid in rats with elevated intraocular pressure and chronic ocular hypertension improved RGC survival and prevented retinal dysfunction such as retinal thinning. Asiatic acid prevented retinal apoptosis in chronic ocular hypertension by preventing the decrease in the Bcl-2:Bax ratio (91).

Madecassic acid protected HRMECs from hypoxia-induced apoptosis, by preventing the decline in the Bax:Bcl-2 ratio and attenuating caspase-3 and caspase-9 cleavage. Madecassic acid also decreased ROS production and lipid peroxidation, and modulated endoplasmic reticulum stress in hypoxic HRMECs (92).

Corosolic acid elicited anti-angiogenic effects in a chorioallantoic membrane assay, characterized by a decrease in the vascular area and density and the number of gap junctions. Although the intravitreal administration of corosolic acid in Wistar rats was safe and well tolerated pharmacological activity was low (93). As with certain other PTs, the clinical use of corosolic acid may be enhanced by improved formulation.

In addition to the PTs mentioned, the activity crude of crude plant extracts that contain triterpenes has been assessed *in vivo*. Such extracts have been tested in rat models of DR and vasculopathy and have been found to exhibit antioxidant and anti-proliferative activities.

1.4 Chemically modified PT derivatives

Naturally occurring PTs have shown favorable pharmacological activity in a number of retinal pathologies. However, their clinical application has been limited by unfavorable pharmacokinetic profiles and adverse effects. Chemical modifications have been adopted in medicinal chemistry strategies to attempt to overcome such barriers. In addition, novel formulation strategies are emerging that would improve the delivery of bioactive PTs to ocular tissues. The structures of semi-synthetic PTs based on OA are shown in Fig 1.2.

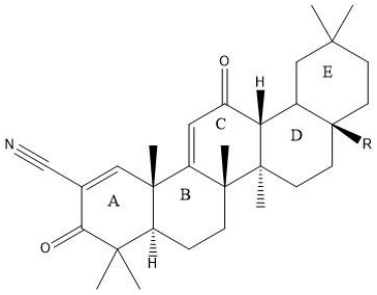

(A) CDDO skeleton

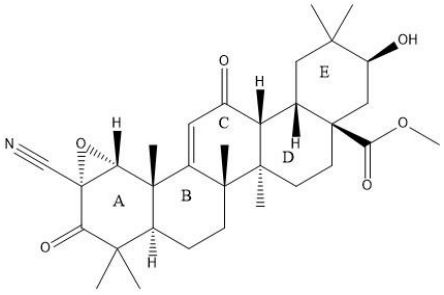

(B) RS9

Compound	Structure of R group
CDDO	COOH
dh404	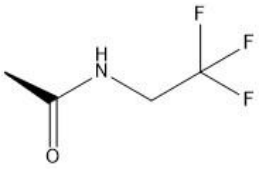
CDDO-Im	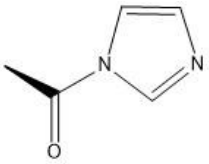
CDDO-Me	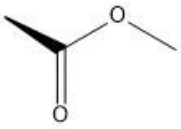
RTA408	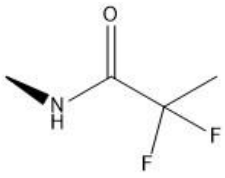

(C) Structures of oleanolic acid derivatives based on CDDO

Figure 1.2 Structures of chemically modified OA derivatives

1.4.1 CDDO and dh404

CDDO (2-cyano-3,12-dioxo-oleana-1,9-dien-28-oic acid, also known as bardoxolone or RTA 401; where R=COOH in Fig. 2C) is a potent semi-synthetic derivative of OA. Further structural modifications have been introduced to produce a series of CDDO analogues, including dh404 (R=$CONHCH_2CF_3$ and where the unsaturated bond in the C-ring of CDDO is reduced; Fig 2C), CDDO methyl ester (CDDO-Me), RTA408 and CDDO-imidazolide (CDDO-Im) (Fig. 1.2C). One phase I clinical study on CDDO in patients with solid tumor reported at least 1 μM blood concentration (effective preclinical concentration) can be reached at 38.4 $mg/m^2/h$ dose with 5-day continuous intravenous infusion for every 28-days (94).

The CDDO analogues are potent activators of Nrf2, which is the master regulator of the Nrf2-inducible gene battery of antioxidant genes in response to oxidative stress. Under normal conditions, Nrf2 is present in the cytoplasm bound to Kelch like-ECH-associated protein 1 (Keap1) and Cullin 3. In a normoxic environment this complex may be rapidly degraded by ubiquitination. However, in oxidative stress, Nrf2 is translocated to the nucleus and activates the transcription of genes that enhance the antioxidant response, including NAD(P)H quinone oxidoreductase 1 (NQO1), glutamate-cysteine ligase catalytic subunit (GCLC), glutamate-cysteine ligase regulatory subunit (GCLM), sulfiredoxin 1 (SRXN1), thioredoxin reductase 1, HO-1 and glutathione S-transferase. Nrf2 and its downstream genes are a major component of the antioxidant defence against the pathogenesis of retinal injuries like Age-related macular degeneration (AMD), DR, choroidal neovascularization, I/R injury, posterior uveitis and glaucoma (95-101), Indeed, Nrf2 knockout animals exhibit increased retinal degeneration and retinopathy (95-101). The capacity of CDDO analogues to activate the Nrf2-inducible gene battery affords protection to the retina.

Deliyanti et al. (102) reported the antioxidant and anti-inflammatory activities of dh404. In the OIR mouse model, dh404 activated the major Nrf2-responsive genes NQO1, glutathione synthase, HO-1 and GCLM. dh404 also alleviated inflammation by decreasing TNFα, CCL2 and ICAM-1 expression and also prevented vascular leakage by restoring VEGF *in vitro* and *in vivo* (Table 1.2).

Similar findings were made in a rat model of diabetes (103). Thus, dh404 activated the Nrf2-responsive genes HO-1 and NQO1 in the retina, attenuated gliosis in in Müller cells by decreasing glial fibrillary acidic protein and suppressed the proinflammatory TNFα, IL-6, ICAM-1 and monocyte chemotactic protein 1 (MCP-1). dh404 also prevented vascular leakage from the diabetic rat retina by inhibiting the increase in albumin and VEGF, and decreased angiopoietin 2.

1.4.2 CDDO-Im

As mentioned, the Nrf2-inducible gene battery is important in maintaining the survival of ocular tissues after exposure to prooxidant stresses. Like dh404, CDDO-Im (2-Cyano-3,12-dioxooleana-1,9-dien-28-imidazolide) attenuated ROS production in the murine photoreceptor 661W cells and minimised I/R injury in mice by upregulating the major Nrf2-inducible genes NQO1, GCLC, GCLM and HO-1 (104). Similar findings were reported by *Himori et al.,* CDDO-Im protected mouse eyes *in vivo* and RGC cells *in vitro* against oxidative stress (105). Two further CDDO derivatives - CDDO-trifluoroethyl-amide (CDDO-TFEA) and CDDO-ethyl-amide (CDDO-EA)- potently activated NQO1 activity in 661W cells in a concentration dependent fashion within the nanomolar range (106). CDDO-TFEA decreased light-induced retinal damage by preventing thinning of the outer nuclear layer (ONL) and increasing retinal NQO1 and GCLC expression in BALB/c mice (106).

1.4.3 CDDO-Me

CDDO-Me (also known as RTA402, bardoxolone methyl or CDDO-methyl ester) activates Nrf2 and inhibits NF-κB. CDDO-Me has been evaluated in ~30 clinical trials for potential application in a range of pathological conditions, including renal diseases, diabetes and pulmonary hypertension (https://clinicaltrials.gov). A phase I clinical trial of CDDO-Me in patients with tumor by *Hong* (107) reported the maximum tolerated dose is 900 mg/d in when orally administrated once a day for 21 days in a 28-day cycle, with Cmax to be 24.7±13.3 ng/mL and Cmin to be 8.8±4.3 ng/mL. CDDO-Me also has low bioavailability, but it can be improved in an amorphous spray dried dispersion (SDD) dosage form (108).

CDDO-Me preserved the integrity of the blood brain barrier, protected endothelial cells and upregulated tight junction proteins (109). CDDO-Me is highly potent in its protective actions against oxidative stress. Thus, CDDO-Me protected the mouse retina against I/R injury by abrogating superoxide levels and inhibiting retinal vascular degeneration, as well as activating Nrf2 target genes such as NQO1, GCLM, GCLC and HO-1 (110).

1.4.4 RTA408

RTA408 (also known as omaveloxolone) is the only OA analogue to date that has been evaluated in clinical trials of corneal endothelial cell loss, ocular pain and ocular inflammation following cataract surgery (NCT02128113, NCT02065375). RTA408 is protective in human fetal RPE cells at low concentrations (≤100 nM) and inhibits H_2O_2-induced apoptosis and necrosis, by increasing the Bcl-2:Bax ratio and inhibiting H_2O_2-induced protein glutathionylation (111). As an Nrf2 activator, RTA408 promotes cell survival by increasing the expression of Nrf2, HO-1, NQO1, superoxide dismutase-2 (SOD2), catalase, glutaredoxin-1 (GRX1) and thioredoxin-1 (TRX1) (111). Clinical studies on patients with Friedreich' ataxia (112) and solid tumors (113) have the similar PK profile (AUC, Cmax, $t_{1/2}$) at low oral doses (20 mg/d), and RTA408 showed a dose-dependent manner between 2.5 mg/d to 300 mg/d (112).

1.4.5 RS9

Nakagami et al. (114) used CDDO as a lead compound to prepare a series of derivatives using microbial transformation. One of the products - termed RS9 - carries an epoxide moiety in the A-ring, an esterified carboxylate substituent at the D/E-ring junction and a hydroxyl group in the E-ring. RS9 was more potent than CDDO-Me in inhibiting *t*-BHP-induced RPE cell death, mediated via Nrf2 activation and leading to increased expression of NQO1, HO-1 and GCLM. Multiple doses of RS9 (114), increased NQO1 and HO-1 expression in the retina of neonatal rats. Other studies corroborated these findings in murine photoreceptor and ARPE-19 cells (115, 116). Indeed, when formulated with PLA-0020, RS9 protected the retina from light-induced ONL thinning in zebrafish and $NaIO_3$-mediated oxidative damage in ARPE-19 cells (116). RS9 also suppressed neovascularization in the OIR rat model and inhibited blood brain barrier hyperpermeability produced in rabbits by administration of glycated albumin. In contrast, CDDO-Me was relatively ineffective. The potency of RS9 was corroborated in another study (117). Thus, RS9 increased the expression of HO-1 and NQO1 mRNAs at a low dose (1 and 3 mg/kg), whereas CDDO-Me only activated HO-1 expression at much higher doses (10 mg/kg). Again, RS9 improved the endothelial cell barrier *in vitro* and *in vivo* assays.

RS9 was also reported to be effective in certain gene-related retinal diseases. For example, *Nakagami* (118) showed that RS9 significantly inhibited ONL in rhodopsin Pro347Leu transgenic rabbits by activating the Nrf2-targeted genes NQO1 and HO-1

(Table 2). This finding suggested that activation of the Nrf2-Keap1 signaling pathway could delay RP pathogenesis due to rhodopsin gene mutations.

Apart from the OA analogues, very few other PTs have been subject to structural modifications by medicinal chemistry or chemical biology approaches. Betulinic acid is structurally similar to OA but has a substituted cyclopentane E-ring in place of the cyclohexane system. Several betulinic acid derivatives with improved aqueous solubility had improved cytoprotective activity and safety in RPE and Müller cells. Antioxidant activities were mediated by attenuating the activation of Akt, Erk1/2 and JNK pathways(119, 120).

1.5 Conclusions

In summary, the potential of PTs and their derivatives for the treatment retinal pathologies includes cytoprotective, antioxidant, neuroprotective, anti- angiogenic and anti-inflammatory effects; these have been assessed in a number of studies (Table 1.1 and 1.2). Important considerations in future studies to assess PTs include:

1) That retinal cell damage *in vitro* or retinal degeneration *in vivo* may be caused by several injurious stimuli, including light, chemicals, ischemia and physical injury. Retinal damage and disease development are complex processes that involve multiple contributory mechanisms and can be exacerbated by coincident diseases, such as diabetes and hypertension. Inflammatory and metabolic indicators may be useful endpoints to monitor retinal degeneration.

2) Retinal damage and retinal diseases are related to altered cellular signaling pathways. Many PTs also modulate such pathways, *eg.* OA derivatives activate the Nrf2 gene battery and GL inhibits HMGB1. Cytoprotection afforded by PTs could enhance insight into the pathogenesis of retinal diseases that may lead to new therapies.

3) Most PTs exhibit diverse biological activities so that off-target actions may produce side effects during treatment.

4) The reported synergism between PTs and glucocorticoids suggests that effective compounds could be used at lower doses when used in combination.

5) Chemical modification of PTs may improve aqueous solubility and pharmacokinetic properties of active agents. For example, CDDO analogues are more potent and exhibit greater retinal protection than the parent compound OA. However, precautions are necessary because chemical modification can also alter the bioactivities of analogues. For example, GL is a HMGB1 inhibitor with retina-protective actions, while CBX is a 11β-HSD1 inhibitor, and may elicit retinal toxicity.

6) In addition to structural modifications, changes in the route of administration and

formulation are other ways to improve their pharmacokinetic and pharmacodynamic profiles. For example, intravitreal injections can enhance topical drug concentrations and nano-scale formulations may achieve superior drug delivery and bioavailability. This is also potentially important because some PTs are toxic at higher doses.

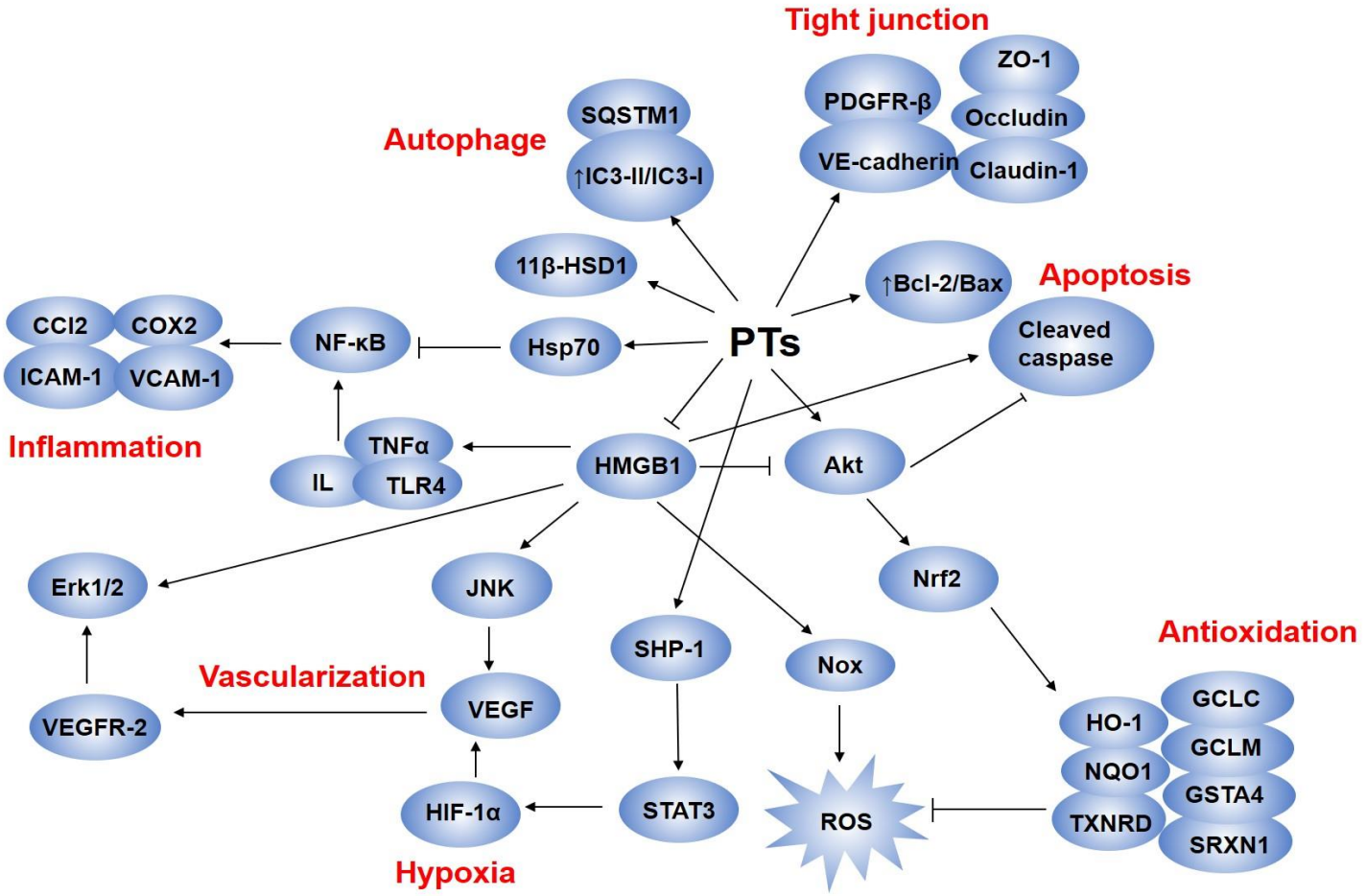

Figure 1.3 Signaling pathways of PTs

Table 1.1 Summary of pharmacological effects and mechanisms of of pentacyclic triterpenoids in the retina

Drug	*In vitro* model	*In vivo* model	Disease model	Pharmacological effects	Pharmacological/ Pathologic improvements	Molecular mechanism	Reference
Glycyrrhizin (GL)		Rabbits	Ocular hypertension	Reduce ocular hypertension	↓ ocular hypertension, improve electrophysiological parameters (flash electroretinogram and flash visual evoked potential), compensate for changes in ocular metabolism induced by triamcinolone acetate	Improve electrophysiological parameters, regulate metabolism	(15)
	ARPE-19 cells	Mice	Sodium iodate induced damage	Cytoprotective	Mice: ↓apoptosis and ROS, ↓retina thinning, ↓drusen number, ↑ the amplitude of 'a-wave' in photoreceptors and 'b-wave' in bipolars	ARPE-19 cells: ↑p-Akt, ↑Nrf2, ↑HO-1	(12)

Rat RGC-5 cells		Advanced glycation end products (ages)–induced vascular endothelial growth factor A (VEGF-A) production	Anti-angiogenic	↓VEGF-A by blocking HMGB1, ↓JNK2/3 activation	(19)
	Rats	Diabetes	Neuroprotective	↓brain-derived neurotrophic factor (BDNF)	(22)
	Rats	Diabetes	Anti-angiogenic, anti-inflammatory	↓CXC chemokine receptor type 4 (CXCR4), ↓HIF-1α, ↓Early growth response protein 1 (Egr-1), ↓Non-receptor tyrosine-protein kinase TYK2 (TYK2), ↓Stromal cell-derived factor 1 (CXCL12)	(21)
	Rats	Diabetes	Anti-inflammatory	↓HMGB-1, ↓NF-κB activation, ↑occludin	(18)
	Rats	Diabetes	Anti-inflammatory	↓HMGB1, ↓Erk1/2, ↑synaptophysin, ↑tyrosine hydroxylase, ↑glutamine synthetase, ↑glyoxalase 1,↓	(23)

						glutamate	
	Primary human retinal endothelial cells (REC)	Mice	REC: high glucose Mice: ischemia/reperfusion (I/R)	Anti-inflammatory, neuroprotective	Mice: ↓ the loss of retinal thickness, ↓ cell number loss in the ganglion cell layer, ↓degenerate capillary cell numbers	REC: ↓HMGB1,↓TLR4, ↓TNFα,↓cleaved caspase-3; ↑p-Akt	(14)
		Rats	Diabetes			↓ROS, ↓Nox2, ↓p47phox, ↓p22phox, ↓Poly [ADP-ribose] polymerase 1 (PARP-1), ↓cleaved caspase-3	(13)
Carbenoxolone (CBX)		Rats	Dry eye syndrome (DES)	Cytoprotective	↓ocular surface damage, ↓tear reduction,↑ corneal thickness, ↓apoptosis in conjunctival epithelium	↓11β-HSD1, ↓TNFα, ↓IL-6, ↓Bax/Bcl-2	(37)
AKBA		Mice	Hypoxia in OIR	Cytoprotective		↑SHP-1 activity, expression and phosphorylation, ↓p-STAT3, ↓HIF-1α, ↓VEGF, ↓phospho-Vascular endothelial growth factor receptor	(57)

						2 (p-VEGFR-2)	
	HRMECs	Mice	OIR	Anti-angiogenic	HRMECs: ↓cell proliferation, ↓ migration, ↓tube formation Mice: ↓neovascularization	HRMECs: ↓p-STAT3 Mice: ↑SHP-1 activity and expression, ↓p-STAT3, ↓VEGF, p-VEGFR-2	(58)
Celastrol	ARPE-19 cells, RAW264.7 cells	Mice	Retinal degeneration induced by bright light	Anti-inflammatory, anti-oxidative	Mice: ↓ONL loss, ↑scotopic a-wave and b-wave amplitudes, ↓ photoreceptor apoptosis, ↓retinal inflammation, ↓leukostasis, ↓reactive gliosis, ↓microglial activation	ARPE-19: ↓ROS, ↓HO-1, ↓IL1β, ↓CCL2 RAW264.7: ↓TNFα, ↓ICAM-1,↓IL1β, ↓CCL2 Mice:↓ IL1β,↓Ccl2, ↓COX2, ↓TNFα	(64)
	ARPE-19 cells		Inflammation caused by LPS	Anti-inflammatory		↓IL-6, ↓NF-κB p65 phosphorylation, ↑Hsp70	(67)
		Rats	Optic nerve crush (ONC)	Cytoprotective	↑RGC survival, ↓body weight,	↑Heat shock factor protein 2(Hsf2), ↓TNFα	(66)
		Rats	Hypertension-induced degeneration	Cytoprotective	↑RGC survival		(65)

Escin	ARPE-19 cells, primary murine RPE cells		H_2O_2-induced cytotoxicity	Anti-oxidative, cytoprotective	↓murine RPE cell damage (low concentration), ↓cell apoptosis	↓ROS, ↓lipid peroxidation; ↑HO-1, ↑NQO1, ↑Sulfiredoxin-1 (SRXN1), ↑ Nrf2 phosphorylation,↑ Akt phosphorylation	(72)
	ARPE-19 cells, HUVECs		BRB breakdown	Cytoprotective	HUVECs: improved tight junction	HUVECs: combination of triamcinolone acetonide and escin: ↑occludin, ↑ZO-1, ↑glucocorticoid receptor expression	(73)
		Rats	Ischemia, BRB leakage	Cytoprotective	Escin: ↓retinal thickness; combination of triamcinolone acetonide and escin: ↓BRB permeability	↑occludin	(74)
Ursolic acid (UA)	Human RPE cells		Broad light irritation	Cytoprotective		↓NF-κB activation, ↑ROS	(88)
	Human RPE cells		UV-induced oxidative stress	Cytoprotective	↓apoptosis, ↓cell death	↓p53, ↓ NF-κB activation	(89)
Oleanolic acid (OA)	HUVEC cells	Mice	Angiogenesis	Anti-angiogenic	HUVECs and mice: ↓angiogenesis	HUVEC cells: ↓VEGFR-2, ↓Erk1/2	(121)

OA/UA nanoparticles with PLGA		Rabbits		Anti-inflammatory			(90)
Asiatic acid		Rat	Increased intraocular pressure (OIP), glaucoma	Cytoprotective	Rat: ↑RGC survival, ↓retinal thinning, ↓apoptosis, ↑photopic negative response amplitudes in COHT	↑Bcl-2; ↓Bax, ↓caspase-3	(91)
Madecassic Acid	Human Retinal Microvascular Endothelial Cells (hRMECs)		Hypoxia-induced oxidative stress	Antioxidative	↓ER stress	↓cleaved caspase-3, ↓cleaved caspase-9, ↓cleaved caspase-12, ↓Bax, ↓ROS, ↓malondialdehyde, ↓LDH,↓glucose-regulated protein 78 (GRP78),↓ CHOP, ↓inositol-requiring kinase/endonuclease 1α (IRE1α),↓cleaved activating transcription factor 6 (ATF6), ↓ATF4 nuclear translocation,↓ p-Erk,	(92)

						↓p- eukaryotic initiation factor 2 (p-eIF2α); ↑Bcl-2,↑glutathione peroxidase (GSH-PX), ↑SOD	
Corosolic acid	ARPE-19 cells	Eggs, rats	Angiogenesis	Anti-angiogenic	Eggs: ↓vascular area, ↓ number of junctions, ↓vessels length and lacunarity		(93)

Table 1.2 Summary of pharmacological effects and mechanisms of of chemically modified pentacyclic triterpenoids in the retina

Drug	*In vitro* model	*In vivo* model	Disease model	Effects	Pharmacological effects	Molecular mechanism	Reference
dh404	Primary astrocyte and rat primary Müller cells	Mice	OIR	Antioxidative, anti-vascularization	Phase II OIR: ↓Müller cell damage, ↓ vascular leakage, ↓leukostasis,↓Iba1-positive microglia	Phase I OIR: ↑VEGF in the retina. In astrocytes:↓ROS, ↑NQO1, ↑glutathione synthase,↑ HO-1 , ↓glial fibrillary acidic protein (GFAP), ↓TNFα,↓ iNOS Phase II OIR:↓ VEGF, ↓erythropoietin, ↓p-Erk/Erk ratio, ↓ROS, ↓GFAP, ↓MCP-1 ; ↑NQO1, ↑GCLM, ↑HO-1 ; ↓ ICAM-1, ↓Vascular cell adhesion protein 1 (VCAM-1), ↓TNFα	(102)

	Rat primary Mülller cells	Rats	Diabetes	Antioxidative		Retina:↓ albumin, ↓ROS, ↓VEGF, ↓angiopoietin-2,↓ TNF-α, ↓IL-6, ↓ICAM-1, ↓MCP-1,↓ 8-OHdG,↓ Nox1, ↓Nox2, ↓Nox4, ↓p22phox, ;↑HO-1, ↑NQO1, Müller cells:↓ GFAP, ↓VEGF, ↓MCP-1, ↓IL-6, ↓TNFα, ↓Nox1, ↓Nox4, ↓p22phox; ↑HO-1, ↑NQO1	(103)
CDDO-Im	RGCs	Mice	Axonal damage	Antioxidative		Mice: ↑NQO1, ↑HO-1, ↑GCLM, ↑GCLC, ↑GSTA4, ↑TXNRD	(105)
	ARPE-19 cell, 661W cells		*t*-BHP induced oxidative stress in ARPE-19 and 661W cells	Anti-oxidative, cytoprotective	ARPE-19 and 661W: ↑cell survival	ARPE-19: ↑NQO1, ↑HO-1, ↑ p-Akt, ↓ROS	(106)
	661W cells	Mice	I/R	Neuroprotective	Mice: ↓neuronal cell loss	661W: ↑NQO1, ↑HO-1, ↑GCLM, ↑GCLC, ↓ROS Mice: ↑NQO1, ↑HO-1, ↑GCLM, ↑GCLC,	(104)

						↑glutathione S-transferase Mu 1 (GSTM1), ↑thioredoxin reductase 1 (TXNRD1)	
CDDO-TFEA	ARPE-19 cell, 661W cells	Mice	*t*-BHP induced oxidative stress in ARPE-19 and 661W cells, light induced retinal damage in mice	Anti-oxidative, cytoprotective	661W: ↑cell survival, Mice: ↑ONL thickness	ARPE-19: ↑NQO1, ↑HO-1 Mice: ↑NQO1, ↑GCLC	(106)
CDDO-EA	ARPE-19 cells		*t*-BHP induced oxidative stress in ARPE-19 cells	Anti-oxidative, cytoprotective		ARPE-19: ↑NQO1, ↑HO-1	(106)
CDDO-Me		Mice	Focal cerebral ischemia	Suppress BBB permeability	↓hemorrhagic transformation, ↓BBB permeability	↑ZO-1, ↑claudin-5, ↑VE-cadherin, ↑CD31, ↑Platelet-derived growth factor receptorβ (PDGFR-β)	(109)
		Wilde type mice	I/R	Neuroprotective, inhibit I/R	↓superoxide levels, ↓retinal vascular degeneration	↑NQO1, ↑GCLM, ↑GCLC, ↑HO-1	(110)
RTA408	Human RPE cells		H_2O_2-induced cytotoxicity	Cytoprotective	↓apoptosis and necrosis, ↑cell survival	↑Bcl-2, ↑Nrf2 expression and nuclear transformation, ↑NQO1, ↑ HO-1,	

						↑SOD2, ↑catalase, ↑glutaredoxin-1 (GRX1), ↑thioredoxin-1 (TRX1); ↓Bax, ↓ROS, ↓ glutathionylation	
RS9		Rhodopsin Pro347Leu Rabbits	Retinitis pigmentosa	Inhibit ONL thinning	↓ONL thinning, cell loss	↑NQO1, HO-1, ↓IL-6	(118)
	ARPE-19 cells	Rats, rabbits	*t*-BHP in ARPE-19, BRB hypermeability in rabbits	antioxidative, inhibit neovascularization, inhibit BRB permeability	Rats: ↓neovascularization Rabbits: ↓BRB hyperpermeability	ARPE-19: ↑NQO1, ↑ HO-1, ↑GCLM Rats: ↑NQO1, ↑ HO-1	(114)
	HRMEC cells	Mice, monkey	Microvascular endothelial barrier dysfunction, choroidal neovascularization	Suppress ocular angiogenesis and hypermeability	HRMECs: ↓cell migration, ↓microvascular endothelial barrier dysfunction Monkey: ↓vascular leakage	HRMECs: ↑HO-1, ↑NQO1, ↑Nrf2, ↑PDGFR-β, ↑VE-cadherin, ↑ZO-1, ↑claudin-5, ↓VEGF	(117)
	ARPE-19 cells	Zebrafish	Non-exudative model in ARPE-19 cells, light-irritated retina degeneration in zebrafish	Cytoprotective	ARPE-19: ↑cell survival Zebrafish: ↓ONL thining, ↑ LC3-positive autophagosome	ARPE-19: ↑HO-1, ↑ microtubule-associated protein light chain 3-II (LC3-II) /LC3-1, ↑sequestosome-1	(116)

						(SQSTM1) zebrafish: ↑LC3-II, ↑SQSTM1	
	661W cells	Mice	Light irradiation	Cytoprotective	661W: ↑cell survival Mice: ↓retinal degeneration ↓ONL thining,	661W: ↑NQO1, HO-1, GCLM Mice:↑HO-1 and its activation, ↑Nrf2 activation	(115)
Betulinic acid derivative H7	RPE cells		Hypoxia-induced oxidative stress	Anti-oxidative	↑cell survival, ↓apoptosis and necrosis	↓ROS, ↓ Akt, Erk1/2, JNK	(119)
Betulinic acid derivatives H5, H7	Müller cells		Excitotoxicity-induced oxidative stress	Anti-oxidative	↑cell survival, ↓necrosis	↓ROS, ↓ Akt, Erk1/2, JNK	(120)

1.6 Objectives of this thesis

This thesis aims to investigate the protective potentials of betulin, betulinic acid and their derivatives in human RPE and Müller cells with testifying the idea of applying nano-technology in improving cellular effects of these compounds. The relevant specific aims are:

1. To investigate the protective effect of betulin, betulinic acid and their derivatives against $CoCl_2$-induced hypoxia in ARPE-19 and human primary RPE cells and study signaling pathways involved in this effect (Chapter 2).
2. To investigate the protective effect of betulin, betulinic acid and their derivatives against glutamate-induced excitotoxicity in MIO-M1 cells and study signaling pathways involved in this effect (Chapter 3).
3. To evaluate the influence of liposome-encapsulated betulinic derivatives and investigate the protective effect of these new formulations in MIO-M1 and ARPE-19 cells (Chapter 4).

References

1. Grossniklaus HE, Geisert EE, Nickerson JM. Introduction to the retina. PROG MOL BIOL TRANSL SCI. 134: Elsevier; 2015. p. 383-96.

2. Grimm C, Willmann G. Hypoxia in the eye: a two-sided coin. HIGH ALT MED BIOL. 2012;13(3):169-75.

3. McMurry J BTe. The organic chemistry of biological pathways. ROBERTS AND CO, COLORADO。 2005;Ch3:pp93-160.

4. Muffler K, Leipold D, Scheller M-C, Haas C, Steingroewer J, Bley T, et al. Biotransformation of triterpenes. PROCESS BIOCHEM. 2011;46(1):1-15.

5. Dzubak P, Hajduch M, Vydra D, Hustova A, Kvasnica M, Biedermann D, et al. Pharmacological activities of natural triterpenoids and their therapeutic implications. NAT PROD REP. 2006;23(3):394-411.

6. Sheng H, Sun H. Synthesis, biology and clinical significance of pentacyclic triterpenes: a multi-target approach to prevention and treatment of metabolic and vascular diseases. NAT PROD REP. 2011;28(3):543-93.

7. Li J, Cao H, Liu P. Glycyrrhizic acid in the treatment of liver diseases: literature review. Biomed Res Int. 2014:872139.

8. Pastorino G, Cornara L, Soares S, Rodrigues F, Oliveira MBP. Liquorice (Glycyrrhiza glabra): A phytochemical and pharmacological review. PHYTOTHER RES. 2018;32(12):2323-39.

9. https://www.drugbank.ca/drugs/DB13751.

10. van Rossum TG, Vulto AG, Hop WC, Schalm SW. Pharmacokinetics of intravenous glycyrrhizin after single and multiple doses in patients with chronic hepatitis C infection. CLIN THER. 1999;21(12):2080-90.

11. Yamamura Y, Kotaki H, Tanaka N, Aikawa T, Sawada Y, Iga T. The pharmacokinetics of glycyrrhizin and its restorative effect on hepatic function in patients with chronic hepatitis and in chronically carbon-tetrachloride-intoxicated rats. BIOPHARM DRUG DISPOS. 1997;18(8):717-25.

12. He H, Wei D, Liu H, Zhu C, Lu Y, Ke Z, et al. Glycyrrhizin protects against sodium iodate-induced RPE and retinal injury though activation of AKT and Nrf2/HO-1 pathway. J CELL MOL MED. 2019;23(5):3495-504.

13. Mohammad G, Alam K, Nawaz MI, Siddiquei MM, Mousa A, El-Asrar AMA. Mutual enhancement between high-mobility group box-1 and NADPH oxidase-derived reactive oxygen species mediates diabetes-induced upregulation of retinal apoptotic markers. J PHYSIOL BIOCHEM. 2015;71(3):359-72.

14. Liu L, Jiang Y, Steinle JJ. Inhibition of HMGB1 protects the retina from ischemia-reperfusion,

as well as reduces insulin resistance proteins. PLOS ONE. 2017;12(5):e0178236.

15. Song Z, Gong Y, Liu H, Ren Q, Sun X. Glycyrrhizin could reduce ocular hypertension induced by triamcinolone acetonide in rabbits. MOL VIS. 2011;17:2056.

16. Li J, Shi J, Sun Y, Zheng F. Glycyrrhizin, a Potential Drug for Autoimmune Encephalomyelitis by Inhibiting High-Mobility Group Box 1. DNA CELL BIOL. 2018;37(12):941-6.

17. El-Asrar AMA, Alam K, Garcia-Ramirez M, Ahmad A, Siddiquei MM, Mohammad G, et al. Association of HMGB1 with oxidative stress markers and regulators in PDR. MOL VIS. 2017;23:853.

18. Mohammad G, Siddiquei MM, Othman A, Al-Shabrawey M, El-Asrar AMA. High-mobility group box-1 protein activates inflammatory signaling pathway components and disrupts retinal vascular-barrier in the diabetic retina. EXP EYE RES. 2013;107:101-9.

19. Lee J-J, Hsiao C-C, Yang I-H, Chou M-H, Wu C-L, Wei Y-C, et al. High-mobility group box 1 protein is implicated in advanced glycation end products–induced vascular endothelial growth factor A production in the rat retinal ganglion cell line RGC-5. MOL VIS. 2012;18:838.

20. El-Asrar AMA, Nawaz MI, Kangave D, Geboes K, Ola MS, Ahmad S, et al. High-mobility group box-1 and biomarkers of inflammation in the vitreous from patients with proliferative diabetic retinopathy. MOL VIS. 2011;17:1829.

21. Abu El-Asrar AM, Mohammad G, Nawaz MI, Siddiquei MM. High-mobility group box-1 modulates the expression of inflammatory and angiogenic signaling pathways in diabetic retina. CURR EYE RES. 2015;40(11):1141-52.

22. El-Asrar A, Ahmed M, Nawaz MI, Siddiquei MM, Al-Kharashi AS, Kangave D, et al. High-mobility group box-1 induces decreased brain-derived neurotrophic factor-mediated neuroprotection in the diabetic retina. MEDIATORS INFLAMM. 2013;2013.

23. El-Asrar A, Ahmed M, Mairaj Siddiquei M, Nawaz MI, Geboes K, Mohammad G. The proinflammatory cytokine high-mobility group box-1 mediates retinal neuropathy induced by diabetes. MEDIATORS INFLAMM. 2014;2014.

24. Tu JH, He YJ, Chen Y, Fan L, Zhang W, Tan ZR, et al. Effect of glycyrrhizin on the activity of CYP3A enzyme in humans. EUR J CLIN PHARMACOL. 2010;66(8):805-10.

25. Sun H, Wang J, Lv J. Effects of glycyrrhizin on the pharmacokinetics of paeoniflorin in rats and its potential mechanism. PHARM BIOL. 2019;57(1):550-4.

26. Liao S, Jin X, Li J, Zhang T, Zhang W, Shi W, et al. Effects of Silymarin, Glycyrrhizin, and Oxymatrine on the Pharmacokinetics of Ribavirin and Its Major Metabolite in Rats. PHYTOTHER RES. 2016;30(4):618-26.

27. Zhao Q, Wang Y, Wang H, Feng L. Effects of glycyrrhizin on the pharmacokinetics of puerarin in rats. XENOBIOTICA. 2018;48(11):1157-63.

28. Ao Y, Chen J, Yue J, Peng RX. Effects of 18alpha-glycyrrhizin on the pharmacodynamics and pharmacokinetics of glibenclamide in alloxan-induced diabetic rats. EUR J PHARMACOL.

2008;587(1-3):330-5.

29. Han L, Wang R, Wu B, Gu Y, Yuan Y. Effect of diammonium glycyrrhizinate on pharmacokinetics of omeprazole by regulating cytochrome P450 enzymes and plasma protein binding rate. XENOBIOTICA. 2019;49(8):975-80.

30. Tu JH, Hu DL, Dai LL, Sun Y, Fan L, Zhang M, et al. Effect of glycyrrhizin on CYP2C19 and CYP3A4 activity in healthy volunteers with different CYP2C19 genotypes. XENOBIOTICA. 2010;40(6):393-9.

31. Chen L, Yang J, Davey AK, Chen YX, Wang JP, Liu XQ. Effects of diammonium glycyrrhizinate on the pharmacokinetics of aconitine in rats and the potential mechanism. XENOBIOTICA. 2009;39(12):955-63.

32. Yan M, Fang PF, Li HD, Xu P, Liu YP, Wang F, et al. Lack of effect of continuous glycyrrhizin administration on the pharmacokinetics of the P-glycoprotein substrate talinolol in healthy volunteers. EUR J CLIN PHARMACOL. 2013;69(3):515-21.

33. Guo L, Cui Y, Hao K. Effects of glycyrrhizin on the pharmacokinetics of asiatic acid in rats and its potential mechanism. PHARM BIOL. 2018;56(1):119-23.

34. Yan G, Zhang H, Wang W, Li Y, Mao C, Fang M, et al. Investigation of the influence of glycyrrhizin on the pharmacokinetics of celastrol in rats using LC-MS and its potential mechanism. XENOBIOTICA. 2017;47(7):607-13.

35. https://www.drugbank.ca/drugs/DB02329.

36. Suzuki T, Sasano H, Kaneko C, Ogawa S, Darnel AD, Krozowski ZS. Immunohistochemical distribution of 11β-hydroxysteroid dehydrogenase in human eye. MOL CELL ENDOCRINOL. 2001;173(1-2):121-5.

37. Na Y-J, Choi K-J, Park SB, Sung H-R, Jung WH, Kim HY, et al. Protective effects of carbenoxolone, an 11β-HSD1 inhibitor, against chemical induced dry eye syndrome. APOPTOSIS. 2017;22(11):1441-53.

38. Pan F, Mills SL, Massey SC. Screening of gap junction antagonists on dye coupling in the rabbit retina. VIS NEUROSCI. 2007;24(4):609-18.

39. Lampe PD, Lau AF. The effects of connexin phosphorylation on gap junctional communication. INT J BIOCHEM CELL BIOL. 2004;36(7):1171-86.

40. Pottek M, Hoppenstedt W, Janssen-Bienhold U, Schultz K, Perlman I, Weiler R. Contribution of connexin26 to electrical feedback inhibition in the turtle retina. J COMP NEUROL. 2003;466(4):468-77.

41. McMahon MJ, Packer OS, Dacey DM. The classical receptive field surround of primate parasol ganglion cells is mediated primarily by a non-GABAergic pathway. J NEUROSCI. 2004;24(15):3736-45.

42. Cusato K, Bosco A, Rozental R, Guimarães CA, Reese BE, Linden R, et al. Gap junctions mediate bystander cell death in developing retina. J NEUROSCI. 2003;23(16):6413-22.

43. Vaney DI, Nelson JC, Pow DV. Neurotransmitter coupling through gap junctions in the retina. J NEUROSCI. 1998;18(24):10594-602.

44. Packer OS, Dacey DM. Synergistic center-surround receptive field model of monkey H1 horizontal cells. J VIS. 2005;5(11):9-.

45. Bramley JR, Wiles EM, Sollars PJ, Pickard GE. Carbenoxolone blocks the light-evoked rise in intracellular calcium in isolated melanopsin ganglion cell photoreceptors. PLOS ONE. 2011;6(7):e22721.

46. Kamermans M, Fahrenfort I, Schultz K, Janssen-Bienhold U, Sjoerdsma T, Weiler R. Hemichannel-mediated inhibition in the outer retina. SCIENCE. 2001;292(5519):1178-80.

47. Khamidakh AA, Juuti-Uusitalo K, Larsson K, Skottman H, Hyttinen J. Intercellular Ca2+ wave propagation in human retinal pigment epithelium cells induced by mechanical stimulation. EXP EYE RES. 2013;108:129-39.

48. Kihara AH, Santos TO, Osuna-Melo EJ, Paschon V, Vidal KS, Akamine PS, et al. Connexin-mediated communication controls cell proliferation and is essential in retinal histogenesis. INT J DEV NEUROSCI. 2010;28(1):39-52.

49. Xia Y, Nawy S. The gap junction blockers carbenoxolone and 18β-glycyrrhetinic acid antagonize cone-driven light responses in the mouse retina. VIS NEUROSCI. 2003;20(4):429-35.

50. Verweij J, Hornstein EP, Schnapf JL. Surround antagonism in macaque cone photoreceptors. J NEUROSCI. 2003;23(32):10249-57.

51. Vessey JP, Lalonde MR, Mizan HA, Welch NC, Kelly ME, Barnes S. Carbenoxolone inhibition of voltage-gated Ca channels and synaptic transmission in the retina. J NEUROPHYSIOL. 2004;92(2):1252-6.

52. Ammon H. Boswellic acids and their role in chronic inflammatory diseases. ADV EXP MED BIOL. 2016, 928: 291-327.

53. Al-Yasiry ARM, Kiczorowska B. Frankincense-therapeutic properties. POSTEPY HIG MED DOSW (ONLINE). 2016;70:380-391.

54. Roy NK, Deka A, Bordoloi D, Mishra S, Kumar AP, Sethi G, et al. The potential role of boswellic acids in cancer prevention and treatment. CANCER LETT. 2016;377(1):74-86.

55. Lyons BL, Smith RS, Hurd RE, Hawes NL, Burzenski LM, Nusinowitz S, et al. Deficiency of SHP-1 protein-tyrosine phosphatase in “viable motheaten” mice results in retinal degeneration. INVEST OPHTHALMOL VIS SCI. 2006;47(3):1201-9.

56. Geraldes P, Hiraoka-Yamamoto J, Matsumoto M, Clermont A, Leitges M, Marette A, et al. Activation of PKC-δ and SHP-1 by hyperglycemia causes vascular cell apoptosis and diabetic retinopathy. NAT MED. 2009;15(11):1298.

57. Mei S, Cammalleri M, Azara D, Casini G, Bagnoli P, Dal Monte M. Mechanisms underlying somatostatin receptor 2 down-regulation of vascular endothelial growth factor expression in response to hypoxia in mouse retinal explants. J PATHOL. 2012;226(3):519-33.

58. Lulli M, Cammalleri M, Fornaciari I, Casini G, Dal Monte M. Acetyl-11-keto-β-boswellic acid reduces retinal angiogenesis in a mouse model of oxygen-induced retinopathy. EXP EYE RES. 2015;135:67-80.

59. Riva A, Morazzoni P, Artaria C, Allegrini P, Meins J, Savio D, et al. A single-dose, randomized, cross-over, two-way, open-label study for comparing the absorption of boswellic acids and its lecithin formulation. PHYTOMEDICINE. 2016;23(12):1375-82.

60. Sterk V, Büchele B, Simmet T. Effect of food intake on the bioavailability of boswellic acids from a herbal preparation in healthy volunteers. PLANTA MED. 2004;70(12):1155-60.

61. Tausch L, Henkel A, Siemoneit U, Poeckel D, Kather N, Franke L, et al. Identification of human cathepsin G as a functional target of boswellic acids from the anti-inflammatory remedy frankincense. J IMMUNOL. 2009;183(5):3433-42.

62. Abdel-Tawab M, Werz O, Schubert-Zsilavecz M. Boswellia serrata: an overall assessment of in vitro, preclinical, pharmacokinetic and clinical data. CLIN PHARMACOKINET. 2011;50(6):349-69.

63. Chen S-R, Dai Y, Zhao J, Lin L, Wang Y, Wang Y. A mechanistic overview of triptolide and celastrol, natural products from Tripterygium wilfordii Hook F. FRONT PHARMACOL. 2018;9:104.

64. Bian M, Du X, Cui J, Wang P, Wang W, Zhu W, et al. Celastrol protects mouse retinas from bright light-induced degeneration through inhibition of oxidative stress and inflammation. J NEUROINFLAMMATION. 2016;13(1):50.

65. Gu L, Kwong JM, Yadegari D, Yu F, Caprioli J, Piri N. The effect of celastrol on the ocular hypertension-induced degeneration of retinal ganglion cells. NEUROSCI LETT. 2018;670:89-93.

66. Kyung H, Kwong JM, Bekerman V, Gu L, Yadegari D, Caprioli J, et al. Celastrol supports survival of retinal ganglion cells injured by optic nerve crush. BRAIN RES. 2015;1609:21-30.

67. Paimela T, Hyttinen JM, Viiri J, Ryhänen T, Karjalainen RO, Salminen A, et al. Celastrol regulates innate immunity response via NF-κB and Hsp70 in human retinal pigment epithelial cells. PHARMACOL RES. 2011;64(5):501-8.

68. Huang Y, Zhou D, Hang T, Wu Z, Liu J, Xu Q, et al. Preparation, characterization, and assessment of the antiglioma effects of liposomal celastrol. ANTICANCER DRUGS. 2012;23(5):515-24.

69. Kim JE, Lee MH, Nam DH, Song HK, Kang YS, Lee JE, et al. Celastrol, an NF-κB inhibitor, improves insulin resistance and attenuates renal injury in db/db mice. PLOS ONE. 2013;8(4):e62068.

70. Sirtori CR. Aescin: pharmacology, pharmacokinetics and therapeutic profile. PHARMACOL RES. 2001;44(3):183-93.

71. Cheong DH, Arfuso F, Sethi G, Wang L, Hui KM, Kumar AP, et al. Molecular targets and anti-cancer potential of escin. CANCER LETT. 2018;422:1-8.

72. Wang K, Jiang Y, Wang W, Ma J, Chen M. Escin activates AKT-Nrf2 signaling to protect retinal pigment epithelium cells from oxidative stress. BIOCHEM BIOPHYS RES COMMUN. 2015;468(4):541-7.
73. Zhang F, Man X, Yu H, Liu L, Li Y. Synergistic protective effects of escin and low-dose glucocorticoids against vascular endothelial growth factor-induced blood-retinal barrier breakdown in retinal pigment epithelial and umbilical vein endothelial cells. MOL MED REP. 2015;11(2):1372-7.
74. Zhang F, Li Y, Zhang L, Mu G. Synergistic protective effects of escin and low-dose glucocorticoids on blood-retinal barrier breakdown in a rat model of retinal ischemia. MOL MED REP. 2013;7(5):1511-5.
75. Wu X, Liu L, Zhang M, Wu D, Wang Y, Sun Y, et al. Simultaneous analysis of isomers of escin saponins in human plasma by liquid chromatography-tandem mass spectrometry: application to a pharmacokinetic study after oral administration. J CHROMATOGR B ANALYT TECHNOL BIOMED LIFE SCI. 2010;878(11-12):861-7.
76. Lin C, Wen X, Sun H. Oleanolic acid derivatives for pharmaceutical use: a patent review. EXPERT OPIN THER PAT. 2016;26(6):643-55.
77. Zhao H, Zhou M, Duan L, Wang W, Zhang J, Wang D, et al. Efficient synthesis and anti-fungal activity of oleanolic acid oxime esters. MOLECULES. 2013;18(3):3615-29.
78. Pollier J, Goossens A. Oleanolic acid. Phytochemistry. 2012;77:10-5.
79. Ayeleso T, Matumba M, Mukwevho E. Oleanolic acid and its derivatives: biological activities and therapeutic potential in chronic diseases. MOLECULES. 2017;22(11):1915.
80. Fai YM, Tao CC. A review of presence of oleanolic acid in natural products. NATURA PRODA MEDICA. 2009;2:77-290.
81. Song M, Hang TJ, Wang Y, Jiang L, Wu XL, Zhang Z, et al. Determination of oleanolic acid in human plasma and study of its pharmacokinetics in Chinese healthy male volunteers by HPLC tandem mass spectrometry. J PHARM BIOMED ANAL. 2006;40(1):190-6.
82. Jeong DW, Kim YH, Kim HH, Ji HY, Yoo SD, Choi WR, et al. Dose-linear pharmacokinetics of oleanolic acid after intravenous and oral administration in rats. BIOPHARM DRUG DISPOS. 2007;28(2):51-7.
83. Jeong DW, Kim YH, Kim HH, Ji HY, Yoo SD, Choi WR, et al. Dose-linear pharmacokinetics of oleanolic acid after intravenous and oral administration in rats. BIOPHARM DRUG DISPOSITION. 2007;28(2):51-7.
84. Woźniak Ł, Skąpska S, Marszałek K. Ursolic acid—a pentacyclic triterpenoid with a wide spectrum of pharmacological activities. MOLECULES. 2015;20(11):20614-41.
85. Hussain H, Green IR, Ali I, Khan IA, Ali Z, Al-Sadi AM, et al. Ursolic acid derivatives for pharmaceutical use: a patent review (2012-2016). EXPERT OPIN THER PAT. 2017;27(9):1061-72.
86. Liao Q, Yang W, Jia Y, Chen X, Gao Q, Bi K. LC-MS determination and pharmacokinetic

studies of ursolic acid in rat plasma after administration of the traditional Chinese medicinal preparation Lu-Ying extract. YAKUGAKU ZASSHI. 2005;125(6):509-15.

87. Wang W, Zhang W, Jiang Y, Wang X, Zhang X, Liu H, et al. Preparation of ursolic acid-phospholipid complex by solvent-assisted grinding method to improve dissolution and oral bioavailability. PHARM DEV TECHNOL. 2020;25(1):68-75.

88. Lee YH, Kumar NC, Glickman RD. Modulation of photochemical damage in normal and malignant cells by naturally occurring compounds. PHOTOCHEM PHOTOBIOL. 2012;88(6):1385-95.

89. Lee Y-H, Wang E, Kumar N, Glickman RD. Ursolic acid differentially modulates apoptosis in skin melanoma and retinal pigment epithelial cells exposed to UV–VIS broadband radiation. APOPTOSIS. 2014;19(5):816-28.

90. Alvarado HL, Abrego G, Garduño-Ramirez ML, Clares B, Calpena AC, García ML. Design and optimization of oleanolic/ursolic acid-loaded nanoplatforms for ocular anti-inflammatory applications. NANOMED NANOTECHNOL BIOL MED. 2015;11(3):521-30.

91. Huang W, Hu F, Sun X-h. Asiatic acid prevents retinal ganglion cell apoptosis in a rat model of glaucoma. FRONT NEUROSCI. 2018;12:489.

92. Yang B, Xu Y, Hu Y, Luo Y, Lu X, Tsui CK, et al. Madecassic Acid protects against hypoxia-induced oxidative stress in retinal microvascular endothelial cells via ROS-mediated endoplasmic reticulum stress. BIOMED PHARMACOTHER. 2016;84:845-52.

93. Toledo CR, Pereira VV, Dourado LFN, Paiva MRB, Silva-Cunha A. Corosolic acid: antiangiogenic activity and safety of intravitreal injection in rats eyes. DOC OPHTHALMOL. 2019;138(3):181-94.

94. Speranza G, Gutierrez ME, Kummar S, Strong JM, Parker RJ, Collins J, et al. Phase I study of the synthetic triterpenoid, 2-cyano-3, 12-dioxoolean-1, 9-dien-28-oic acid (CDDO), in advanced solid tumors. CANCER CHEMOTHER PHARMACOL. 2012;69(2):431-8.

95. Datta S, Cano M, Ebrahimi K, Wang L, Handa JT. The impact of oxidative stress and inflammation on RPE degeneration in non-neovascular AMD. PROG RETIN EYE RES. 2017;60:201-18.

96. Lambros ML, Plafker SM. Oxidative stress and the Nrf2 anti-oxidant transcription factor in age-related macular degeneration. ADV EXP MED BIOL. 2016;854:67-72..

97. Bellezza I. Oxidative Stress in Age-Related Macular Degeneration: Nrf2 as Therapeutic Target. FRONT PHARMACOL. 2018;9:1280.

98. Kowluru RA, Mishra M. Epigenetic regulation of redox signaling in diabetic retinopathy: Role of Nrf2. FREE RADIC BIOL MED. 2017;103:155-64.

99. Nakagami Y. Nrf2 is an attractive therapeutic target for retinal diseases. OXID MED CELL LONGEV. 2016; 2016:7469326.

100. Liu X-F, Zhou D-D, Xie T, Hao J-L, Malik TH, Lu C-B, et al. The Nrf2 Signaling in Retinal

Ganglion Cells under Oxidative Stress in Ocular Neurodegenerative Diseases. INT J BIOL SCI. 2018;14(9):1090.

101. Sachdeva MM, Cano M, Handa JT. Nrf2 signaling is impaired in the aging RPE given an oxidative insult. EXP EYE RES. 2014;119:111-4.

102. Deliyanti D, Lee JY, Petratos S, Meyer CJ, Ward KW, Wilkinson-Berka JL, et al. A potent Nrf2 activator, dh404, bolsters antioxidant capacity in glial cells and attenuates ischaemic retinopathy. CLIN SCI. 2016;130(15):1375-87.

103. Deliyanti D, Alrashdi SF, Tan SM, Meyer C, Ward KW, de Haan JB, et al. Nrf2 activation is a potential therapeutic approach to attenuate diabetic retinopathy. INVEST OPHTHALMOL VIS SCI. 2018;59(2):815-25.

104. Xu Z, Cho H, Hartsock MJ, Mitchell KL, Gong J, Wu L, et al. Neuroprotective role of Nrf2 for retinal ganglion cells in ischemia-reperfusion. J NEUROCHEM. 2015;133(2):233-41.

105. Himori N, Yamamoto K, Maruyama K, Ryu M, Taguchi K, Yamamoto M, et al. Critical role of Nrf2 in oxidative stress-induced retinal ganglion cell death. J NEUROCHEM. 2013;127(5):669-80.

106. Pitha-Rowe I, Liby K, Royce D, Sporn M. Synthetic triterpenoids attenuate cytotoxic retinal injury: cross-talk between Nrf2 and PI3K/AKT signaling through inhibition of the lipid phosphatase PTEN. INVEST OPHTHALMOL VIS SCI. 2009;50(11):5339-47.

107. Hong DS, Kurzrock R, Supko JG, He X, Naing A, Wheler J, et al. A phase I first-in-human trial of bardoxolone methyl in patients with advanced solid tumors and lymphomas. CLIN CANCER RES. 2012;18(12):3396-406.

108. Thomas M. A preliminary evaluation of bardoxolone methyl for the treatment of diabetic nephropathy. EXPERT OPIN DRUG METAB TOXICOL. 2012;8(8):1015-22.

109. Imai T, Takagi T, Kitashoji A, Yamauchi K, Shimazawa M, Hara H. Nrf2 activator ameliorates hemorrhagic transformation in focal cerebral ischemia under warfarin anticoagulation. NEUROBIOL DIS. 2016;89:136-46.

110. Wei Y, Gong J, Yoshida T, Eberhart CG, Xu Z, Kombairaju P, et al. Nrf2 has a protective role against neuronal and capillary degeneration in retinal ischemia–reperfusion injury. FREE RADIC BIOL MED. 2011;51(1):216-24.

111. Liu X, Ward K, Xavier C, Jann J, Clark AF, Pang I-H, et al. The novel triterpenoid RTA 408 protects human retinal pigment epithelial cells against H_2O_2-induced cell injury via NF-E2-related factor 2 (Nrf2) activation. REDOX BIOL. 2016;8:98-109.

112. Reisman SA, Gahir SS, Lee CI, Proksch JW, Sakamoto M, Ward KW. Pharmacokinetics and pharmacodynamics of the novel Nrf2 activator omaveloxolone in primates. DRUG DES DEVEL THER. 2019;13:1259-70.

113. Creelan BC, Gabrilovich DI, Gray JE, Williams CC, Tanvetyanon T, Haura EB, et al. Safety, pharmacokinetics, and pharmacodynamics of oral omaveloxolone (RTA 408), a synthetic triterpenoid, in a first-in-human trial of patients with advanced solid tumors. ONCO TARGETS

THER. 2017;10:4239-50.
114. Nakagami Y, Masuda K, Hatano E, Inoue T, Matsuyama T, Iizuka M, et al. Novel N rf2 activators from microbial transformation products inhibit blood–retinal barrier permeability in rabbits. BR J PHARMACOL. 2015;172(5):1237-49.
115. Inoue Y, Shimazawa M, Noda Y, Nagano R, Otsuka T, Kuse Y, et al. RS 9, a novel Nrf2 activator, attenuates light-induced death of cells of photoreceptor cells and Müller glia cells. J NEUROCHEM. 2017;141(5):750-65.
116. Saito Y, Kuse Y, Inoue Y, Nakamura S, Hara H, Shimazawa M. Transient acceleration of autophagic degradation by pharmacological Nrf2 activation is important for retinal pigment epithelium cell survival. REDOX BIOL. 2018;19:354-63.
117. Nakamura S, Noguchi T, Inoue Y, Sakurai S, Nishinaka A, Hida Y, et al. Nrf2 Activator RS9 Suppresses Pathological Ocular Angiogenesis and Hyperpermeability. INVEST OPHTHALMOL VIS SCI. 2019;60(6):1943-52.
118. Nakagami Y, Hatano E, Inoue T, Yoshida K, Kondo M, Terasaki H. Cytoprotective effects of a novel Nrf2 activator, RS9, in rhodopsin Pro347Leu rabbits. CURR EYE RES. 2016;41(8):1123-6.
119. Cheng Z, Yao W, Zheng J, Ding W, Wang Y, Zhang T, et al. A derivative of betulinic acid protects human Retinal Pigment Epithelial (RPE) cells from cobalt chloride-induced acute hypoxic stress. EXP EYE RES. 2019;180:92-101.
120. Cheng Z, Zhang T, Zheng J, Ding W, Wang Y, Li Y, et al. Betulinic acid derivatives can protect human Müller cells from glutamate-induced oxidative stress. EXP CELL RES. 2019;383(1):111509.
121. Lee D-H, Lee J, Jeon J, Kim K-J, Yun J-H, Jeong H-S, et al. Oleanolic Acids Inhibit Vascular Endothelial Growth Factor Receptor 2 Signaling in Endothelial Cells: Implication for Anti-Angiogenic Therapy. MOL CELLS. 2018;41(8):771.

Chapter 2

A derivative of betulinic acid protects human Retinal Pigment Epithelial (RPE) cells from cobalt chloride-induced acute hypoxic stress

Abstract

The Retinal Pigment Epithelium (RPE) is a monolayer of cells located above the choroid. It mediates human visual cycle and nourishes photoreceptors. Hypoxia-induced oxidative stress to RPE is a vital cause of retinal degeneration such as the Age-related Macular Degeneration. Most of these retinal diseases are irreversible with no efficient treatment, therefore protecting RPE cells from hypoxia stress is an important way to prevent or slow down the progression of retinal degeneration. Betulinic acid (BA) and betulin (BE) are pentacyclic triterpenoids with anti-oxidative property, but little is known about their effect on RPE cells. We investigated the protective effect of BA, BE and their derivatives against cobalt chloride-induced hypoxia stress in RPE cells. Human ARPE-19 cells were exposed to BA, BE and their eighteen derivatives (named as H3-H20) that we customized through replacing moieties at C3 and C28 positions. We found that cobalt chloride reduced cell viability, increased Reactive Oxygen Species (ROS) production as well as induced apoptosis and necrosis in ARPE-19 cells. Interestingly, the pretreatment of H7 (3-O-acetyl-glycyl- 28-O-glycyl-betulinic acid) effectively protected cells from acute hypoxia stress induced by cobalt chloride. Our immunoblotting results suggested that this derivative attenuated the cobalt chloride-induced activation of Akt, Erk1/2 and JNK pathways. All findings were further validated in human primary RPE cells. In summary, this BA derivate has protective effect against the acute hypoxic stress in human RPE cells and may be developed into a candidate agent effective in the prevention of prevalent retinal diseases.

2.1 Introduction

Our capacity to see the world starts in the retina, a thin layer of neural tissue at the back of the eye. The processing of light information relies on the visual cycle, where retinoids are exchanged between photoreceptors and the Retinal Pigment Epithelium (RPE). This cycle converts light energy into electrical signals for visual processing within the neural retina (1). The RPE monolayer is located just outside the neural retina, between the outer neural layer of photoreceptors (rods and cones) and the underlying vascular choroid. RPE is responsible for selectively transporting molecules between the vascular choroid and outer neural retina as well as the phagocytosis of shredded photoreceptor outer segments (2). RPE is also the main producer of angiogenic factors in the retina (3). Furthermore, RPE cells are able to absorb excess light and protect the retina from phototoxicity (4), thus pathologic damage to RPE is a vital cause of many retinal diseases (5-9).

Age-related macular degeneration (AMD) is the most prevalent, irreversible retinal disease (1), which accounts for 8.7% blindness worldwide with an increasing morbidity (10, 11). It is also the leading cause of blindness among those aged over 50 years. There are two main types of AMD: “dry” (atrophic) and “wet” (neovascular). The dry form is associated with chronic loss of photoreceptors and RPE cell death (12); whereas wet AMD involves with choroidal neovascularization (CNV), new vessel growth originated from the choroid to the subretinal space (13). Anti-VEGF drugs can be used to treat wet AMD, but there is no therapy for dry AMD now.

Due to a high metabolic rate and oxygen level, exposure to light as well as abundance of polyunsaturated fatty acids, RPE cells are prone to oxidative damage caused by the imbalance of generation and elimination of reactive oxygen species (ROS) (4, 7, 14, 15). In addition, antioxidant ability declines with aging (16), which further leads to ROS level increase and potentiates retinal degeneration. Hypoxia-induced oxidation in RPE cells is a vital cause of dry AMD (9, 17), and RPE is thought to be the prime early target of this disease (18), therefore it is important to protect RPE cells from hypoxia in order to prevent or slow down the progression of retinal degenerations.

In the current study, we investigated the protective effect of betulinic acid (BA), betulin (BE) and their chemical derivatives on hypoxia-induced oxidative stress in human RPE cell line. BE and BA are both pentacyclic triterpenoids extracted from the bark of birch trees; BA is more biologically active than its precursor BE. These natural compounds have been shown to have anti-oxidative, anti-cancer, anti-inflammatory, anti-microbial, anti-viral and anti-diabetic properties (19, 20). Publications have reported that BA and BE can effectively protect various cell types from oxidative

damages (21-23); however, little is known about their effects on retinal cells. It is known that the solubility of BA and BE in the gastrointestinal tract and their bioavailability in the body are low (24, 25). According to the studies on their structure-effect relationship, chemical modifications at the position C3 and C28 were considered to be preferable in improving their solubility and bioavailability with reduced cytotoxicity (24, 25). We synthesized a series of BA and BE derivatives with replacing various moieties at C3 and C28 positions previously (26, 27). In this study, we evaluated the anti-oxidative potentials of BA, BE and their 18 derivatives in human RPE cells with cobalt chloride-induced hypoxic stress.

2.2 Materials and methods

2.2.1 Reagents and chemicals

Fetal Bovine Serum (FBS) and Dulbecco's Modified Eagle Medium (DMEM) were purchased from Thermo Scientific (Lidcombe, NSW, Australia). Dimethyl sulfoxide (DMSO), thiazolyl blue tetrazoliuM bromide (MTT), Betulinic Acid (BA, named as H1 in this thesis) and cobalt chloride were purchased from Sigma-Aldrich (Castle Hill, NSW, Australia). Betulinic acid derivatives were in house synthesized and customized as described before (26, 27). 2′,7′-Dichlorodihydrofluorescein diacetate (CM-H_2DCFDA) was obtained from Thermo Scientific (Lidcombe, NSW, Australia). FITC annexin V apoptosis detection kit was purchased from BD Bioscience (North Ryde, NSW, Australia). PVDF membrane was obtained from Merck Millipore (Bayswater, VIC, Australia). Phospho-Akt (Ser473), Akt (pan), phospho-p44/42 MAPK (Erk) (Thr202/Tyr204), p44/42 MAPK (Erk) phosphor-SAPK/JNK (Thr183/Tyr185) (81E11), SAPK/JNK and α-Tubulin (DM1A) antibodies were obtained from Genesearch Pty Ltd (Arundel, QLD, Australia); p-p38 Antibody (D-8) and p38α/β Antibody (A-12) antibodies were purchased from Bio-strategy Laboratory Products (Tingalpa, QLD, Australia); β-actin antibody was obtained from Sigma-Aldrich (Castle Hill, NSW, Australia). Horseradish peroxidase-conjugated goat anti-rabbit and anti-mouse IgG was purchased from Bio-strategy Laboratory Products (Tingalpa, QLD, Australia). Protein signal was detected with the SuperSignal West Pico Chemiluminescent Substrate (Thermo Scientific, Lidcombe, NSW, Australia).

2.2.2 Cell culture

Human retinal pigment epithelium (ARPE-19) cell line was purchased from American Type Culture Collection (ATCC). Cells were maintained at 37 °C and 5% CO_2 with Dulbecco's modified Eagle medium suppled with 10% FBS (v/v) and 1% L-Glutamine.

Three postmortem human eyes (age range, 38-69 years, postmortem delay < 16 hours) were requested through the Lions NSW Eye Bank and used to isolate primary RPE cells with human ethical approval from The University of Sydney human Research Ethics Committee. As described previously (28), after removing the anterior segment, the neurosensory retina and vitreous from the eyes, the eyecups were washed with phosphate buffered saline (PBS, pH 7.4). Trypsin-EDTA was used to remove the cells at 37 °C for 45 min. The RPE was gently dissected from the Bruch's membrane with pipetting. The cells were collected into DMEM supplied with 4.5 g/L glucose, 2 mM L-glutamine and 20% FBS. Primary RPE cells were maintained in flasks at 37 °C with 5% CO_2 and used between passages 2 to 5 in the following experiments.

2.2.3 Cytotoxicity and anti-hypoxic assay

ARPE-19 cells were seeded into 96-well plates (3×10^4 cells/well) and cultured overnight to reach confluence. In the cytotoxicity study, cells were treated with 10 μM H1-H20 compound in DMEM plus 1% FBS (v/v) for 24 h and DMSO was used as the vehicle control. To determine the anti-hypoxic effect of H1-H20, cells were further incubated with 8 mM cobalt chloride for 4 h before measuring cell viability.

Cell viability was performed using MTT assay as shown before (29-37). In details, cells were incubated with 0.5 mg/mL MTT solution for 2 h in dark and washed with phosphate-buffered saline (PBS, pH 7.4; 0.001 M KH_2PO_4, 0.154 M NaCl, 0.003 M Na_2HPO_4). 100 μL DMSO was then added into each well and shake at room temperature for 10 min. The absorbance was measured at 550 nm with the BioRad Model 680 microplate reader (Bio-rad, Gladesville, NSW, Australia).

2.2.4 Measurement of intracellular Reactive Oxygen Species (ROS)

ROS level was measured with CM-H_2DCFDA reagent as to the manufacture's manual. Briefly, cells were seeded into 96-well plates (3×10^4 cells/well) and pretreated

with each compound for 24 h, then incubated with 2 μM CM-H_2DCFDA for 1 h at 37 ℃ in dark. Cells were then washed with PBS three times and measured at Ex/Em: 485 nm/535 nm by the PerkinElmer VictorTM X4 Multimode plate reader (PerkinElmer, Melbourne, VIC, Australia). Readings were subtracted by that of control (cells treated with vehicle). The changes of compound treated cells were calculated as the fold of control.

2.2.5 Apoptotic assay

Similar to our published studies before (38-40), ARPE-19 cells (1.8×10^5 cells/well) were seeded on 24-well plates and incubated with each compound for 24 h at 37 °C. Cells were collected after exposure to 10 mM cobalt chloride for 4 h. Cells were stained with annexin V-FITC and propidium iodide (PI) according to the manufacturer's protocol. Samples were analyzed with Guava easy®cyte flow cytometer (Merck Millipore, Bayswater, VIC, Australia).

2.2.6 Western blot

ARPE-19 cells were lysed with NP-40 lysis buffer (50 mM Tris, 150 mM NaCl, 1% IGEPAL, pH 7.8) supplied with protease inhibitor cocktail and centrifuged at 15,000 rpm for 10 min at 4℃. Protein samples was separated by electrophoresis using 10% SDS-PAGE gels and transferred onto PVDF membranes. After blocking with 5% non-fat milk in PBST for 30 min at room temperature, immunoblots were probed with different primary antibodies overnight at 4 ℃. After washing, the blots were probed with secondary antibodies for 1 h at room temperature. Blots were washed and incubated with the SuperSignal West Pico Chemiluminescent Substrate (Thermo Scientific, Lidcombe, NSW, Australia).

2.2.7 Statistics

All the data are presented as mean ± standard deviation (SD). Student's *t*-test was used to evaluate differences between cobalt chloride treated and control group. Two-way ANOVA was used to compare the compound treated groups *vs*. control group. $p<0.05$ was considered as significant.

2.3 Results

2.3.1 Cytotoxicity of BA, BE and their derivatives

Chemical modifications were made at the C3 and C28 positions of BA and BE (Table 2.1) (26, 27). To elucidate the therapeutic potentials of these compounds, we first evaluated their cytotoxicity in ARPE-19 cells at 10 μM, which concentration is close to the C_{max} reported in murine models (41-44). Compound H1, H11 and H14 had mild cytotoxicity at 10 μM; while compound H2, H4, H6, H9 and H19 had moderate toxicity to the APRE-19 cells (Table 2). The remaining derivatives without significant cytotoxicity were selected for following studies.

Table 2.1 Chemical structures of betulinic acid and its derivatives

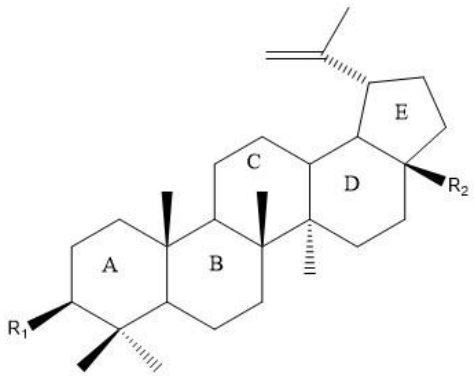

ID	R1	R2
H1 (Betulinic acid)	HO	COOH
H2 (Betulin)	HO	CH_2OH
H3	HO	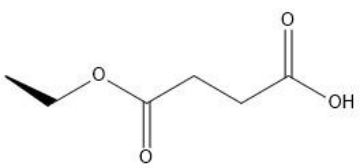

H4	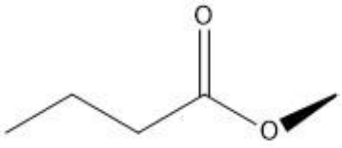	COOH
H5	O=	COOH
H6	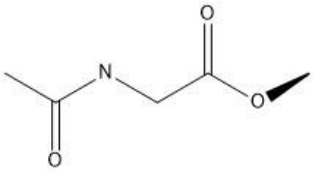	COOH
H7	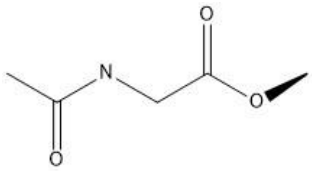	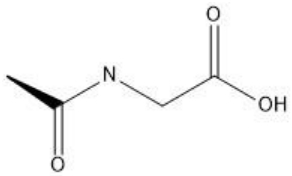
H8	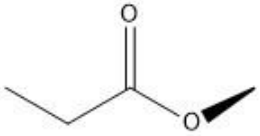	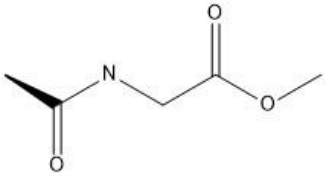
H9	HO	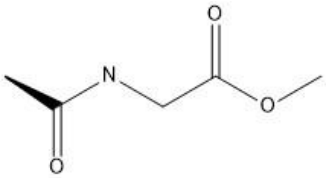
H10	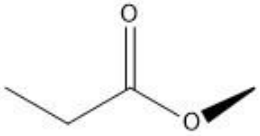	COOH
H11	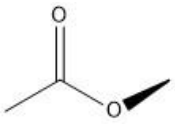	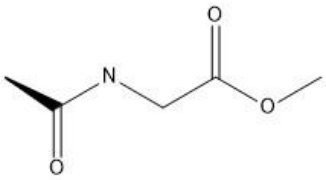
H12	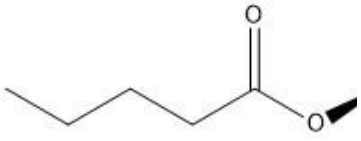	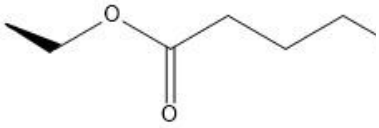

H13

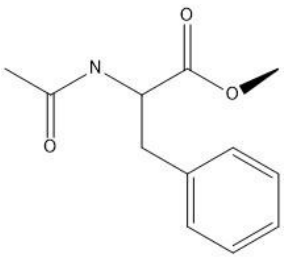

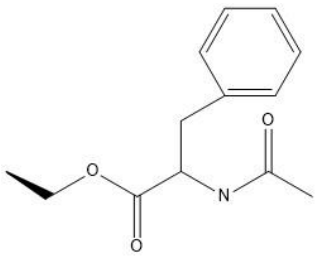

H14

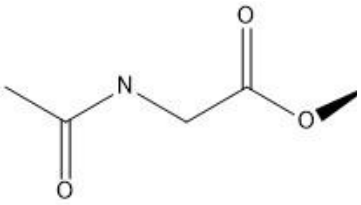

CH_2OH

H15

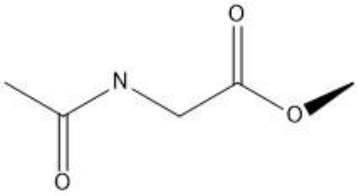

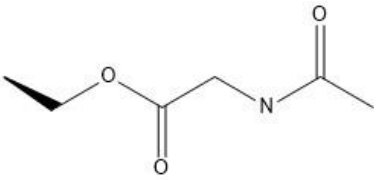

H16

HO

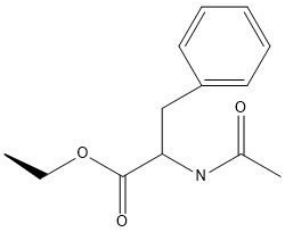

H17

HO

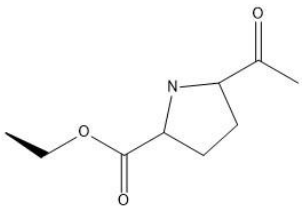

H18

HO

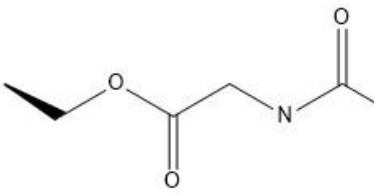

H19

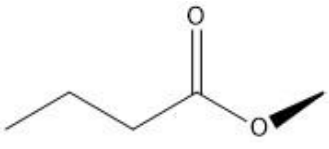

CH_2OH

H20

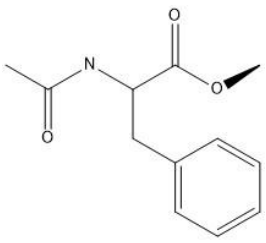

CH_2OH

Table 2.2 Cell toxicity of betulinic acid and its derivatives in ARPE-19 cells

Cells were pre-treated with 10 μM of betulinic acid or its derivatives for 24 h and cell viability was then assessed with MTT assay. Data was presented as the percentage of cell viability with compound treatment as to that of DMSO control treated cells.

Compound	Viability (%) (AVG±SD)
Control	100.0±6.3
H1***	82.7±5.2
H2***	66.8±7.1
H3	106.8±8.3
H4***	56.8±7.9
H5	98.9±5.8
H6***	54.7±8.8
H7	95.8±9.2
H8	100.3±2.9
H9***	59.6±3.3
H10	91.9±9.4
H11***	84.0±4.0
H12	97.5±3.3
H13	102.8±4.0
H14**	88.5±1.5
H15	100.2±12.9
H16	105.0±5.9
H17	96.7±7.7
H18	99.1±3.4
H19***	69.4±7.6
H20	107.8±7.8

**p<0.01 *vs* Control, ***p<0.001 vs Control, t-test

2.3.2 Protective effect of BA, BE and their derivatives on ARPE-19 cells with cobalt chloride-induced hypoxic stress

Cobalt chloride is an iron analogue often used for mimicking hypoxic conditions in the RPE cells (13, 45-47) and has been widely used in disease-relevant studies including

cancers and retinal diseases (48). We established an acute hypoxia *in vitro* model in this study to explore the protective effect of BA, BE and their derivatives. We treated the ARPE-19 cells with various concentrations of cobalt chloride for 4 h. We performed an initial screening to assess the cell viability with the treatment of cobalt chloride at the concentrations varying from 1 to 20 mM (data not shown). We found all concentrations caused certain levels of reduction in cell viability; the maximum effect was observed at 10 mM and above. 8 mM cobalt chloride decreased approximately 50% of cell viability and this concentration was used in the following experiments.

Next, we assessed the protective effect of BA, BE and their non-cytotoxic derivatives on ARPE-19 cells with cobalt chloride-induced hypoxia stress. Cells were pre-treated with BA, H3, H5, H7, H8, H10, H12, H13, H15, H16, H17, H18 or H20 compound (10 μM) for 24 h, followed by cobalt chloride for 4 h, then cell viabilities were assessed with MTT assay (Table 2.3). We found that H7 (3-O-acetyl-glycyl- 28-O-glycyl-betulinic acid) compound can significantly attenuate the cytotoxicity induced by cobalt chloride (Table 2.4). Therefore, this compound was chosen to be further studied.

Table 2.3 The protective effect of betulinic acid and its derivatives on hypoxia induced by cobalt chloride in the ARPE-19 cells

Cells were pre-treated with 10 μM of betulinic acid or its derivatives for 24h and then incubated with or without 8 mM cobalt chloride for additional 4 h. Then cell viability was assessed with MTT assay. Data was presented as the percentage of cell viability as to that of 0.1% DMSO control treated cells.

Treatment	Viability (%) (AVG±SD)
Control	100.0±6.9
Control+$CoCl_2$	51.7±6.9
H3	100.9±13.5
H3+ $CoCl_2$	56.8±4.9
H5	94.0±11.3
H5+ $CoCl_2$	56.3±2.9
H7	89.2±2.9
H7+ $CoCl_2$	61.6±5.1
H8	100.6±12.3
H8+ $CoCl_2$	58.1±4.9
H10	92.0±12.6

H10+ $CoCl_2$	49.4±4.2
H12	94.3±8.3
H12+ $CoCl_2$	47.0±6.1
H13	105.6±5.7
H13+ $CoCl_2$	50.5±7.7
H15	93.2±5.2
H15+ $CoCl_2$	52.3±6.1
H16	105.7±6.3
H16+ $CoCl_2$	57.5±7.7
H17	102.7±9.8
H17+ $CoCl_2$	56.1±9.8
H18	101.6±5.4
H18+ $CoCl_2$	57.1±6.8
H20	112.7±6.9
H20+ $CoCl_2$	56.1±3.8

Table 2.4 The protective effect of betulinic acid and its derivatives on hypoxia induced by cobalt chloride in the ARPE-19 cells (Control as 100%)

Re-analysis of the data from Table 2.3. Data as presented as the percentage of anti-hypoxia effect of compound treatment (the viability of betulinic derivatives pre-treated cells without cobalt chloride treatment vs. that with cobalt chloride treatment) as to that of DMSO control.

Treatment	**Anti-hypoxic effect (%) (AVG±SD)**
control	100.0±6.9
H3	111.9±4.9
H5	116.0±2.9
H7#	**133.8±4.9**
H8	111.8±4.9
H10	104.0±4.2
H12	96.6±6.1
H13	92.6±7.7
H15	108.7±6.1
H16	105.4±7.7
H17	105.7±3.2

H18	108.9±6.8
H20	96.4±3.8

#p<0.05, two way ANOVA

2.3.3 H7 suppresses $CoCl_2$-induced hypoxic stress in the ARPE-19 cells

ARPE-19 cells were pre-treated with different concentrations of H7 (0-15 μM) for 24 h followed by cobalt chloride exposure. The pretreatment of 10 μM or higher concentration of H7 exhibited significant anti-hypoxic effect compared to control (Fig 2.1A); therefore, 10 μM were selected as the optimal treatment condition in the following studies.

The treatment of cobalt chloride elevates ROS level which leads to oxidative damage in ARPE-19 cells (46). We found cobalt chloride markedly increased the cellular ROS level in the control group; whereas H7 significantly attenuated such oxidative stress (~5.49 folds increase in the DMSO control group *vs*. the ~2.66 folds increase in the H7 treated group, Fig 2.1B). This result indicated that H7 protects ARPE-19 cells by scavenging ROS.

Furthermore, we adopted annexin V-FITC/PI dual staining assay to evaluate the rescue effect of H7 compound. We found moderate apoptosis and necrosis with cobalt chloride treatment; while H7 pre-treatment significantly reduced cellular apoptosis (5.96%±2.41% *vs*. 13.06%±2.69% of control, Fig 2.1C) and necrosis (4.14±1.32% *vs.* 17.32±4.36% of control, Fig. 1D). This suggested that H7 exhibited protective effect through decreasing both cellular apoptosis and necrosis induced by cobalt chloride.

A

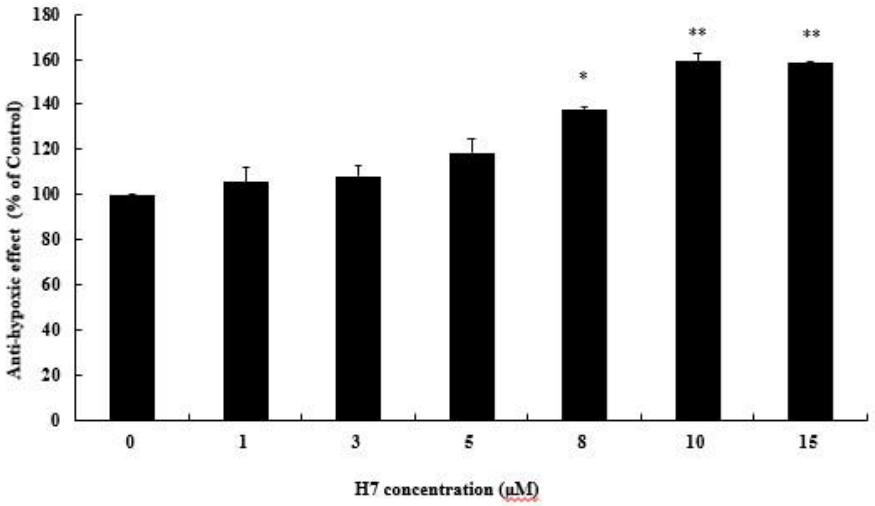
Anti-hypoxic effect (% of Control)
180
160
140
120
100
80
60
40
20
0
*
**
**
0
1
3
5
8
10
15
H7 concentration (μM)

B

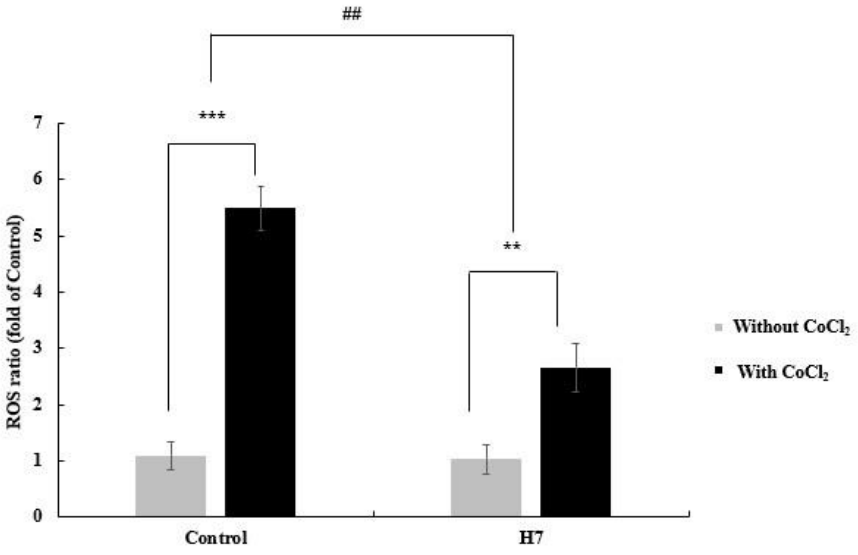
##
***
**
ROS ratio (fold of Control)
7
6
5
4
3
2
1
0
Control
H7
Without CoCl2
With CoCl2

C

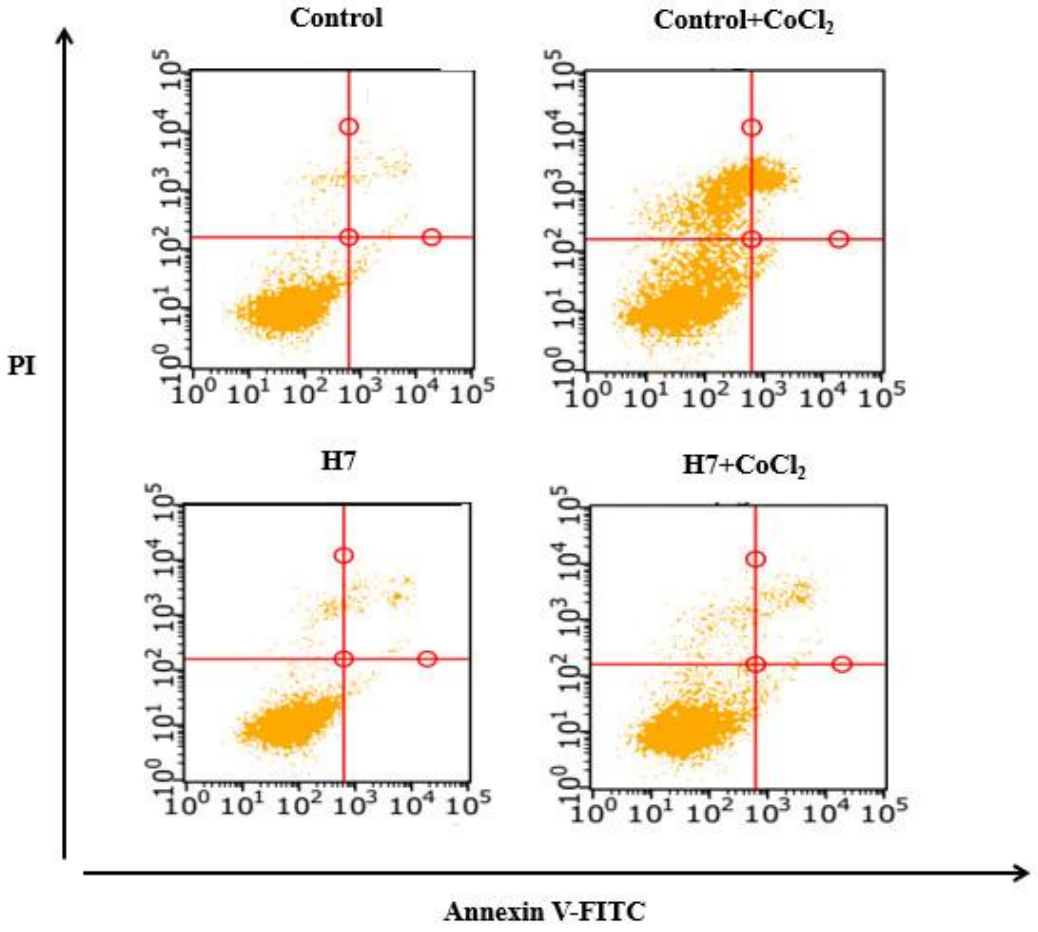
Control
Control+CoCl2
H7
H7+CoCl2
PI
Annexin V-FITC

D

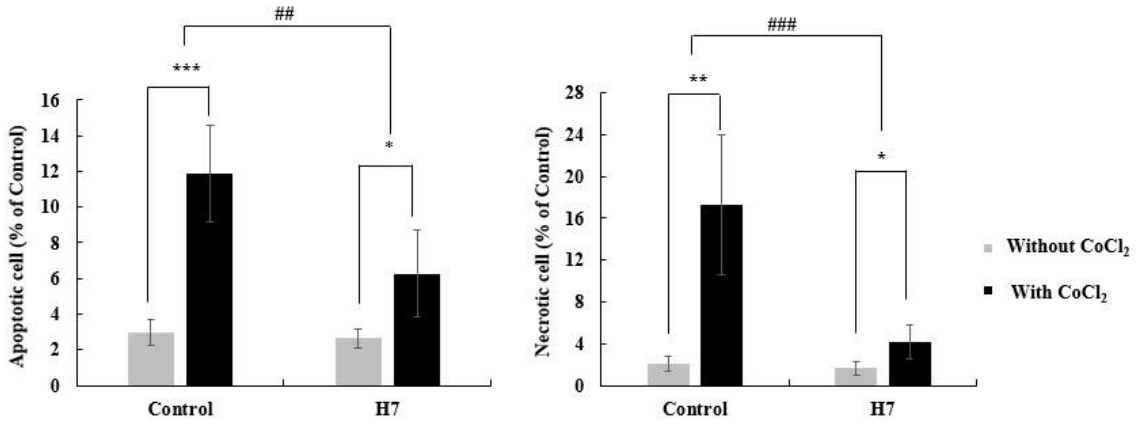
Apoptotic cell (% of Control)
Necrotic cell (% of Control)
Control
H7
Without CoCl2
With CoCl2

Figure 2.1 H7 protects ARPE-19 cells from cobalt chloride-induced cell death

(A) ARPE-19 cells were pre-treated with different concentrations of H7 (1-15 μM) for 24 h, followed by 8 mM $CoCl_2$ for 4 h. DMSO was used as vehicle control. Anti-hypoxic effect of H7 was analyzed by MTT method as described in Materials and Methods. Data were shown as percentage of control. (B) ARPE-19 cells were pre-treated with or without 10 μM H7 for 24 h, followed with or without 8 mM $CoCl_2$ for 4 h. DMSO was used as vehicle control. ROS level was assessed by CM-H_2DCFDA method as described in 2.2.4. Data were shown as folds of control. (C) ARPE-19 cells were pre-treated with or without 10 μM H7 for 24 h, followed with or without 8 mM $CoCl_2$ for 4 h. DMSO was used as vehicle control. Cell apoptosis and necrosis were analyzed by annexin/PI staining method as described in 2.2.5. Representative image was demonstrated in the figure. (D) Analysis of cell apoptosis and necrosis of Fig. 2.1C. Data was shown as percentage of control. Data were presented as mean ± STD, n=3. *p<0.05, **p<0.01, ***p<0.001, t-test; ##p<0.01, ###p<0.001, two-way ANOVA.

2.3.4 H7 attenuated the activation of Akt, Erk1/2 and JNK pathways induced by oxidative stress in RPE

Akt, Erk1/2 and JNK signaling are major pathways involved in RPE survival and oxidative stress (15, 18, 49-55); therefore, we investigated the involvement of these signaling pathways in cobalt chloride stressed RPE cells with or without H7 pretreatment. We found that Akt, Erk1/2 and JNK pathways were significantly activated in the ARPE-19 cells under cobalt chloride-induced stress (Fig. 2.2). The activations were markedly inhibited with H7 pre-treatment (Akt: 2.01 ± 0.25 fold of increase in the H7 group vs. 3.78 ± 0.54 fold of increase in the control group; Erk: 1.54 ± 0.26 fold of increase in the H7 group vs. 8.94 ± 2.65 fold of increase in the control group; JNK: 3.13 ± 0.56 fold of increase in the H7 group vs. 61.02 ± 10.32 fold of increase in the control group).

A

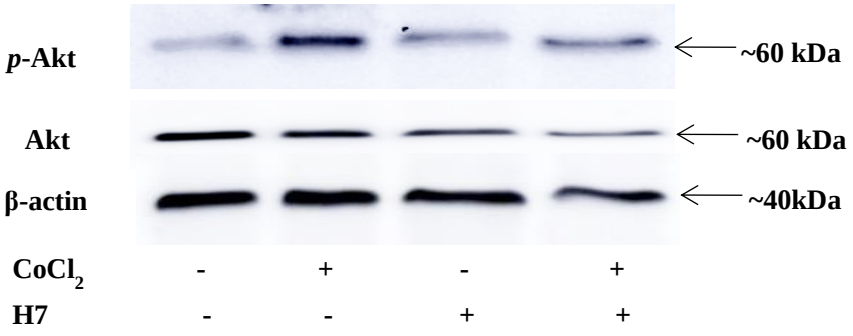
p-Akt
~60 kDa
Akt
~60 kDa
β-actin
~40kDa
CoCl2 - + - +
H7 - - + +

B

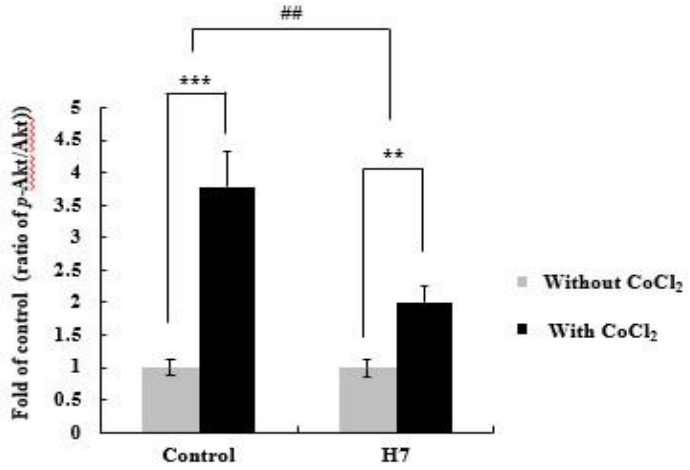
##
***
**
Fold of control (ratio of p-Akt/Akt))
5
4.5
4
3.5
3
2.5
2
1.5
1
0.5
0
Control
H7
Without CoCl2
With CoCl2

C

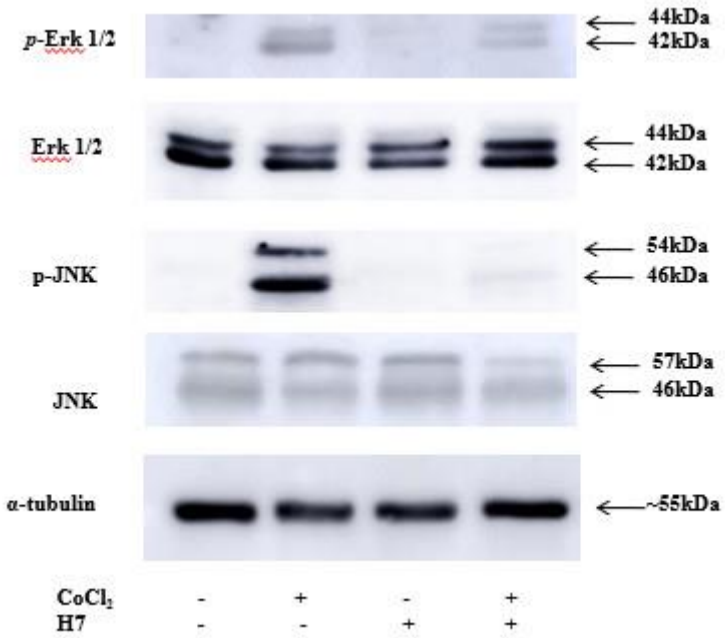
p-Erk 1/2
44kDa
42kDa
Erk 1/2
44kDa
42kDa
p-JNK
54kDa
46kDa
JNK
57kDa
46kDa
α-tubulin
~55kDa
CoCl2 - + - +
H7 - - + +

D

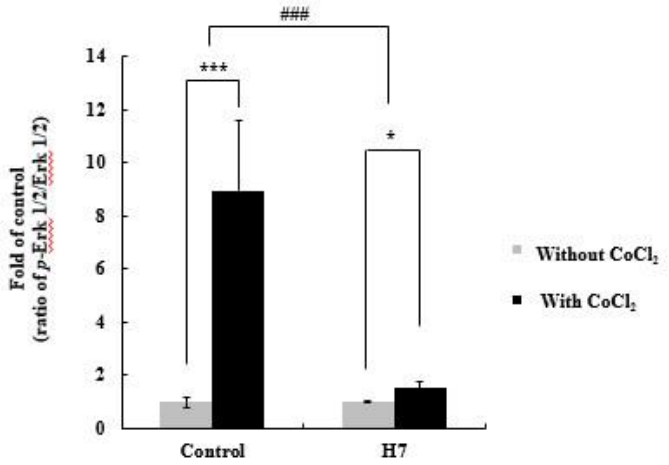
###
***
*
Fold of control
(ratio of p-Erk 1/2/Erk 1/2)
0
2
4
6
8
10
12
14
Control
H7
Without CoCl2
With CoCl2

E

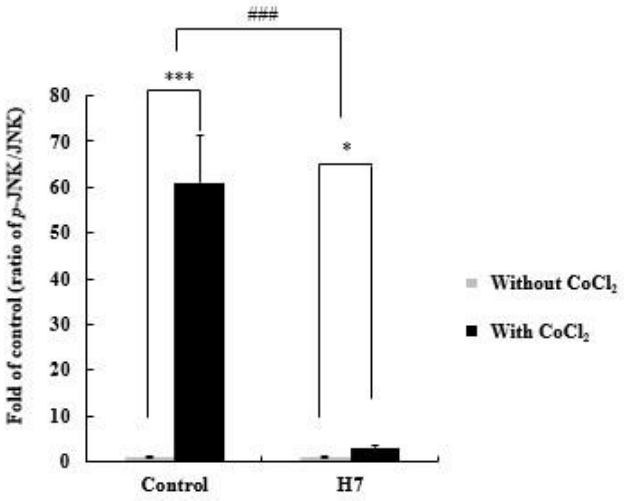

Figure 2.2 H7 inhibits cobalt chloride-induced Akt, Erk1/2 and JNK activation in the ARPE-19 cells

ARPE-19 cells were pre-treated with or without 10 μM H7 for 24 h, followed with or without 8 mM $CoCl_2$ for 4 h. DMSO was used as control. Phosphorylated- and total-Akt (A and B), -Erk1/2 and -JNK (C, D and E) were detected with western blot. β-actin and α-tubulin were included as loading controls. Representative image was demonstrated in (A) and (C). Results in (B), (D) and (E) were presented as mean ± STD, n=3. *p<0.05, **p<0.01, ***p<0.001, t-test; ##p<0.01, ###p<0.001, two-way ANOVA.

2.3.5 H7 suppresses $CoCl_2$-induced hypoxic stress in human primary RPE cells

We further verified our findings in the primary RPE cells cultured from three healthy donors without known retinal disorders. Initial testing indicated that 12 μM of cobalt chloride was optimal in inducing significant hypoxia in the primary RPE cells (~50% viability *vs*. control); therefore, this concentration was used in the experiments conducted on human primary RPE cells. Consistently, H7 showed a pronounced protective effect on cobalt chloride-induced hypoxia in the primary RPE cells at a concentration dependent manner (Fig. 2.3A). Our preliminary data showed that the treatment of 15 μM H7 demonstrated a better effect compared to that of 10 μM; therefore, this concentration was chosen as the preferred condition in the following experiments. It was also noted that at this concentration, there was no significant

cytotoxicity observed in the primary RPE cells (data not shown). H7 pre-treatment suppressed the cobalt chloride-induced activation of Erk and JNK in all primary RPE cells from three different donors (Fig. 2.3D). It inhibited the upregulation of Akt signaling in 2 out 3 primary RPE cell lines (Fig. 2.3B); while the Akt signaling in one of the primary RPE cell lines was not changed upon cobalt chloride treatment. The unresponsiveness of Akt signaling to cobalt chloride in this primary PRE cell line might be associated with the genetic variation of individuals. However, to explore the actual reason underpinning such unresponsiveness is beyond the scope of this study.

A

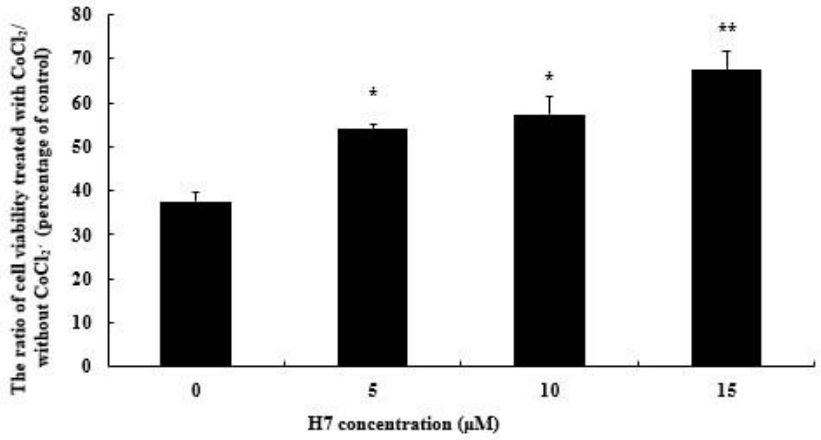

B

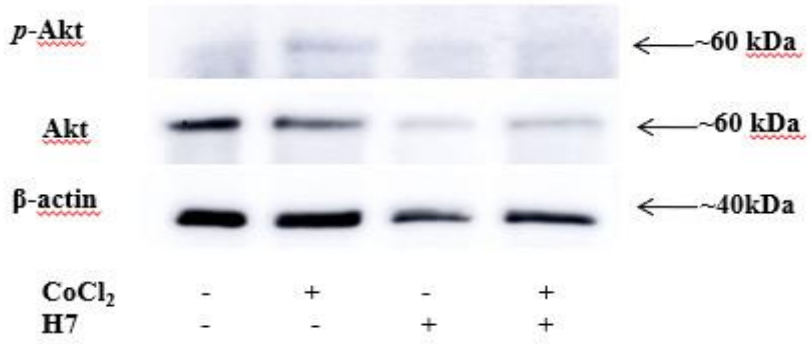

C

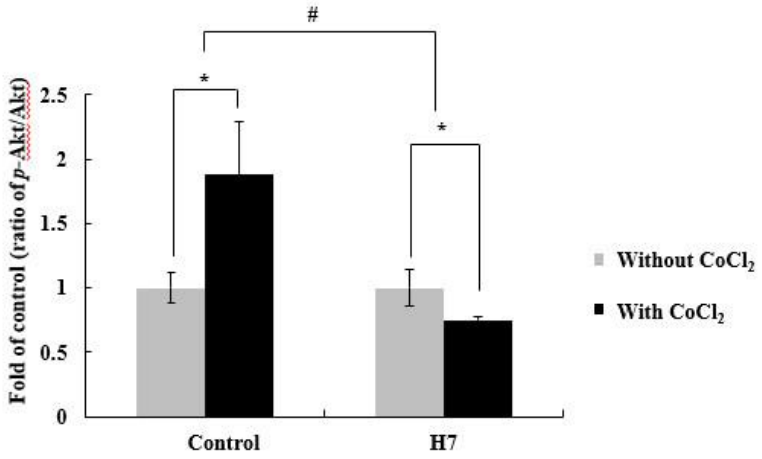
#
*
*
Fold of control (ratio of p-Akt/Akt)
2.5
2
1.5
1
0.5
0
Control
H7
Without CoCl2
With CoCl2

D

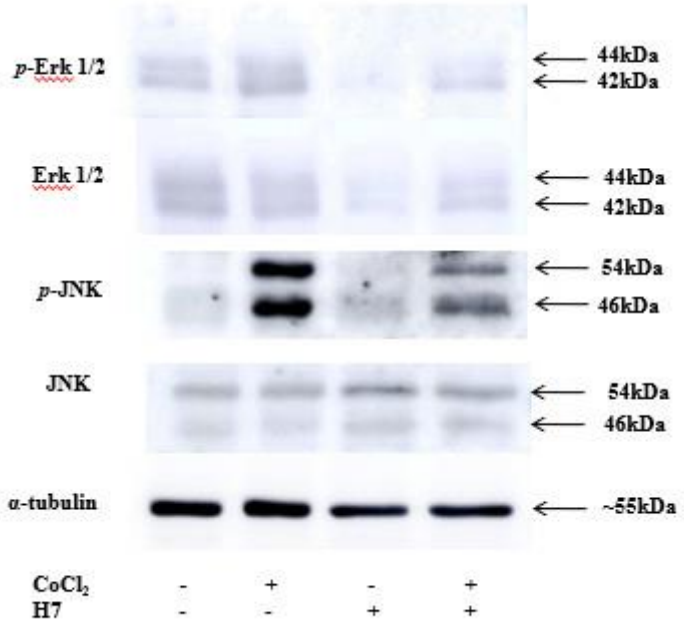
p-Erk 1/2
44kDa
42kDa
Erk 1/2
44kDa
42kDa
p-JNK
54kDa
46kDa
JNK
54kDa
46kDa
α-tubulin
~55kDa
CoCl2 - + - +
H7 - - + +

E

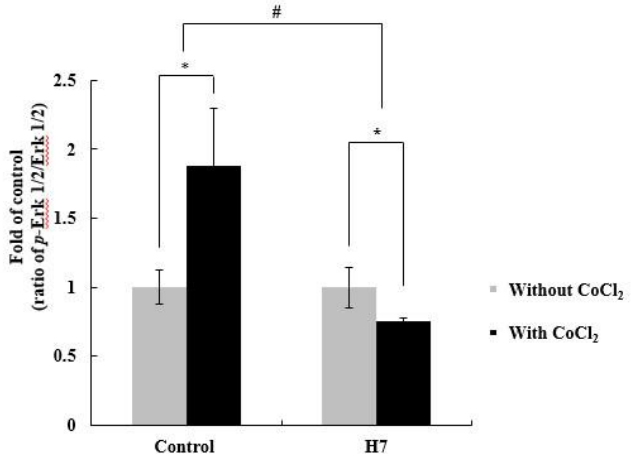

F

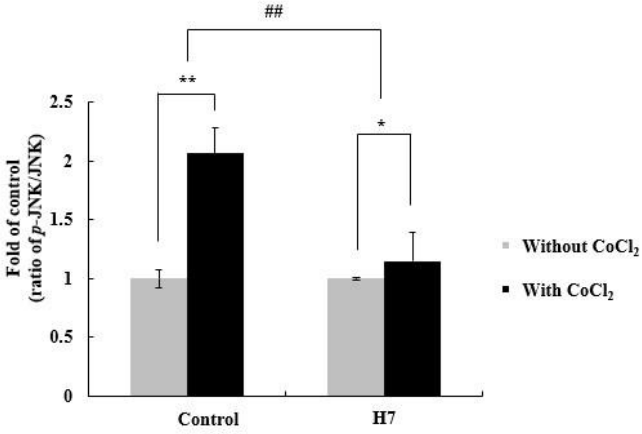

Figure 2.3 H7 suppressed hypoxic assaults and inhibits cobalt chloride-induced Akt, Erk1/2 and JNK activation in human primary RPE cells

(A) Human primary RPE cells were pre-treated with different concentrations of H7 (5-15 μM) for 24 h, followed by 12 mM $CoCl_2$ for 4 h. DMSO was used as control. Anti-hypoxic effect of H7 was analyzed by MTT method as described in 2.2.3. Data was shown as percentage of control. (B-E) Human primary RPE cells were pre-treated with or without 10 μM H7 for 24 h, followed with or without 8 mM $CoCl_2$ for 4 h. DMSO was used as control. Phosphorylated- and total-Akt (B and C), -ERK and -JNK (D, E and F) were detected with western blot. β-actin and α-tubulin were included as loading controls. Representative image was demonstrated in the figure. Data in (A), (C), (E) and (F) were represented as mean ± STD, n=3. *$p<0.05$, **$p<0.01$, t-test; #$p<0.05$, ##$p<0.01$, two-way ANOVA.

2.4 Discussion

RPE cells are essential to human retina and vision (2-9). Oxidative stress to RPE cells greatly potentiates human retinal degenerative diseases (4, 7, 9, 14, 15, 17). Apoptosis of RPE cells was widely observed upon oxidation induced by cobalt chloride, H_2O_2, UVB etc. (18, 56-63); previous studies also demonstrated cellular necrosis due to oxidative stress (49, 64). Most early-year research concluded that apoptosis is a major mechanism for RPE cell death in response to oxidative stress in AMD, but more and more recent studies indicated that necrosis is the primary consequence of RPE cell death in AMD (65). Among the oxidative stimuli, cobalt chloride is a chemical hypoxia mimetic agent that has been widely used to induce hypoxic assault in the RPE cells (46, 59, 62, 66-68). Furthermore, literature suggested that the oxidation-induced apoptosis and/or necrosis of RPE cells could be involved with multiple signaling pathways (13, 47, 69, 70).

The anti-oxidative effect of BA and BE was widely reported in *in vitro* and *in vivo* studies (21-23, 71-74). In this study, we were the first to investigate the anti-hypoxic effect of BA, BE and their derivatives (H3-H20) on human RPE cells. As there is no previous *in vivo* pharmacokinetic report on derivatives in this Chapter, we used 10 μM for drug screening, which is close to *in vivo* condition of BA (41-44). However, there may exist some limitations in this concentration selection: firstly, different animals, disease models, administration methods and dosages will contribute to different PK profile; secondly, the derivatives may have different plasma concentrations to its parental compound due to different structures and bioavailability. Considering the large number of candidates, this concentration could better mimic the practical drug effect *in vivo* and is suitable for drug screening.

Consistent with previous reports (55, 75), we observed both apoptosis and necrosis upon the acute treatment of cobalt chloride in human ARPE-19 cells (Fig. 1C and 1D). Then we found that compound H7 possesses the relatively best protective effect among all these compounds (Table 2.4), which significantly decreased the induced apoptosis and necrosis of RPE cells (Fig. 1C and 1D).

The derivatives H6, H7, H14 and H15 are structurally similar (Table 2.1). They differ at the C28 position, but the moieties at their C3 position remain the same. We noticed that H6 with a carboxylic acid group was associated with a pronounced cytotoxicity followed by H14 with a hydroxyl group residue at C28 position; while H7 and H15 with residues less hydrophilic at this position have little toxicity to RPE cells (Table 2.2). Aldehyde group of H15 has higher oxidative potential than the carboxylic acid group of H7 at C28 position, so it is plausible that H7 has better anti-oxidative effect

than H15.

Cobalt chloride induced ROS production in the RPE cells (46, 66). In the current study, we observed a significant elevation of ROS level in the ARPE-19 cells with the treatment of cobalt chloride; while pretreatment with H7 greatly attenuated the cellular ROS production (Fig. 2.1B). Moreover, our data indicated that the cyto-protective effect of H7 was accompanied with markedly counteracting the hypoxia-induced Akt, Erk and JNK activation (Fig. 2.2). Such findings were further verified using human primary RPE cells (Fig. 3). It is interesting that although Hypoxia-inducible Factor 1α (HIF-1α) and Vascular Endothelial Growth Factor (VEGF) were shown to be the major protein factors involved with the anti-hypoxic effect of several agents in the previous reports (76-78), there was no significant influence of H7 treatment on the expressions of these two factors observed in our study (data not shown).

Arising evidence suggested that mitogen-activated protein kinase (MAPK) pathway is involved in cell proliferation (15, 79-81). MAPK superfamily includes three major signaling pathways: extracellular signal-regulated kinases (Erk), p38 and c-jun N-termnal kinases (JNK). Erk can generally be stimulated by growth factors, while p38 and JNK are more likely to be activated by cellular stress including inflammation, UV irradiation, oxidative stress, hypoxia and ischemia (18, 81). ROS elevation stimulates Erk, JNK and Akt pathways in various cell types (82); therefore, it is not surprising to find the activation of these three signaling pathways accompanied with an increased ROS level upon cobalt chloride-induced acute hypoxic stress in RPE cells in this study.

Erk is closely involved with the oxidative damage in human RPE cells (18, 80, 83). Glotin *et al.* (18) reported that a transient but not prolonged Erk activation was involved in the acute oxidative spike of t-BHP; neither JNK nor p38 were involved in this process. Koinzer *et al.* (84) also demonstrated a biphasic role of Erk in the RPE cells upon tBH treatment, where Erk phosphorylation is time-dependent (it was observed 30 min after the tBH treatment but decreased after 1 h, and then phosphor-Erk level increased again after 4h). *Tsao et al.* (83) also revealed the protective role of Erk to H_2O_2-induced oxidative stress in the RPE. Therefore, it is plausible that H7 attenuated the activation of Erk protected the RPE cells from hypoxic stress in our study.

The role of JNK pathway in cell death remains controversial. Generally speaking, whether JNK is pro-apoptotic or apoptotic, largely depends on cell type, stimulus, other signaling pathways and the duration of activation (51, 85). The previous study showed that JNK was activated in cobalt chloride-treated ARPE-19 cells, which effect could be suppressed in the presence of the anti-oxidative compound Ginsenoside Rg-1 (58). In addition, the activation of JNK signaling was also observed in ARPE-19 cell death under other oxidation stimuli like 4-HNE and H_2O_2 (86-88) and also under UV-C

irradiation (80). And it has been demonstrated that mRNA and protein level of JNK was upregulated in ARPE-19 cells exposed to A2E (a prominent cytotoxic side product of retinoids) and/or blue light; however, JNK inhibition resulted in a further increase of cell death (89). These evidences suggested an apoptotic role of JNK in RPE cells. In contrast, *Cao et al.* demonstrated a pro-apoptotic role of JNK in ARPE-19 cells that JNK inhibition was observed with cellular apoptosis under UV-B exposure, while EGCG attenuated such oxidative damage partially via blocking the decreased phosphorylation of JNK (57). Our study is consistent with some of the previous observations (58, 80, 86-89) that JNK signaling was activated due to the acute treatment of cobalt chloride and H7 is potent in suppressing such effect (Fig. 2.3C and 2.3D).

Akt activation is widely observed in the RPE and other cell types after exposure to oxidative stress (55, 60, 90, 91). It has been shown to mediate the cyto-protective effect of various compounds in the RPE (63, 90, 92) as well as the programmed necrosis in neurons (52). And our study suggested that the anti-hypoxic and cyto-protective effect of H7 is partially mediated through deactivating Akt pathway.

There is also evidence obtained from animal and patient studies verifying that Akt and MAPK pathways are closely associated with dry AMD. Akt activation was found in the AMD mice model (93). Erk activation was observed both in mice model and dry AMD patients (94). And biphasic Erk activation after oxidative assaults was reported in primary mouse RPE cells (95). *Makarev et al.* used "AMD Medicine" software to analyze signaling pathways and discovered significant activation of Akt and MAPK (Erk, p38, JNK) involved in dry AMD (96).

A meta-analysis of more than 1,000 people showed a strong enrichment of JNK in AMD patients (97). And the activation of Akt and MAPK pathways is a hallmark of RPE damage and dry AMD progression, which indicates Akt and MAPK pathways may be the potential targets in the treatment of AMD. We found H7 can attenuate the activation of these pathways induced by oxidative stress, which suggested that H7 is a promising candidate agent to protect RPE cells from hypoxic stress and prevent the progress of retinal degenerations.

2.5 Conclusion

We found that the betulinic acid derivative H7 (3-O-acetyl-glycyl- 28-O-glycyl-betulinic acid) is safe and effective in protecting RPE cells from cobalt chloride-induced hypoxia stress. H7 pretreatment can significantly improve cell viability through decreasing cellular ROS level as well as inhibiting apoptosis and necrosis under hypoxic stress. We also found activation of Akt, Erk1/2 and JNK signaling induced by

hypoxia stress in RPE can be attenuated by H7 pretreatment. Therefore, H7 may be a candidate agent to be used in the prevention of untreatable dry AMD and other hypoxia-related retinal diseases.

Acknowledgements

We want to thank Professor Paul Groundwater for his help in chemical description. This work was supported by internal grants of the School of Pharmacy, the University of Sydney. Dr. Fanfan Zhou is the Equity Fellowship holder of the University of Sydney.

References

1. Travis GH, Golczak M, Moise AR, Palczewski K. Diseases caused by defects in the visual cycle: retinoids as potential therapeutic agents. ANNU REV PHARMACOL TOXICOL. 2007;47:469-512.

2. Simo R, Villarroel M, Corraliza L, Hernandez C, Garcia-Ramirez M. The retinal pigment epithelium: something more than a constituent of the blood-retinal barrier--implications for the pathogenesis of diabetic retinopathy. J BIOMED BIOTECHNOL. 2010;2010:190724.

3. Nagineni CN, Raju R, Nagineni KK, Kommineni VK, Cherukuri A, Kutty RK, et al. Resveratrol Suppresses Expression of VEGF by Human Retinal Pigment Epithelial Cells: Potential Nutraceutical for Age-related Macular Degeneration. AGING DIS. 2014;5(2):88-100.

4. Plafker SM, O'Mealey GB, Szweda LI. Mechanisms for countering oxidative stress and damage in retinal pigment epithelium. INT REV CELL MOL BIOL. 298: Elsevier; 2012. p. 135-77.

5. Ao J, Wood JP, Chidlow G, Gillies MC, Casson RJ. Retinal pigment epithelium in the pathogenesis of age-related macular degeneration and photobiomodulation as a potential therapy? CLIN EXP OPHTHALMOL. 2018;46(6):670-86.

6. Cai J, Nelson KC, Wu M, Sternberg Jr P, Jones DP. Oxidative damage and protection of the RPE. PROG RETIN EYE RES. 2000;19(2):205-21.

7. Fanjul-Moles ML, López-Riquelme GO. Relationship between oxidative stress, circadian rhythms, and AMD. OXID MED CELL LONGEV. 2016;2016.

8. Khandhadia S, Lotery A. Oxidation and age-related macular degeneration: insights from molecular biology. EXPERT REV MOL MED. 2010;12.

9. Grimm C, Willmann G. Hypoxia in the eye: a two-sided coin. HIGH ALT MED BIOL. 2012;13(3):169-75.

10. Jonas JB. Global prevalence of age-related macular degeneration. LANCET GLOB HEALTH. 2014;2(2):e65-6.

11. Wong WL, Su X, Li X, Cheung CM, Klein R, Cheng CY, et al. Global prevalence of age-related macular degeneration and disease burden projection for 2020 and 2040: a systematic review and meta-analysis. LANCET GLOB HEALTH. 2014;2(2):e106-16.

12. Bowes Rickman C, Farsiu S, Toth CA, Klingeborn M. Dry age-related macular degeneration: mechanisms, therapeutic targets, and imaging. INVEST OPHTHALMOL VIS SCI. 2013;54(14):ORSF68-80.

13. Park H, Lee DS, Yim MJ, Choi YH, Park S, Seo SK, et al. 3,3'-Diindolylmethane inhibits VEGF expression through the HIF-1alpha and NF-kappaB pathways in human retinal pigment epithelial cells under chemical hypoxic conditions. INT J MOL MED. 2015;36(1):301-8.

14. Masuda T, Shimazawa M, Hara H. Retinal diseases associated with oxidative stress and the

effects of a free radical scavenger (edaravone). OXID MED CELL LONGEV. 2017;2017.

15. Ung L, Pattamatta U, Carnt N, Wilkinson-Berka JL, Liew G, White AJ. Oxidative stress and reactive oxygen species: a review of their role in ocular disease. CLIN SCI (LOND). 2017;131(24):2865-83.

16. Golden TR, Hinerfeld DA, Melov S. Oxidative stress and aging: beyond correlation. AGING CELL. 2002;1(2):117-23.

17. Kurihara T, Westenskow PD, Gantner ML, Usui Y, Schultz A, Bravo S, et al. Hypoxia-induced metabolic stress in retinal pigment epithelial cells is sufficient to induce photoreceptor degeneration. ELIFE. 2016;5:e14319.

18. Glotin A-L, Calipel A, Brossas J-Y, Faussat A-M, Tréton J, Mascarelli F. Sustained versus transient ERK1/2 signaling underlies the anti-and proapoptotic effects of oxidative stress in human RPE cells. INVEST OPHTHALMOL VIS SCI. 2006;47(10):4614-23.

19. Muceniece R, Namniece J, Nakurte I, Jekabsons K, Riekstina U, Jansone B. Pharmacological research on natural substances in Latvia: Focus on lunasin, betulin, polyprenol and phlorizin. PHARMACOL RES. 2016;113(Pt B):760-70.

20. Rastogi S, Pandey MM, Kumar Singh Rawat A. Medicinal plants of the genus Betula--traditional uses and a phytochemical-pharmacological review. J ETHNOPHARMACOL. 2015;159:62-83.

21. Peng J, Lv Y-C, He P-P, Tang Y-Y, Xie W, Liu X-Y, et al. Betulinic acid downregulates expression of oxidative stress-induced lipoprotein lipase via the PKC/ERK/c-Fos pathway in RAW264. 7 macrophages. BIOCHIMIE. 2015;119:192-203.

22. Szuster-Ciesielska A, Kandefer-Szerszeñ M. Protective effects of betulin and betulinic acid against ethanol-induced cytotoxicity in HepG2 cells. PHARMACOL REP. 2005;57(5):588.

23. Zhu L, Yi X, Zhao J, Yuan Z, Wen L, Pozniak B, et al. Betulinic acid attenuates dexamethasone-induced oxidative damage through the JNK-P38 MAPK signaling pathway in mice. BIOMED PHARMACOTHER. 2018;103:499-508.

24. Cavazos-Garduno A, Ochoa Flores AA, Serrano-Nino JC, Martinez-Sanchez CE, Beristain CI, Garcia HS. Preparation of betulinic acid nanoemulsions stabilized by omega-3 enriched phosphatidylcholine. ULTRASON SONOCHEM. 2015;24:204-13.

25. Mullauer FB, Kessler JH, Medema JP. Betulinic acid, a natural compound with potent anticancer effects. ANTICANCER DRUGS. 2010;21(3):215-27.

26. Ding W, Sun M, Luo S, Xu T, Cao Y, Yan X, et al. A 3D QSAR study of betulinic acid derivatives as anti-tumor agents using topomer CoMFA: model building studies and experimental verification. MOLECULES. 2013;18(9):10228-41.

27. Ding W, Zhang S, Zhu M, Wang S, Xu T, Qu H, et al. A 3D-QSAR Study on Betulinic Acid Derivatives as Anti-Tumor Agents and the Synthesis of Novel Derivatives for Modeling Validation. ANTICANCER AGENTS MED CHEM. 2017;17(4):566-75.

28. Chan T, Zhu L, Madigan MC, Wang K, Shen W, Gillies MC, et al. Human organic anion transporting polypeptide 1A2 (OATP1A2) mediates cellular uptake of all-trans-retinol in human retinal pigmented epithelial cells. BR J PHARMACOL. 2015;172(9):2343-53.
29. Wang K, Zhu X, Yao Y, Yang M, Zhou F, Zhu L. Corosolic acid induces cell cycle arrest and cell apoptosis in human retinoblastoma Y-79 cells via disruption of MELK-FoxM1 signaling. ONCOL REP. 2018;39(6):2777-86.
30. Wang K, Zhu X, Zhang K, Zhou F, Zhu L. Neuroprotective effect of tetramethylpyrazine against all-trans-retinal toxicity in the differentiated Y-79 cells via upregulation of IRBP expression. EXP CELL RES. 2017;359(1):120-8.
31. Zhu X, Wang K, Zhang K, Zhou F, Zhu L. Induction of oxidative and nitrosative stresses in human retinal pigment epithelial cells by all-trans-retinal. EXP CELL RES. 2016;348(1):87-94.
32. Zhu X, Wang K, Zhang K, Tan X, Wu Z, Sun S, et al. Tetramethylpyrazine Protects Retinal Capillary Endothelial Cells (TR-iBRB2) against IL-1beta-Induced Nitrative/Oxidative Stress. INT J MOL SCI. 2015;16(9):21775-90.
33. Liu Y, Gao D, Zhang X, Liu Z, Dai K, Ji B, et al. Antitumor drug effect of betulinic acid mediated by polyethylene glycol modified liposomes. MATER SCI ENG C MATER BIOL APPL. 2016;64:124-32.
34. Wang K, Zhu X, Zhang K, Zhou F, Zhu L. Gas1 Knockdown Increases the Neuroprotective Effect of Glial Cell-Derived Neurotrophic Factor Against Glutamate-Induced Cell Injury in Human SH-SY5Y Neuroblastoma Cells. CELL MOL NEUROBIOL. 2016;36(4):603-11.
35. Zhu X, Wang K, Zhang K, Lin X, Zhu L, Zhou F. Puerarin Protects Human Neuroblastoma SH-SY5Y Cells against Glutamate-Induced Oxidative Stress and Mitochondrial Dysfunction. J BIOCHEM MOL TOXICOL. 2016;30(1):22-8.
36. Zhu X, Wang K, Zhang K, Zhu L, Zhou F. Ziyuglycoside II induces cell cycle arrest and apoptosis through activation of ROS/JNK pathway in human breast cancer cells. TOXICOL LETT. 2014;227(1):65-73.
37. Wang K, Zhu X, Zhang K, Wu Z, Sun S, Zhou F, et al. Neuroprotective Effect of Puerarin on Glutamate-Induced Cytotoxicity in Differentiated Y-79 Cells via Inhibition of ROS Generation and Ca(2+) Influx. INT J MOL SCI. 2016;17(7).
38. Zhu X, Xie M, Wang K, Zhang K, Gao Y, Zhu L, et al. The effect of puerarin against IL-1beta-mediated leukostasis and apoptosis in retinal capillary endothelial cells (TR-iBRB2). MOL VIS. 2014;20:1815-23.
39. Zhu X, Wang K, Zhang K, Pan Y, Zhou F, Zhu L. Polyphyllin I Induces Cell Cycle Arrest and Cell Apoptosis in Human Retinoblastoma Y-79 Cells through Targeting p53. ANTICANCER AGENTS MED CHEM. 2018.
40. Zhu X, Wang K, Yao Y, Zhang K, Zhou F, Zhu L. Triggering p53 activation is essential in ziyuglycoside I-induced human retinoblastoma WERI-Rb-1 cell apoptosis. J BIOCHEM MOL

TOXICOL. 2018;32(1).

41. Godugu C, Patel AR, Doddapaneni R, Somagoni J, Singh M. Approaches to improve the oral bioavailability and effects of novel anticancer drugs berberine and betulinic acid. PLOS ONE. 2014;9(3):e89919.

42. Kumar P, Singh AK, Raj V, Rai A, Keshari AK, Kumar D, et al. Poly (lactic-co-glycolic acid)-loaded nanoparticles of betulinic acid for improved treatment of hepatic cancer: characterization, in vitro and in vivo evaluations. INT J NANOMEDICINE. 2018;13:975.

43. Li Y, Guo S, Hua T, Wang Y, Wei D, Zhao M, et al. Comparative pharmacokinetics of triterpenic acids in normal and immunosuppressed rats after oral administration of Jujubae Fructus extract by UPLC-MS/MS. J CHROMATOGR B ANALYT TECHNOL BIOMED LIFE SCI. 2018;1077-1078:13-21.

44. Udeani GO, Zhao GM, Geun Shin Y, Cooke BP, Graham J, Beecher CW, et al. Pharmacokinetics and tissue distribution of betulinic acid in CD-1 mice 1. BIOPHARM DRUG DISPOS. 1999;20(8):379-83.

45. Lai YH, Hu DN, Rosen R, Sassoon J, Chuang LY, Wu KY, et al. Hypoxia-induced vascular endothelial growth factor secretion by retinal pigment epithelial cells is inhibited by melatonin via decreased accumulation of hypoxia-inducible factors-1alpha protein. CLIN EXP OPHTHALMOL. 2017;45(2):182-91.

46. Li KR, Zhang ZQ, Yao J, Zhao YX, Duan J, Cao C, et al. Ginsenoside Rg-1 protects retinal pigment epithelium (RPE) cells from cobalt chloride (CoCl2) and hypoxia assaults. PLOS ONE. 2013;8(12):e84171.

47. Wang S, Du S, Wu Q, Hu J, Li T. Decorin Prevents Retinal Pigment Epithelial Barrier Breakdown Under Diabetic Conditions by Suppressing p38 MAPK Activation. INVEST OPHTHALMOL VIS SCI. 2015;56(5):2971-9.

48. Masoud GN, Li W. HIF-1alpha pathway: role, regulation and intervention for cancer therapy. ACTA PHARM SIN B. 2015;5(5):378-89.

49. Hanus J, Anderson C, Wang S. RPE necroptosis in response to oxidative stress and in AMD. AGEING RES REV. 2015;24:286-98.

50. Hecquet C, Lefevre G, Valtink M, Engelmann K, Mascarelli F. Activation and role of MAP kinase-dependent pathways in retinal pigment epithelium cells: JNK1, P38 kinase, and cell death. INVEST OPHTHALMOL VIS SCI. 2003;44(3):1320-9.

51. Klettner A. Oxidative stress induced cellular signaling in RPE cells. FRONT BIOSCI (SCHOL ED). 2012;4(2):392-411.

52. Liu Q, Qiu J, Liang M, Golinski J, Van Leyen K, Jung J, et al. Akt and mTOR mediate programmed necrosis in neurons. CELL DEATH DIS. 2014;5(2):e1084.

53. Mochizuki T, Asai A, Saito N, Tanaka S, Katagiri H, Asano T, et al. Akt protein kinase inhibits non-apoptotic programmed cell death induced by ceramide. J BIOL CHEM. 2002;277(4):2790-7.

54. Nebreda AR, Porras A. p38 MAP kinases: beyond the stress response. TRENDS BIOCHEM SCI. 2000;25(6):257-60.

55. Yang P, Peairs JJ, Tano R, Jaffe GJ. Oxidant-mediated Akt activation in human RPE cells. INVEST OPHTHALMOL VIS SCI.2006;47(10):4598-606.

56. Cai J, Wu M, Nelson KC, Sternberg P, Jones DP. Oxidant-induced apoptosis in cultured human retinal pigment epithelial cells. INVEST OPHTHALMOL VIS SCI. 1999;40(5):959-66.

57. Cao G, Chen M, Song Q, Liu Y, Xie L, Han Y, et al. EGCG protects against UVB-induced apoptosis via oxidative stress and the JNK1/c-Jun pathway in ARPE19 cells. MOL MED REP. 2012;5(1):54-9.

58. Zhao H, Zhou M, Duan L, Wang W, Zhang J, Wang D, et al. Efficient synthesis and anti-fungal activity of oleanolic acid oxime esters. MOLECULES. 2013;18(3):3615-29.

59. Liu Z, Chen J, Huang W, Zeng Z, Yang Y, Zhu B. Ginsenoside Rb1 protects rat retinal ganglion cells against hypoxia and oxidative stress. MOL MED REP. 2013;8(5):1397-403.

60. Yan T, Bi H, Wang Y. Wogonin modulates hydroperoxide-induced apoptosis via PI3K/Akt pathway in retinal pigment epithelium cells. DIAGN PATHOL. 2014;9(1):154.

61. Shao L, Zhou Z, Cai Y, Castro P, Dakhov O, Shi P, et al. Celastrol suppresses tumor cell growth through targeting an AR-ERG-NF-κB pathway in TMPRSS2/ERG fusion gene expressing prostate cancer. PLOS ONE. 2013;8(3):e58391.

62. Cervellati F, Cervellati C, Romani A, Cremonini E, Sticozzi C, Belmonte G, et al. Hypoxia induces cell damage via oxidative stress in retinal epithelial cells. FREE RADIC RES. 2014;48(3):303-12.

63. Baek S-M, Yu S-Y, Son Y, Hong HS. Substance P promotes the recovery of oxidative stress-damaged retinal pigmented epithelial cells by modulating Akt/GSK-3β signaling. MOL VIS. 2016;22:1015.

64. Hanus J, Kolkin A, Chimienti J, Botsay S, Wang S. 4-Acetoxyphenol Prevents RPE Oxidative Stress–Induced Necrosis by Functioning as an NRF2 Stabilizer. INVEST OPHTHALMOL VIS SCI. 2015;56(9):5048-59.

65. Hanus J, Anderson C, Wang S. RPE necroptosis in response to oxidative stress and in AMD. AGEING RES REV. 2015;24(Pt B):286-98.

66. King RE, Kent KD, Bomser JA. Resveratrol reduces oxidation and proliferation of human retinal pigment epithelial cells via extracellular signal-regulated kinase inhibition. CHEM BIOL INTERACT. 2005;151(2):143-9.

67. Park H, Lee D-S, Yim M-J, Choi YH, Park S, Seo S-K, et al. 3, 3'-Diindolylmethane inhibits VEGF expression through the HIF-1α and NF-κB pathways in human retinal pigment epithelial cells under chemical hypoxic conditions. INT J MOL MED. 2015;36(1):301-8.

68. Rosen R, Vagaggini T, Chen Y, Hu D-N. Zeaxanthin inhibits hypoxia-induced VEGF secretion by RPE cells through decreased protein levels of hypoxia-inducible factors-1α. BIOMED RES INT.

2015;2015.

69. Li G-Y, Fan B, Zheng Y-C. Calcium overload is a critical step in programmed necrosis of ARPE-19 cells induced by high-concentration H_2O_2. BIOMED ENVIRON SCI. 2010;23(5):371.

70. Yang P, Peairs JJ, Tano R, Jaffe GJ. Oxidant-mediated Akt activation in human RPE cells. INVEST OPHTHALMOL VIS SCI. 2006;47(10):4598-606.

71. Lu Q, Xia N, Xu H, Guo L, Wenzel P, Daiber A, et al. Betulinic acid protects against cerebral ischemia–reperfusion injury in mice by reducing oxidative and nitrosative stress. NITRIC OXIDE. 2011;24(3):132-8.

72. Steinkamp-Fenske K, Bollinger L, Xu H, Yao Y, Horke S, Förstermann U, et al. Reciprocal regulation of endothelial nitric-oxide synthase and NADPH oxidase by betulinic acid in human endothelial cells. J PHARMACOL EXP THER. 2007;322(2):836-42.

73. Yi J, Zhu R, Wu J, Wu J, Tan Z. Ameliorative effect of betulinic acid on oxidative damage and apoptosis in the splenocytes of dexamethasone treated mice. INT IMMUNOPHARMACOL. 2015;27(1):85-94.

74. Yi J, Zhu R, Wu J, Wu J, Xia W, Zhu L, et al. In vivo protective effect of betulinic acid on dexamethasone induced thymocyte apoptosis by reducing oxidative stress. PHARMACOL REP. 2016;68(1):95-100.

75. Zha X, Wu G, Zhao X, Zhou L, Zhang H, Li J, et al. PRDX6 protects ARPE-19 cells from oxidative damage via PI3K/AKT signaling. CELL PHYSIOL BIOCHEM. 2015;36(6):2217-28.

76. Alzhrani RM, Alhadidi Q, Bachu RD, Shah Z, Dey S, Boddu SH. Tanshinone IIA Inhibits VEGF Secretion and HIF-1alpha Expression in Cultured Human Retinal Pigment Epithelial Cells under Hypoxia. CURR EYE RES. 2017;42(12):1667-73.

77. Wu J, Ke X, Fu W, Gao X, Zhang H, Wang W, et al. Inhibition of Hypoxia-Induced Retinal Angiogenesis by Specnuezhenide, an Effective Constituent of Ligustrum lucidum Ait., through Suppression of the HIF-1alpha/VEGF Signaling Pathway. MOLECULES. 2016;21(12).

78. Wu J, Ke X, Wang W, Zhang H, Ma N, Fu W, et al. Aloe-emodin suppresses hypoxia-induced retinal angiogenesis via inhibition of HIF-1alpha/VEGF pathway. INT J BIOL SCI. 2016;12(11):1363-71.

79. Kyosseva SV. Targeting MAPK signaling in age-related macular degeneration. OPHTHALMOL EYE DIS. 2016;8:OED. S32200.

80. Roduit R, Schorderet DF. MAP kinase pathways in UV-induced apoptosis of retinal pigment epithelium ARPE19 cells. APOPTOSIS. 2008;13(3):343-53.

81. Cargnello M, Roux PP. Activation and function of the MAPKs and their substrates, the MAPK-activated protein kinases. MICROBIOL MOL BIOL REV. 2011;75(1):50-83.

82. Görlach A, Dimova EY, Petry A, Martínez-Ruiz A, Hernansanz-Agustín P, Rolo AP, et al. Reactive oxygen species, nutrition, hypoxia and diseases: problems solved? REDOX BIOL. 2015;6:372-85.

83. Tsao Y-P, Ho T-C, Chen S-L, Cheng H-C. Pigment epithelium-derived factor inhibits oxidative stress-induced cell death by activation of extracellular signal-regulated kinases in cultured retinal pigment epithelial cells. LIFE SCI. 2006;79(6):545-50.

84. Koinzer S, Reinecke K, Herdegen T, Roider J, Klettner A. Oxidative stress induces biphasic ERK1/2 activation in the RPE with distinct effects on cell survival at early and late activation. CURR EYE RES. 2015;40(8):853-7.

85. Lin A, Dibling B. The true face of JNK activation in apoptosis. AGING CELL. 2002;1(2):112-6.

86. Sharma A, Sharma R, Chaudhary P, Vatsyayan R, Pearce V, Jeyabal PV, et al. 4-Hydroxynonenal induces p53-mediated apoptosis in retinal pigment epithelial cells. ARCH BIOCHEM BIOPHYS. 2008;480(2):85-94.

87. Ho TC, Yang YC, Cheng HC, Wu AC, Chen SL, Chen HK, et al. Activation of mitogen-activated protein kinases is essential for hydrogen peroxide -induced apoptosis in retinal pigment epithelial cells. APOPTOSIS. 2006;11(11):1899-908.

88. Qin S, McLaughlin AP, De Vries GW. Protection of RPE cells from oxidative injury by 15-deoxy-delta12,14-prostaglandin J2 by augmenting GSH and activating MAPK. INVEST OPHTHALMOL VIS SCI. 2006;47(11):5098-105.

89. Westlund BS, Cai B, Zhou J, Sparrow JR. Involvement of c-Abl, p53 and the MAP kinase JNK in the cell death program initiated in A2E-laden ARPE-19 cells by exposure to blue light. APOPTOSIS. 2009;14(1):31-41.

90. Cheng L-B, Chen C-M, Zhong H, Zhu L-J. Squamosamide derivative FLZ protects retinal pigment epithelium cells from oxidative stress through activation of epidermal growth factor receptor (EGFR)-AKT signaling. INT J MOL SCI. 2014;15(10):18762-75.

91. Chou W-W, Chen K-C, Wang Y-S, Wang J-Y, Liang C-L, Juo S-HH. The role of SIRT1/AKT/ERK pathway in ultraviolet B induced damage on human retinal pigment epithelial cells. TOXICOL IN VITRO. 2013;27(6):1728-36.

92. Kim JH, Kim JH, Jun HO, Yu YS, Min BH, Park KH, et al. Protective Effect of Clusterin from Oxidative Stress–Induced Apoptosis in Human Retinal Pigment Epithelial Cells. INVEST OPHTHALMOL VIS SCI. 2010;51(1):561-6.

93. Lee EJ, Kim N, Kang KH, Kim JW. Phosphorylation/inactivation of PTEN by Akt-independent PI3K signaling in retinal pigment epithelium. BIOCHEM BIOPHYS RES COMMUN. 2011;414(2):384-9.

94. Dridi S, Hirano Y, Tarallo V, Kim Y, Fowler BJ, Ambati BK, et al. ERK1/2 activation is a therapeutic target in age-related macular degeneration. PROC NATL ACAD SCI U S A. 2012;109(34):13781-6.

95. Koinzer S, Reinecke K, Herdegen T, Roider J, Klettner A. Oxidative Stress Induces Biphasic ERK1/2 Activation in the RPE with Distinct Effects on Cell Survival at Early and Late Activation.

CURR EYE RES. 2015;40(8):853-7.

96. Makarev E, Cantor C, Zhavoronkov A, Buzdin A, Aliper A, Csoka AB. Pathway activation profiling reveals new insights into age-related macular degeneration and provides avenues for therapeutic interventions. AGING (ALBANY NY). 2014;6(12):1064.

97. SanGiovanni JP, Lee PH. AMD-associated genes encoding stress-activated MAPK pathway constituents are identified by interval-based enrichment analysis. PLOS ONE. 2013;8(8):e71239.

Chapter 3

Betulinic acid derivatives can protect human Müller cells from glutamate-induced oxidative stress

Abstract

Müller cells are the predominant retinal glial cells. One of the key roles of Müller cells is in the uptake of the neurotransmitter glutamate and in its conversion to glutamine. Müller cell dysfunction due to oxidative stress elicited by high glutamate concentrations can lead to toxicity, which promote the pathogenesis of retinal diseases like diabetic retinopathy and glaucoma. This study investigated the anti-oxidant activity and mechanisms of betulinic acid (BA) and its derivatives in human Müller cells. Human MIO-M1 Müller cells were pre-treated in the presence or absence of BA, BE as well as their derivatives (named H3-H20) followed by incubation with glutamate. Cell viability was evaluated with the MTT and Calcein-AM assays. Reactive oxygen species (ROS) production in MIO-M1 cells was measured using CM-H_2DCFDA and flow cytometry. The activation of cellular apoptosis and necrosis was analysed with annexin V/PI staining and flow cytometry. The modulation of signalling pathways involved in glutamate-mediated cytotoxicity and ROS production was evaluated by immunoblotting. The BA derivatives H3, H5 and H7 exhibited minimal cytotoxicity and significant anti-oxidant activity. These compounds significantly suppressed ROS production and attenuated cellular necrosis elicited by glutamate-induced oxidative stress. The protective effects of H3, H5 and H7 in MIO-M1 cells were associated with the attenuation of Akt, Erk1/2, and JNK signalling. The BA analogues H3, H5 and H7 are protective against glutamate-induced oxidative stress in human Müller cells, and elicit their actions by modulation of the Erk, Akt and JNK signalling pathways. These agents are potential candidate molecules for the prevention or treatment of human retinal diseases.

3.1 Introduction

Müller cells are the predominant neuron-supporting glial cells. Müller cells extend

vertically throughout the retina and are functionally linked with other retinal and neuronal cells in the maintenance of retinal structure and health (1). Thus, Müller cells regulate retinal blood flow (1-4), ion and pH homeostasis (1-3, 5), glucose metabolism and the visual cycle (1, 5), the release of trophic factors (2-5) and the response of photoreceptors to light (2, 3, 5). Together with endothelial cells and pericytes (5), the Müller cells are integral components of the blood-retinal barrier (BRB) that protects the retina from toxins.

As the major excitatory neurotransmitter, glutamate mediates the transmission of visual signals by several retinal cell types including bipolar, photoreceptors and ganglion cells (2). Glutamate is continuously synthesized and released from the synaptic terminal of photoreceptors and acts at postsynaptic receptors on horizontal and bipolar cells (2, 6). A major function of Müller cells is in the uptake and recycling of glutamate to prevent toxicity (1, 4, 5). Glutamate-induced toxicity contributes to retinal loss and impaired vision and may progress to a range of retinal diseases like glaucoma, diabetic retinopathy (DR), ischemia and inherited photoreceptor degeneration (3, 6).

DR and glaucoma are the two most common irreversible ocular diseases in humans. Indeed, DR is the primary cause of blindness in people, who are aged 20-74 years old (https://www.visionaustralia.org) followed by glaucoma (7). The incidence of these conditions is increasing dramatically. Although several potential therapeutic strategies have been tested (*eg*. anti-VEGF therapy, surgery and laser treatment), they remain incurable. Therefore, new approaches to prevent the progression of such retinal diseases are urgently required.

Betulinic acid (BA) and betulin (BE) are both pentacyclic triterpenoids. They are extracted from the bark of birch trees. Literature reports indicate that these agents have anti-cancer, anti-diabetic, anti-inflammatory, anti-microbial, as well as anti-viral properties (8, 9). We recently reported that BA derivatives carrying a range of substituents at positions C3 and C28 (10-12) protected human retinal pigmented epithelial cells against hypoxia (12). These agents also exhibit potent anti-oxidative activities in a range of cell lines (13-15). The present study evaluated these promising agents in the prevention of glutamate-induced oxidative stress in the human MIO-M1 cell line that express markers of mature retinal Müller cells (16-19).

3.2 Materials and methods

3.2.1 Reagents and chemicals

Dulbecco's Modified Eagle Medium (DMEM), CM-H_2DCFDA, Fetal Bovine Serum

(FBS) and Calcein-AM were purchased from Thermo Scientific (Lidcombe, NSW, Australia). Dimethyl sulfoxide (DMSO), L-glutamic acid monosodium salt hydrate and thiazolyl blue tetrazolium bromide (MTT) were obtained from Sigma-Aldrich (Castle Hill, NSW, Australia). BA derivatives were chemically synthesized as described previously (12, 20, 21). The FITC-annexin V apoptosis detection kit was bought from BD Bioscience (North Ryde, NSW, Australia). PVDF membranes were purchased from Merck Millipore (Bayswater, VIC, Australia). Akt (pan), Phospho-Akt (Ser473), p44/42 MAPK (Erk), phospho-p44/42 MAPK (Erk) (Thr202/Tyr204), SAPK/JNK and phospho-SAPK/JNK (Thr183/Tyr185) (81E11) antibodies were obtained from Bio-strategy Laboratory Products (Tingalpa, QLD, Australia) or Genesearch Pty Ltd (Arundel, QLD, Australia). The β-actin antibody was bought from Sigma-Aldrich. Goat anti-mouse and anti-rabbit IgGs conjugated with horseradish peroxidase were obtained from Bio-strategy Laboratory Products.

3.2.2 Cell culture

MIO-M1 cells were maintained in a humidified incubator (5% CO_2) at 37 °C in DMEM (Gibco, Thermo Fisher) containing 10% FBS (v/v) and 1% L-Glutamine.

3.2.3 Cytotoxicity assays

MIO-M1 cells were cultured in 96-well plates (1.2×10^4 cells/well) for 24h. In cytotoxicity studies, cells were treated with BA and its derivatives (10 μM) in DMEM containing 1% FBS (v/v) for 24 h. 0.1% DMSO was applied as the negative control. Cells were then treated with 300 mM glutamate for 4 h prior to MTT assay (22-26). Briefly, cells were treated with MTT solution (0.5 mg/mL) in the dark for 2 h and then washed with phosphate-buffered saline (PBS, 0.154 M NaCl, 0.001 M KH_2PO_4, 0.003 M Na_2HPO_4; pH 7.4). Cells were then treated with DMSO and the plate was shaken for 10 min at room temperature. The absorbance of the treated cells was measured at 550 nm in a microplate reader (Model 680, Bio-Rad, Gladesville, NSW, Australia).

Cell viability was also evaluated using Calcein-AM assays following incubation with glutamate. As mentioned before (17, 27), cells were then washed with PBS and then incubated in the dark with 2 μM Calcein-AM for 0.5h. The fluorescence ratios at the excitation/emission wavelength pair of 485 nm/535 nm were determined in a plate reader (Victor^{TM} X4 Multimode, PerkinElmer, Melbourne, VIC, Australia); ratios were

corrected by subtraction of values in Calcein-AM-free cells.

3.2.4 Apoptotic and necrotic assay

MIO-M1 cells were treated with each of the test compounds (10 µM, 24 h, 37 °C) and then treated with glutamate (300 mM) for 4 h. Cells were collected and as described previously, stained with propidium iodide (PI) and annexin V-FITC (12, 28). Samples were analyzed in a flow cytometer (Guava easy®cyte , Merck Millipore, Bayswater, VIC, Australia).

3.2.5 Intracellular Reactive Oxygen Species (ROS) assay

MIO-M1 cells were treated with each of the test compounds (10 µM, 24 h, 37 °C) and then treated with 300 mM glutamate for 4h. ROS formation was quantified as mentioned before (28). Briefly, cells were treated with CM-H_2DCFDA (1 µM) for 40 min in the dark, washed with PBS and analyzed in a flow cytometer.

3.2.6 Western blot

MIO-M1 cells were harvested and lysed with the lysis buffer containing NP-40 (1% IGEPAL, 50 mM Tris and 150 mM NaCl pH 7.8 supplied with protease inhibitors). Lysate was centrifuged at 15,000 rpm (10 min, 4℃). Protein samples were denatured and separated by electrophoresis. After transferred onto PVDF membranes, the blots were incubated with 5% non-fat milk (in PBST) for 30 min (at room temperature). The blots were incubated with a primary antibody at 4℃ overnight and then washed with PBST for three times. Blots were then incubated with a secondary antibody for 1 h (at room temperature) and then with the chemiluminescent substrate (SuperSignal West Pico, Thermo Scientific, Lidcombe, NSW, Australia). The signals were visualized with the image box (ImageQuant LAS500, GE health care, Silverwater, NSW, Australia).

3.2.7 Statistics

All data are shown as mean ± standard deviation (SD). The Student's *t*-test was used to identify differences between glutamate-treated and control groups, and between

compound-treated and vehicle-treated groups. Two-way ANOVA was used to compare multiple treatment and control groups. $p<0.05$ was considered as significant.

3.3 Results

3.3.1 Cellular toxicity of BA and its derivatives in MIO-M1 cells

In initial studies, we evaluated the cytotoxicity of BA, BE and their analogues in MIO-M1 cells. Cells were treated with individual analogues at 10 μM for 24 h. This concentration was selected, because it is close to the reported C_{max} of BA *in vivo* (29-31). Under these conditions H1, H2, H4, H6, H9 and H19 and, to a lesser extent, H15 were toxic in MIO-M1 cells (Fig. 3.1A). Interestingly, H8 and H20 produced a slight but significant increase in the viability of MIO-M1 cells. Analogues with no apparent effects on cell viability were selected for further analysis.

A

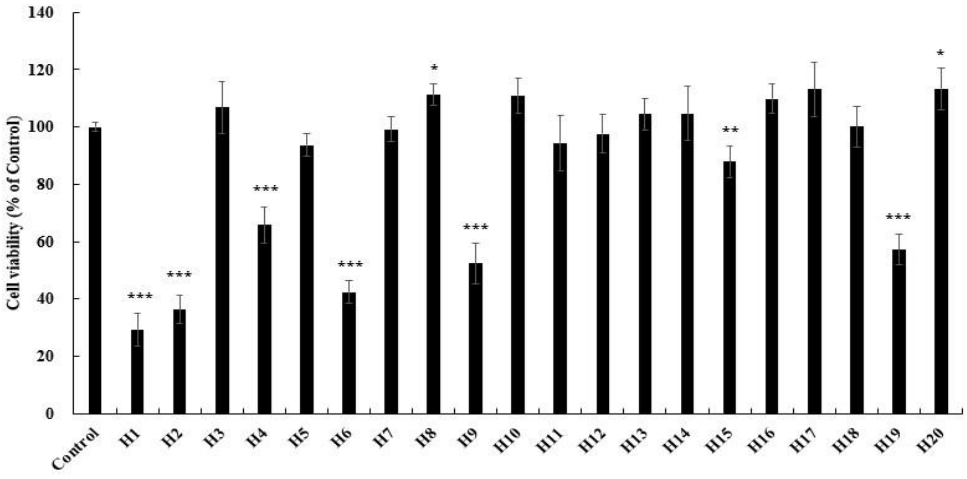

B

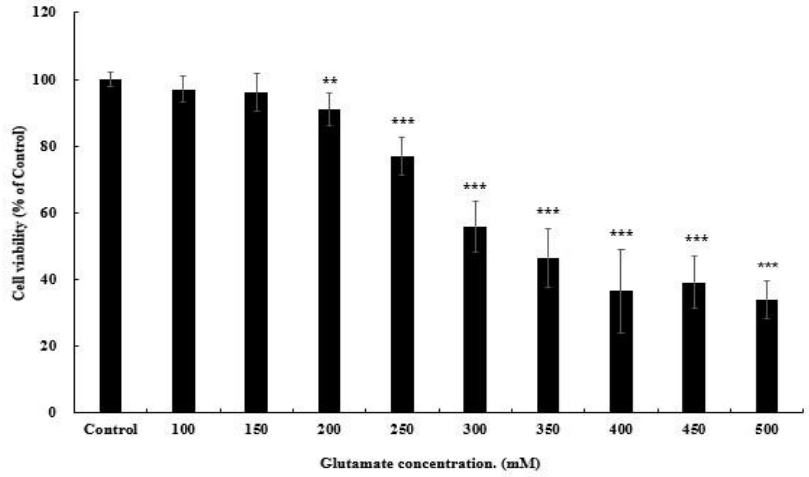

C

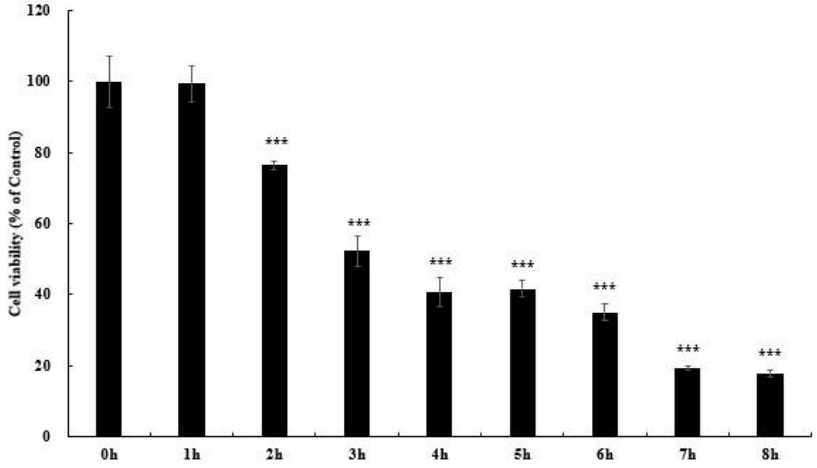

Figure 3.1 Cytotoxicity of BA, its analogues and glutamate in MIO-M1 cells

(A) MIO-M1 cells were incubated with H1-H20 (10 μM) for 24 h and cell viability was measured using the MTT assay. (B) MIO-M1 cells were pre-incubated with glutamate (0-500 mM) for 4 h and cell viability was assessed using the MTT assay. (C) MIO-M1 cells were pre-incubated with glutamate (300 mM) for 0-8 h and cell viability was evaluated with MTT assay. DMSO was adopted as vehicle control. Data are presented as the percentage of control (mean ± SD). *$p<0.05$, **$p < 0.01$, ***$p < 0.001$ vs. control group, t-test.

3.3.2 Protective effect of BA derivatives on MIO-M1 cells against glutamate-induced oxidative stress

Glutamate-induced oxidative stress is considered to be a primary cause of neuronal cell death (32), the prevention of which is a potential approach for the treatment of retinal diseases. The protective actions of BA derivatives were assessed in MIO-M1 cells as a model of acute toxicity (33, 34).

MIO-M1 cells were incubated with glutamate (4 h) over the concentration range 100 to 500 mM. As shown in Fig. 3.1B, glutamate (200-500 mM) significantly decreased cell viability. A concentration of 300 mM was selected for further study as it produced an approximate 50% decrease in cell viability (55.8 ± 7.6 %). From the time dependence study, cell viability was decreased at 2 h and appeared to be maximal at 4 h (Fig. 3.1C). Thus, a 4 h treatment duration was adopted in further studies.

To examine the protective effect of non-cytotoxic BA derivatives against glutamate-induced oxidative stress, MIO-M1 cells were pre-treated with each compound (10 μM) for 24 h prior to the addition of glutamate (300 mM). After 4 h, cell viability was estimated using MTT (Table 3.1), the data was then re-analyzed as shown in Table 3.2. However, all the selected compounds showed significant cyto-protective activity compared to vehicle control, so we need to adopt another method of different mechanism to narrow-down the candidates. By using Calcein-AM assay (Table 3.3 and Table 3.4), H3, H5, H7, H11 and H12 were observed with significant improved cell viability, as H12 exhibited relatively low antioxidative effects (67.6±9.5% in Table 3.2), we will only include H3, H5, H7 and H11 for further studies.

Table 3.1 Cell viability of betulinic acid derivatives with or without glutamate in MIO-M1 cells (MTT assay)

MIO-M1 cells were treated with BA or its derivative (10 μM) for 24 h and then treated with or without glutamate (300 mM) for additional 4 h. Cell viability was evaluated using MTT assay. Data are presented as percentages of cell viability relative to DMSO treated control.

Treatment	Viability (%) (AVG± SD)
Control	100.0±5.2
Control + glutamate	52.6±10.4
H3	93.8±5.3
H3+glutamate	68.3±6.4
H5	90.7±7.1

H5+ glutamate	75.8±5.6
H7	89.6±7.7
H7+ glutamate	75.8±3.9
H8	92.8±4.9
H8+ glutamate	81.2±6.9
H10	104.1±4.2
H10+ glutamate	85.8±7.0
H11	99.8±8.5
H11+ glutamate	85.2±9.4
H12	96.7±8.2
H12+glutamate	65.4±8.6
H13	92.5±3.9
H13+ glutamate	69.1±14.1
H14	94.8±5.1
H14+glutamate	75.2±5.5
H16	94.9±6.1
H16+ glutamate	81.4±6.0
H17	99.3±5.6
H17+ glutamate	72.8±7.6
H18	110.0±7.8
H18+ glutamate	81.5±4.9
H20	101.0±5.9
H20+ glutamate	77.1±7.5

Table 3.2 Anti-oxidative effects of betulinic acid derivatives (MTT assay)

A re-analysis of data in the Table 3.1. Data are shown as the percentage viability of cells pre-treated with betulinic acid derivatives and glutamate divided by that of cells treated with the BA derivative alone.

Treatment	**Anti-oxidative effect (%) (AVG ± SD)**
Control	52.6±11.1
H3	72.8±7.2###
H5	83.5±6.5###
H7	84.6±4.6###
H8	87.5±7.8###
H10	82.4±7.1###

H11	85.4±10.0###
H12	67.6±9.5#
H13	74.7±16.2###
H14	79.3±6.3###
H16	85.7±6.8###
H17	73.3±8.1###
H18	74.1±4.7###
H20	76.3±7.9###

Table 3.3 Cell viability of betulinic acid derivatives with or without glutamate in MIO-M1 cells (Calcein-AM assay)

MIO-M1 cells were treated with BA or its derivative (10 μM) for 24 h and then treated with or without glutamate (300 mM) for additional 4 h. Cell viability was evaluated using Calcein-AM assay. Data are shown as percentages of cell viability relative to DMSO treated control.

Treatment	Viability (%) (AVG ± SD)
Control	100.0±8.7
Control + glutamate	43.6±7.4
H3	107.2±12.4
H3+glutamate	66.3±11.4
H5	106.4±11.7
H5+ glutamate	68.6±9.6
H7	109.7±11.3
H7+ glutamate	74.2±9.7
H8	99.9±10.6
H8+ glutamate	55.4±8.3
H10	101.4±11.9
H10+ glutamate	54.8±7.3
H11	95.3±7.1
H11+ glutamate	56.2±8.9
H12	102.6±6.3
H12+glutamate	57.5±7.3
H13	94.9±5.1
H13+ glutamate	39.9±6.5
H14	107.4±6.3
H14+glutamate	59.9±12.9
H16	105.4±10.1

H16+ glutamate	59.5±11.7
H17	100.4±3.6
H17+ glutamate	49.9±9.0
H18	106.4±8.8
H18+ glutamate	53.8±11.3
H20	105.2±6.9
H20+ glutamate	52.8±12.7

Table 3.4 Anti-oxidative effects of betulinic acid derivatives (Calcein-AM assay)

A re-analysis of data in the Table 3.3. Data are shown as the percentage viability of cells pre-treated with betulinic acid derivatives and glutamate divided by that of cells treated with the BA derivative alone.

Treatment	**Anti-oxidative effect (%) (AVG±SD)**
Control	43.6±7.4
H3	61.9±10.7#
H5	64.5±9.0#
H7	67.6±8.9##
H8	55.4±8.3
H10	54.0±7.2
H11	59.0±9.4##
H12	56.0±7.2#
H13	42.0±6.8
H14	55.7±12.0
H16	56.5±11.1
H17	49.7±9.0
H18	50.6±10.6
H20	50.2±12.1

3.3.3 The BA analogues H3, H5, H7 and H11 attenuated necrosis in MIO-M1 cells elicited by glutamate-induced oxidative stress

Glutamate-mediated oxidative stress has been reported to activate apoptosis and necrosis in neuronal cells, such as HT22, PC12 and ganglion cells (35-38). We utilized annexin V-FITC/PI dual staining to elucidate whether H3, H5, H7 and H11 modulated cell death in glutamate-treated MIO-M1 cells. The data showed that necrosis was the

primary death program in MIO-M1 cells resulting from glutamate-induced oxidative stress (Fig. 3.2A). Pre-treatment with the BA derivatives H3, H5, H7 and H11 attenuated glutamate-dependent necrosis in MIO-M1 cells (Fig. 3.2A and 3.2B).

A

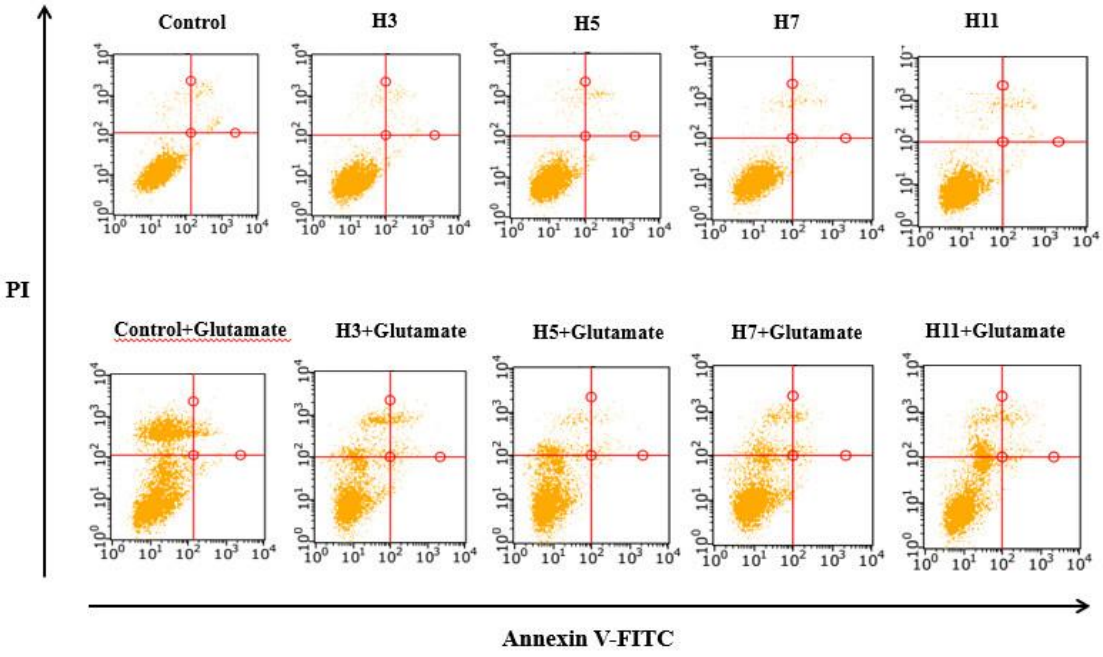

B

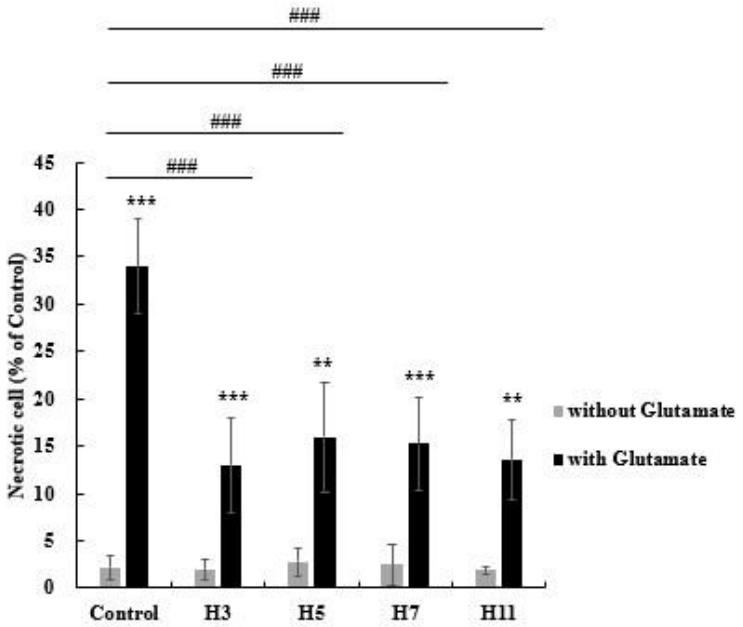

C

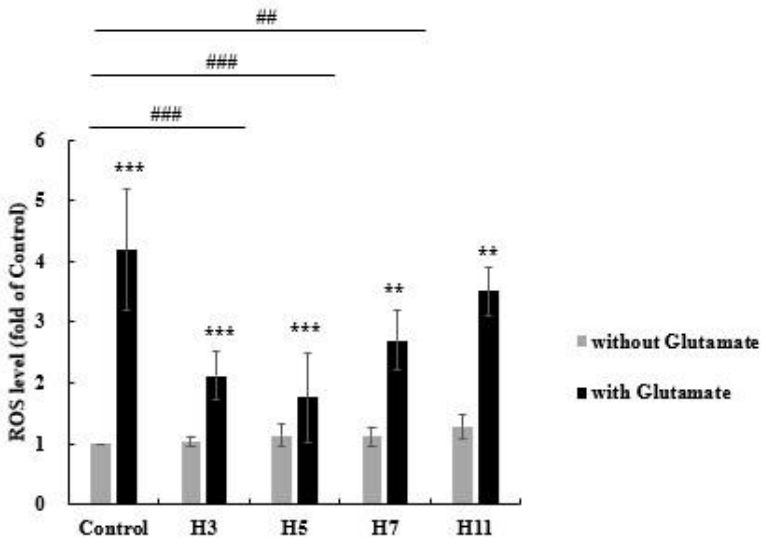

Figure 3.2 The BA analogues H3, H5, H7 and H11 protected MIO-M1 cells from glutamate-induced cell death and modulated ROS production

MIO-M1 cells were incubated with H3, H5, H7 or H11 (10 μM) for 24 h and then treated with or without glutamate (300 mM) for 4 h. (A) Cell apoptosis and necrosis were analyzed by annexin V/PI staining and flow cytometry. Only representative images are shown. (B) Analysis of cell necrosis in (A). Data are shown as percentage of control (mean ± SD). (C) ROS production was quantified in MIO-M1 cells after glutamate treatment (300 mM, 24 h) by CM-H_2DCFDA and flow cytometry. Data are shown as folds of control (mean ± SD). DMSO was adopted as negative control in these experiments. **p < 0.01, ***p < 0.001 vs. corresponding groups without glutamate treatment, t-test; #p<0.05, ##p < 0.01, ###p < 0.001 vs. control groups with or without glutamate, two-way ANOVA.

3.3.4 The BA analogues H3, H5 and H7 suppressed the increase in ROS production in MIO-M1 cells following glutamate treatment

Oxidative stress is a likely consequence of the increase in cellular ROS production following glutamate treatment and could be an early, and perhaps causative, event in toxicity (6). In the present study, we confirmed that glutamate treatment increased cellular ROS production in MIO-M1 cells. The BA analogues H3, H5 and H7 attenuated this increase in ROS formation (Fig. 3.2C); the anti-oxidative activity of H11 was

somewhat lower. Accordingly, H3, H5 and H7 emerged as agents with potential protective actions against glutamate-induced toxicity in MIO-M1 cells by decreasing ROS production.

3.3.5 The cytoprotective agents H3, H5 and H7 modulate Akt, Erk1/2 and JNK signaling in MIO-M1 cells

As shown in Fig. 3, H3, H5 and H7 exhibited time- and concentration-dependent cytoprotection in MIO-M1 cells. Compared to 24h, H3 showed much increased anti-oxidative effect from 48 h, while H5 from 64 h and H7 from 40 h. Anti-oxidative effect of these compounds was significant at concentrations of 5 μM and above (Fig. 3B-D and Supplementary Table 2). To facilitate comparison with earlier findings, we employed a concentration of 10 μM in subsequent mechanistic studies.

A

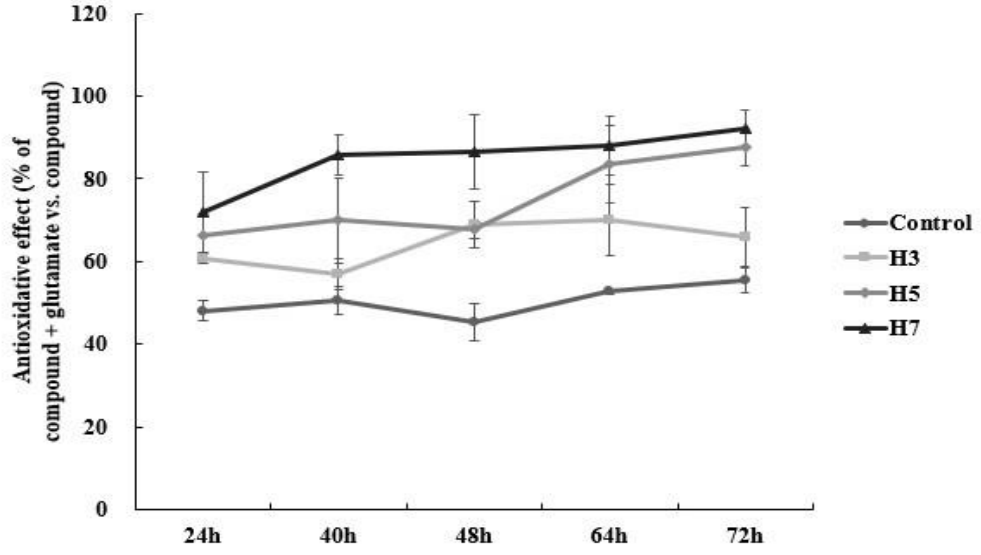

B

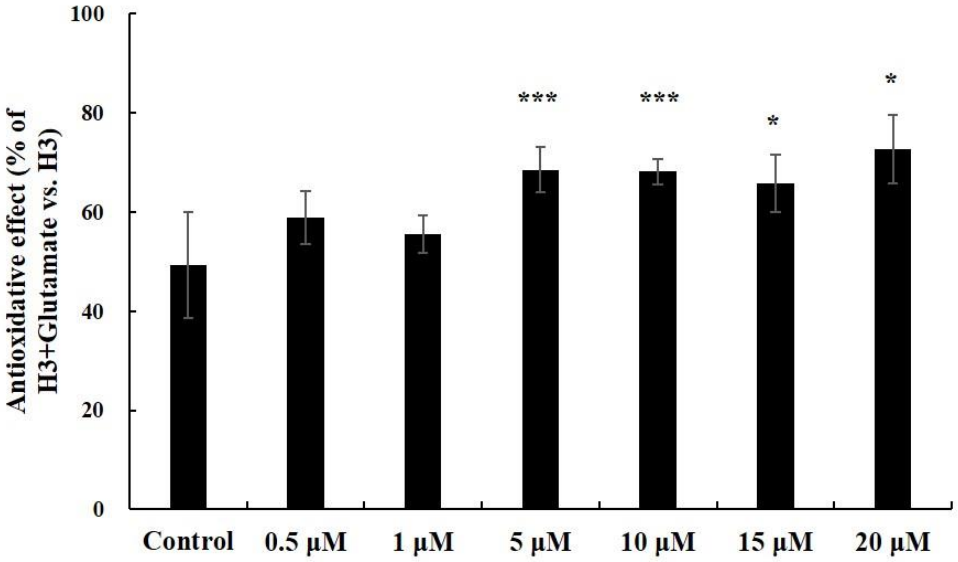
Antioxidative effect (% of H3+Glutamate vs. H3)
100
80
60
40
20
0
***
***
*
*
Control
0.5 μM
1 μM
5 μM
10 μM
15 μM
20 μM

C

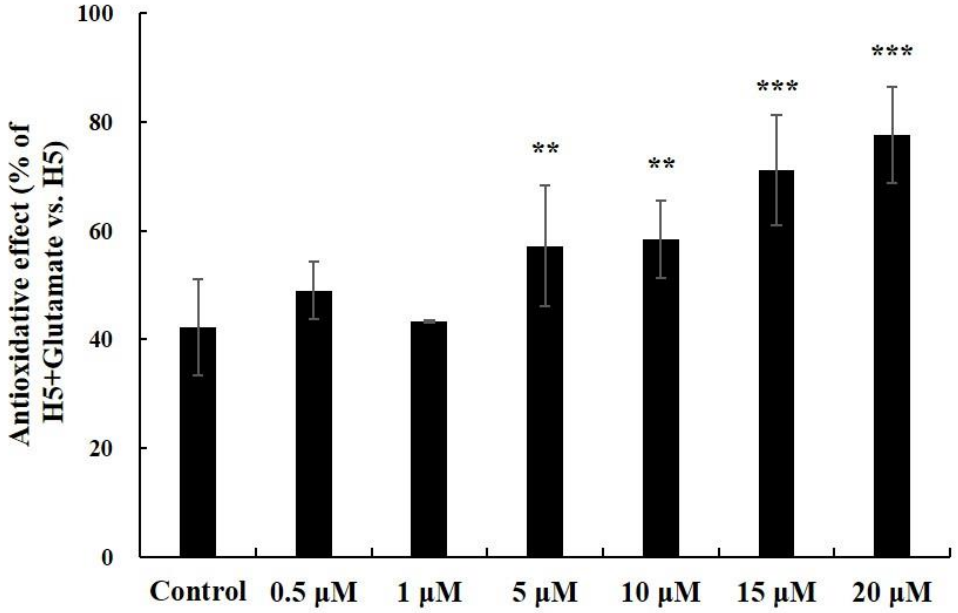
Antioxidative effect (% of H5+Glutamate vs. H5)
100
80
60
40
20
0
**
**
***
***
Control
0.5 μM
1 μM
5 μM
10 μM
15 μM
20 μM

D

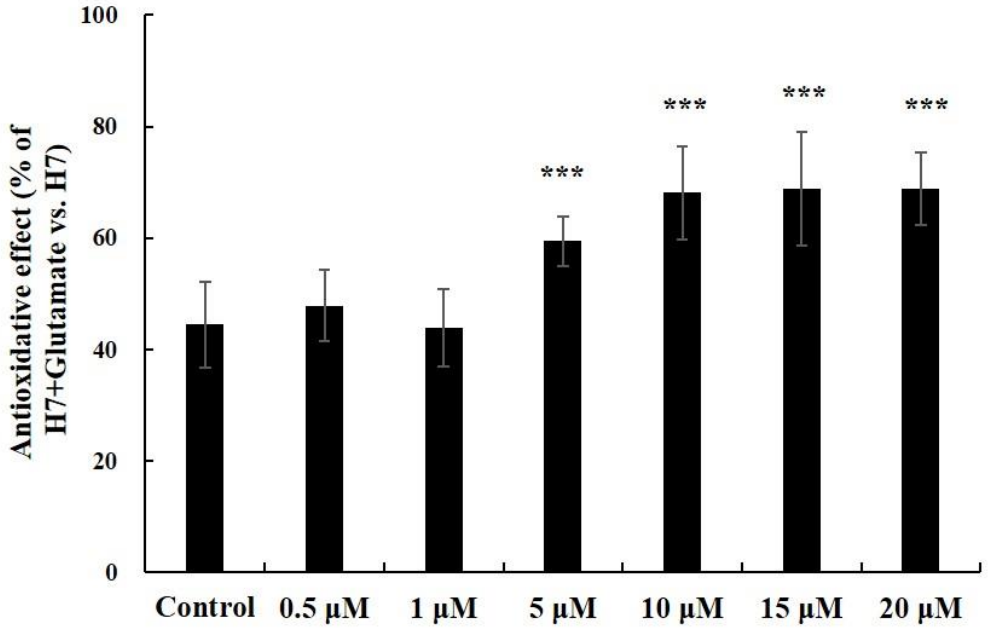

Figure 3.3 Time- and concentration-dependence of the cytoprotective activity of H3, H5 and H7

(A) MIO-M1 cells were incubated with H3, H5 or H7 (10 μM) for 24, 40, 48, 64 or 72 h and then treated with or without glutamate (300 mM) for 4 h. Cell viability was measured using Calcein-AM assay. (B-D) MIO-M1 cells were treated with 0, 0.5, 1, 5, 10, 15 or 20 μM of H3 (B), H5 (C) or H7 (D) for 24 h and then incubated in the presence or absence of 300 mM glutamate for 4 h. Cell viability was measured using Calcein-AM assay. DMSO was used as vehicle control in these experiments. Data are shown as the percentage of control (mean ± SD). **p < 0.01,**p<0.01, ***p < 0.001 vs. control, t-test.

The mitogen-activated protein kinase (MAPK) as well as phosphoinositide-3 kinase (PI3K)/Akt signaling pathways have been widely implicated in glutamate-induced toxicity. From Western blot analysis, the Akt, Erk1/2 and JNK MAPK pathways were activated in MIO-M1 cells following treatment with glutamate (increased phospho-protein expression; Fig. 3.4A). The BA analogues H5 and H7 markedly attenuated the activation of Akt, Erk and JNK pathways, whereas H3 was less effective (Fig. 3.4B-D). Thus, the agents with the greatest capacity to prevent ROS production and cytotoxicity after glutamate treatment also prevented the activation of Akt/MAPK signaling.

A

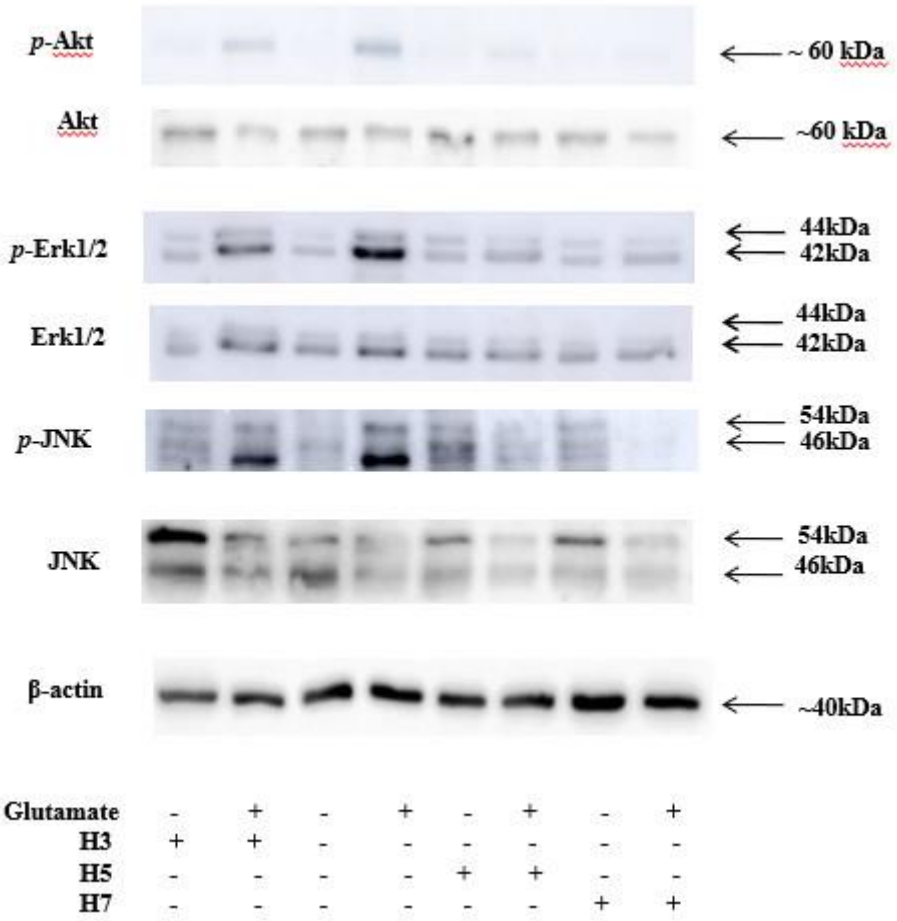
p-Akt
~ 60 kDa
Akt
~60 kDa
p-Erk1/2
44kDa
42kDa
Erk1/2
44kDa
42kDa
p-JNK
54kDa
46kDa
JNK
54kDa
46kDa
β-actin
~40kDa
Glutamate - + - + - + - +
H3 + + - - - - - -
H5 - - - - + + - -
H7 - - - - - - + +

B

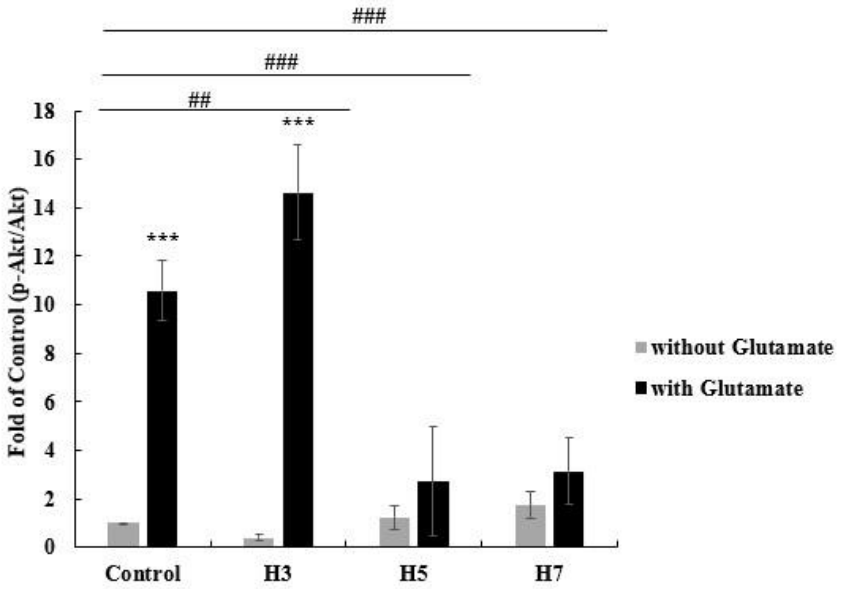
###
###
##
***
***
Fold of Control (p-Akt/Akt)
18
16
14
12
10
8
6
4
2
0
Control
H3
H5
H7
without Glutamate
with Glutamate

C

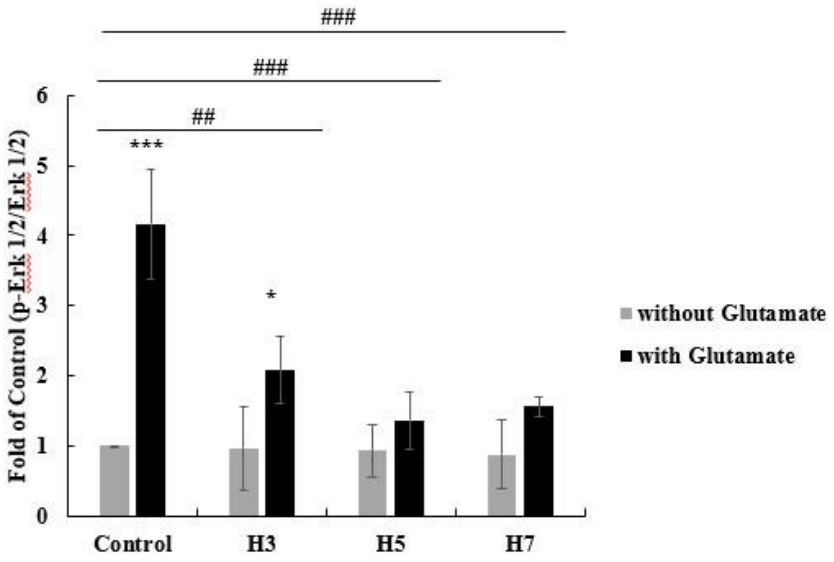

D

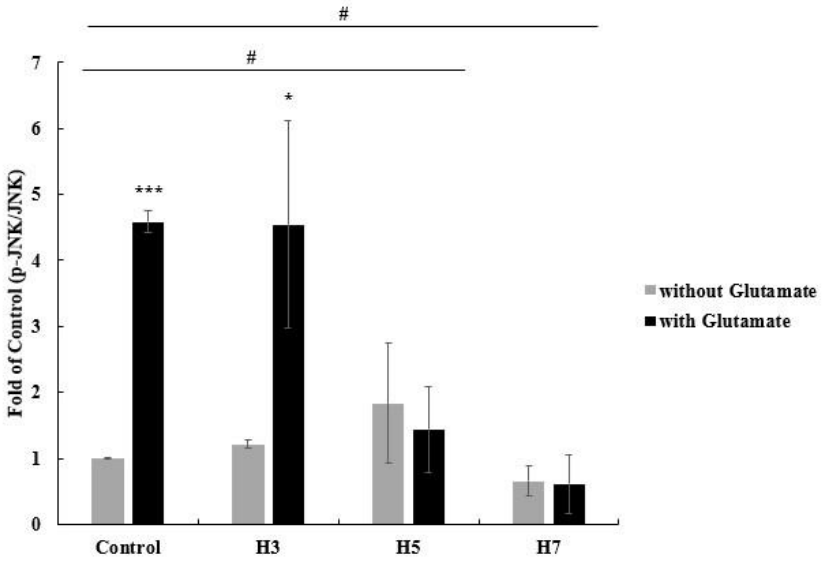

Figure 3.4 Modulation of glutamate-induced Erk, Akt and JNK activation in MIO-M1 cells by the BA analogues H3, H5 and H7

(A) MIO-M1 cells were pre-treated with or without H3, H5 or H7 (10 μM) for 24 h and then incubated with or without glutamate (300 mM) for 4 h. Protein expression of p-Akt/Akt (B), p-Erk /Erk (C), and p-JNK/JNK (D) was evaluated by Western blotting. Intensities of bands were analyzed by densitometry. DMSO was used in control cell treatments and β-actin was included as the control

of sample loading. Data are shown as fold of control (mean ± SD). *p < 0.05, ***p < 0.001 vs. corresponding groups without glutamate, t-test; #p<0.05, ##p < 0.01, ###p < 0.001 vs. control groups with or without glutamate, two-way ANOVA.

3.4 Discussion

Glutamate is an important excitatory neurotransmitter, which level in the CNS is controlled by its uptake and cycling mechanisms. Dysregulation of the glutamate cycle may increase extracellular glutamate leading to inflammation and oxidative stress (2). Müller cells are mainly responsible for the uptake and recycling of glutamate in the retina (1, 4, 5). Under pathological conditions, the dysfunction of Müller cells can lead to an abnormal accumulation of glutamate. The glutamate-induced oxidative stress will consequently cause the damage of Müller and other retinal cells resulting in a range of retinal diseases such as DR and glaucoma (3, 6).

In the human retina, glutamate transporters are shown to be downregulated in pathological conditions such as glaucoma, which is associated with impaired removal of glutamate by glial and neuronal cells, and may lead to the accumulation of glutamate in the extracellular space. Müller cells are the predominant glial cells of the human retina, and are susceptible to the consequences of glutamate accumulation (39). The protection of cells against glutamate-induced oxidative damage is a potentially valuable strategy for the prevention of retinal pathologies.

The present study evaluated a range of BA analogues for the capacity to modulate ROS production and necrosis in MIO-M1 cells after glutamate treatment. We employed two cytotoxicity assays reflecting different cytotoxic mechanisms: The MTT assay assesses cellular metabolic activity, while the Calcein-AM assay reflects endogenous plasma membrane integrity and esterase activity. The data showed that the BA analogues H3, H5, H7 and H11 protect MIO-M1 cells against glutamate toxicity in both assays (Table 3.1- 3.4).

Glutamate toxicity can cause neuronal loss. Both apoptosis and necrosis were activated in cells that were subject to glutamate-induced oxidative stress (35-38, 40-42). The mechanism of cell death following glutamate exposure varies in a cell type- and treatment-related manner (43). In general, mild insults primarily activate apoptosis (35, 37, 38, 41), while acute, intense and excitotoxic stimuli or free-radical related insults are more likely to induce necrosis. Necrosis can be activated rapidly within minutes to hours, whereas apoptosis requires a longer time-frame (44). Thus, *Ankarcrona et al* detected necrosis in cerebellar granule cells soon after glutamate treatment; while apoptosis occurred later and in cells with impaired mitochondrial function (41). We treated MIO-M1 cells with 300 mM glutamate for 4 h, to reflect clinically relevant acute

toxicity in retinal pathologies, such as glaucoma (45).

Glutamate-induced apoptosis and necrosis have also been observed *in vivo*. It has been reported that in albino mice, necrosis of the inner retina was observed a few hours after subcutaneous injection of sodium L-glutamate, which suggested that glutamate at high concentrations can induce retinal cell death (46). *Mitori* also observed retinal apoptosis when glutamate was injected directly into the retina in neonatal rats (47). Glutamate has been shown to elevate the Ca^{2+} concentration in neurons, which increases the uptake into mitochondria and promotes ROS production (48). In the present study, the BA analogues H3, H5, H7 and H11 prevented necrosis in glutamate-treated MIO-M1 cells (Fig. 3.2A and 3.2B). H3, H5 and H7 in particular, also effectively inhibited ROS production (Fig. 3.2C).

The MAPK and PI3K/Akt signaling cascades are implicated in the responses of a number of cell types to ROS (49). The Erk MAPK is primarily considered to be stimulated by growth factors, mitogens and survival factors, resulting in the activation of genes that promote cell growth and differentiation (50-52). Erk pathway proteins are highly expressed in neurons and are also involved in synaptic plasticity, memory and learning (53, 54). However, the Erk pathway also mediates retinal apoptosis and Müller cell death in response to glutamate-induced toxicity (43). In accord with these findings, *Roth et al.,* (55) reported that Erk was activated in Müller cells of the ischemic rat and that the death signal was transmitted to nearby retinal ganglion cells and photoreceptors. ROS-induced Erk phosphorylation in microglia (56), can also stimulate the release of inflammatory factors (56). We previously showed that H7 has protective effect on human RPE cells via modulating the Erk, Akt and JNK pathways (12). In the current study, the Erk pathway was activated in response to increased ROS production in glutamate-treated MIO-M1 cells. Pre-treatment with the BA analogues H3, H5 or H7 effectively attenuated ROS production and necrosis, which suggests that Erk blockade might be employed therapeutically to prevent retinal damage due to glutamate-induced oxidative stress.

The alternate MAPK isoforms p38 and JNK are responsive to cellular stresses like UV irradiation, inflammation, hypoxia, ischemia and oxidative stress (57, 58), as well as to proinflammatory cytokines such as tumor necrosis factors and interleukin-1. Activating the JNK and p38 pathways can promote the expression of genes that mediate cell death (59). The JNK pathway mediates neuropathological events including cellular toxicity (60); while p38 and apoptosis are activated in retinal ganglion cells by the N-methyl-D-aspartic acid (NMDA) receptor agonist NMDA (61). In the present study, JNK was activated in MIO-M1 cells by glutamate; this was attenuated by H5, H7 and, to a lesser extent, H3 (Fig. 3.4D). In contrast, none of the compounds were found to activate the p38 pathway (data not shown).

The PI3K/Akt cascade enhances cell survival in response to injurious stresses, and is also important in CNS development and plasticity (62). In the present study, Akt activation in MIO-M1 cells appeared to be a component of the cellular defense against glutamate-induced oxidative stress, although there have been conflicting reports that Akt is unresponsive to glutamate (63-65), which might reflect differences in cell protocols or cell contexts. Pretreatment of cells with H5 and H7 prevented the glutamate-mediated activation of Akt; in comparison, H3 pretreatment was less effective.

The three signaling pathways under investigation also exhibit crosstalk in response to glutamate *in vivo* and *in vitro*. Thus, p-Erk, p-p38 and p-JNK expression was activated in the ischemic rat retina in a time-dependent pattern (55), and the blockade of the Erk and p38 MAPKs, but not JNK, significantly improved recovery in ischemic retina (55). *Yu et al.* (37) reported the CaMKII-dependent activation of the ASK-1/JNK/p38 cascade in glutamate treated PC12 cells, while activation of p38 and JNK was produced by NMDA exposure (66, 67). *Zhang et al.* (68) demonstrated that increased activity of the major metabotropic glutamate receptor 5 (mGluR5) increased Erk and Akt signaling and promoted retinal progenitor cell proliferation. However, Asomugha *et al* (63) did not replicate these findings in glutamate treated porcine retinal ganglion cells. The findings in the current study demonstrated that the Akt, Erk and JNK cascades were all activated by glutamate in MIO-M1 cells.

The structural requirements for activity in BA analogues are not completely clear. The most active agents were substituted at C3 and C28 in the triterpenoid ring system. Thus, H5 possesses a carbonyl function and a carboxylate group at C3 and C28, respectively. None of the other test analogues carried a C3 carbonyl but several toxic analogues contained a carboxylate at C28. The analogue H7 carries acylglycine substituents at both C3 and C28 (with one being esterified). H3 possesses a hydroxyl group at C3 and a succinate at C28. Although several other analogues also carried a C3 hydroxyl group (H1, H2, H9, H16-H18), these derivatives were either toxic or carried bulky and flexible groups at C28. Further analogues, perhaps based on H5 and H7, could now be prepared to elucidate the structural basis of cyto-protection in greater detail.

3.5 Conclusion

Considered together, several BA analogues have emerged from the present study as potential protective agents against glutamate toxicity in the MIO-M1 Müller cell line. The analogues H5 and H7 and, to a lesser extent, H3, were capable of preventing ROS production, necrosis and the loss of cell viability. The underlying mechanism was

related to attenuation of the glutamate-mediated activation of Akt/MAPK signaling cascades that regulate cell death.

Declarations of interest

The authors declare no conflict of interest.

Acknowledgements

This study received funding support from the internal grants of the School of Pharmacy, the University of Sydney. Dr. Fanfan Zhou received the Equity Fellowship of the University of Sydney during the study.

References

1. Bringmann A, Pannicke T, Grosche J, Francke M, Wiedemann P, Skatchkov SN, et al. Müller cells in the healthy and diseased retina. PROG RETIN EYE RES. 2006;25(4):397-424.

2. Bringmann A, Grosche A, Pannicke T, Reichenbach A. GABA and glutamate uptake and metabolism in retinal glial (Müller) cells. FRONT ENDOCRINOL (LAUSANNE). 2013;4:48.

3. Bringmann A, Wiedemann P. Müller glial cells in retinal disease. OPHTHALMOLOGICA. 2012;227(1):1-19.

4. Coughlin BA, Feenstra DJ, Mohr S. Müller cells and diabetic retinopathy. VISION RES. 2017;139:93-100.

5. Subirada PV, Paz MC, Ridano ME, Lorenc VE, Vaglienti MV, Barcelona PF, et al. A journey into the retina: Müller glia commanding survival and death. EUR J NEUROSCI. 2018;47(12):1429-43.

6. Ishikawa M. Abnormalities in glutamate metabolism and excitotoxicity in the retinal diseases. SCIENTIFICA. 2013;2013.

7. Quigley HA, Broman AT. The number of people with glaucoma worldwide in 2010 and 2020. BR J OPHTHALMOL. 2006;90(3):262-7.

8. Muceniece R, Namniece J, Nakurte I, Jekabsons K, Riekstina U, Jansone B. Pharmacological research on natural substances in Latvia: Focus on lunasin, betulin, polyprenol and phlorizin. PHARMACOL RES. 2016;113(Pt B):760-70.

9. Rastogi S, Pandey MM, Kumar Singh Rawat A. Medicinal plants of the genus Betula--traditional uses and a phytochemical-pharmacological review. J ETHNOPHARMACOL. 2015;159:62-83.

10. Cavazos-Garduno A, Ochoa Flores AA, Serrano-Nino JC, Martinez-Sanchez CE, Beristain CI, Garcia HS. Preparation of betulinic acid nanoemulsions stabilized by omega-3 enriched phosphatidylcholine. ULTRASON SONOCHEM. 2015;24:204-13.

11. Mullauer FB, Kessler JH, Medema JP. Betulinic acid, a natural compound with potent anticancer effects. ANTICANCER DRUGS. 2010;21(3):215-27.

12. Cheng Z, Yao W, Zheng J, Ding W, Wang Y, Zhang T, et al. A derivative of betulinic acid protects human Retinal Pigment Epithelial (RPE) cells from cobalt chloride-induced acute hypoxic stress. EXP EYE RES. 2019;180:92-101.

13. Peng J, Lv Y-C, He P-P, Tang Y-Y, Xie W, Liu X-Y, et al. Betulinic acid downregulates expression of oxidative stress-induced lipoprotein lipase via the PKC/ERK/c-Fos pathway in RAW264. 7 macrophages. BIOCHIMIE. 2015;119:192-203.

14. Szuster-Ciesielska A, Kandefer-Szerszeñ M. Protective effects of betulin and betulinic acid against ethanol-induced cytotoxicity in HepG2 cells. PHARMACOL REP. 2005;57(5):588.

15. Zhu L, Yi X, Zhao J, Yuan Z, Wen L, Pozniak B, et al. Betulinic acid attenuates dexamethasone-

induced oxidative damage through the JNK-P38 MAPK signaling pathway in mice. BIOMED PHARMACOTHER. 2018;103:499-508.

16. Limb GA, Salt TE, Munro PM, Moss SE, Khaw PT. In vitro characterization of a spontaneously immortalized human Muller cell line (MIO-M1). INVEST OPHTHALMOL VIS SCI. 2002;43(3):864-9.

17. Zhang T, Gillies MC, Madigan MC, Shen W, Du J, Grünert U, et al. Disruption of de novo serine synthesis in Müller cells induced mitochondrial dysfunction and aggravated oxidative damage. MOL NEUROBIOL. 2018;55(8):7025-37.

18. Wright P, Kelsall J, Healing G, Sanderson J. Differential expression of cyclin-dependent kinases in the adult human retina in relation to CDK inhibitor retinotoxicity. ARCH TOXICOL. 2019, 93(3):1-13.

19. Netti V, Pizzoni A, Pérez-Domínguez M, Ford P, Pasantes-Morales H, Ramos-Mandujano G, et al. Release of taurine and glutamate contributes to cell volume regulation in human retinal Müller cells: differences in modulation by calcium. J NEUROPHYSIOL. 2018;120(3):973-84.

20. Ding W, Sun M, Luo S, Xu T, Cao Y, Yan X, et al. A 3D QSAR study of betulinic acid derivatives as anti-tumor agents using topomer CoMFA: model building studies and experimental verification. MOLECULES. 2013;18(9):10228-41.

21. Ding W, Zhang S, Zhu M, Wang S, Xu T, Qu H, et al. A 3D-QSAR Study on Betulinic Acid Derivatives as Anti-Tumor Agents and the Synthesis of Novel Derivatives for Modeling Validation. ANTICANCER AGENTS MED CHEM. 2017;17(4):566-75.

22. Wang K, Zhu X, Zhang K, Zhou F, Zhu L. Gas1 knockdown increases the neuroprotective effect of glial cell-derived neurotrophic factor against glutamate-induced cell injury in human SH-SY5Y neuroblastoma cells. CELL MOL NEUROBIOL. 2016;36(4):603-11.

23. Zhu X, Wang K, Yao Y, Zhang K, Zhou F, Zhu L. Triggering p53 activation is essential in ziyuglycoside I-induced human retinoblastoma WERI-Rb-1 cell apoptosis. J BIOCHEM MOL TOXICOL. 2018;32(1):e22001.

24. Zhu X, Wang K, Zhang K, Zhou F, Zhu L. Induction of oxidative and nitrosative stresses in human retinal pigment epithelial cells by all-trans-retinal. EXP CELL RES. 2016;348(1):87-94.

25. Wankun X, Wenzhen Y, Min Z, Weiyan Z, Huan C, Wei D, et al. Protective effect of paeoniflorin against oxidative stress in human retinal pigment epithelium in vitro. MOL VIS. 2011;17:3512.

26. Zhu X, Xue L, Yao Y, Wang K, Tan C, Zhuang M, et al. The FoxM1-ABCC4 axis mediates carboplatin resistance in human retinoblastoma Y-79 cells. ACTA BIOCHIM BIOPHYS SIN (SHANGHAI). 2018;50(9):914-20.

27. Zhang T, Gillies M, Wang Y, Shen W, Bahrami B, Zeng S, et al. Simvastatin Protects Photoreceptors from all-trans-retinal Induced Oxidative Stress with Up-regulation of Interphotoreceptor Retinoid Binding Protein. BR J PHARMACOL. 2019.

28. Wang K, Zhu X, Zhang K, Zhou F, Zhu L. Neuroprotective effect of tetramethylpyrazine against all-trans-retinal toxicity in the differentiated Y-79 cells via upregulation of IRBP expression. EXP CELL RES. 2017;359(1):120-8.

29. Godugu C, Patel AR, Doddapaneni R, Somagoni J, Singh M. Approaches to improve the oral bioavailability and effects of novel anticancer drugs berberine and betulinic acid. PLOS ONE. 2014;9(3):e89919.

30. Kumar P, Singh AK, Raj V, Rai A, Keshari AK, Kumar D, et al. Poly (lactic-co-glycolic acid)-loaded nanoparticles of betulinic acid for improved treatment of hepatic cancer: characterization, in vitro and in vivo evaluations. INT J NANOMEDICINE. 2018;13:975.

31. Udeani GO, Zhao GM, Geun Shin Y, Cooke BP, Graham J, Beecher CW, et al. Pharmacokinetics and tissue distribution of betulinic acid in CD-1 mice. BIOPHARM DRUG DISPOS. 1999;20(8):379-83.

32. Cassano T, Pace L, Bedse G, Michele Lavecchia A, De Marco F, Gaetani S, et al. Glutamate and mitochondria: two prominent players in the oxidative stress-induced neurodegeneration. CURR ALZHEIMER RES. 2016;13(2):185-97.

33. Li P, Shen M, Gao F, Wu J, Zhang J, Teng F, et al. An antagomir to microRNA-106b-5p ameliorates cerebral ischemia and reperfusion injury in rats via inhibiting apoptosis and oxidative stress. MOL NEUROBIOL. 2017;54(4):2901-2921.

34. Stanciu M, Wang Y, Kentor R, Burke N, Watkins S, Kress G, et al. Persistent activation of ERK contributes to glutamate-induced oxidative toxicity in a neuronal cell line and primary cortical neuron cultures. J BIOL CHEM. 2000;275(16):12200-6.

35. Yang E-J, Kim G-S, Jun M, Song K-S. Kaempferol attenuates the glutamate-induced oxidative stress in mouse-derived hippocampal neuronal HT22 cells. FOOD FUNCT. 2014;5(7):1395-402.

36. Bai X, Zhang C, Chen A, Liu W, Li J, Sun Q, et al. Protective effect of edaravone on glutamate-induced neurotoxicity in spiral ganglion neurons. NEURAL PLAST. 2016;2016.

37. Yu L, Wang N, Zhang Y, Wang Y, Li J, Wu Q, et al. Neuroprotective effect of muscone on glutamate-induced apoptosis in PC12 cells via antioxidant and Ca^{2+} antagonism. NEUROCHEM INT. 2014;70:10-21.

38. Yamagishi R, Aihara M. Neuroprotective effect of astaxanthin against rat retinal ganglion cell death under various stresses that induce apoptosis and necrosis. MOL VIS. 2014;20:1796.

39. Ji M, Miao Y, Dong L-D, Chen J, Mo X-F, Jiang S-X, et al. Group I mGluR-mediated inhibition of Kir channels contributes to retinal Müller cell gliosis in a rat chronic ocular hypertension model. J NEUROSCI. 2012;32(37):12744-55.

40. Ankarcrona M, Dypbukt JM, Bonfoco E, Zhivotovsky B, Orrenius S, Lipton SA, et al. Glutamate-induced neuronal death: a succession of necrosis or apoptosis depending on mitochondrial function. NEURON. 1995;15(4):961-73.

41. Hu X, Dai Y, Sun X. Parkin overexpression protects retinal ganglion cells against glutamate

excitotoxicity. MOL VIS. 2017;23:447.

42. Su W, Li Z, Jia Y, Zhuo Y. Rapamycin is neuroprotective in a rat chronic hypertensive glaucoma model. PLOS ONE. 2014;9(6):e99719.

43. Pasha SPBS, Münch R, Schäfer P, Oertel P, Sykes AM, Zhu Y, et al. Retinal cell death dependent reactive proliferative gliosis in the mouse retina. SCI REP. 2017;7(1):9517.

44. Bonfoco E, Krainc D, Ankarcrona M, Nicotera P, Lipton SA. Apoptosis and necrosis: two distinct events induced, respectively, by mild and intense insults with N-methyl-D-aspartate or nitric oxide/superoxide in cortical cell cultures. PROC NATL ACAD SCI U S A. 1995;92(16):7162-6.

45. Yoles E, Schwartz M. Elevation of intraocular glutamate levels in rats with partial lesion of the optic nerve. ARCH OPHTHALMOL. 1998;116(7):906-10.

46. Lucas D, Newhouse J. The toxic effect of sodium L-glutamate on the inner layers of the retina. AMA ARCH OPHTHALMOL. 1957;58(2):193-201.

47. Mitori H, Izawa T, Kuwamura M, Matsumoto M, Yamate J. Developing stage-dependent retinal toxicity induced by L-glutamate in neonatal rats. TOXICOL PATHOL. 2016;44(8):1137-45.

48. Quincozes-Santos A, Bobermin LD, Tramontina AC, Wartchow KM, Tagliari B, Souza DO, et al. Oxidative stress mediated by NMDA, AMPA/KA channels in acute hippocampal slices: neuroprotective effect of resveratrol. TOXICOL IN VITRO. 2014;28(4):544-51.

49. Görlach A, Dimova EY, Petry A, Martínez-Ruiz A, Hernansanz-Agustín P, Rolo AP, et al. Reactive oxygen species, nutrition, hypoxia and diseases: problems solved? REDOX BIOL. 2015;6:372-85.

50. Boulton TG, Nye SH, Robbins DJ, Ip NY, Radzlejewska E, Morgenbesser SD, et al. ERKs: a family of protein-serine/threonine kinases that are activated and tyrosine phosphorylated in response to insulin and NGF. CELL. 1991;65(4):663-75.

51. Irving EA, Bamford M. Role of mitogen-and stress-activated kinases in ischemic injury. J CEREB BLOOD FLOW METAB. 2002;22(6):631-47.

52. Almasieh M, Wilson AM, Morquette B, Vargas JLC, Di Polo A. The molecular basis of retinal ganglion cell death in glaucoma. PROG RETIN EYE RES. 2012;31(2):152-81.

53. Sweatt JD. The neuronal MAP kinase cascade: a biochemical signal integration system subserving synaptic plasticity and memory. J NEUROCHEM. 2001;76(1):1-10.

54. Shiflett MW, Balleine BW. Contributions of ERK signaling in the striatum to instrumental learning and performance. BEHAV BRAIN RES. 2011;218(1):240-7.

55. Roth S, Shaikh AR, Hennelly MM, Li Q, Bindokas V, Graham CE. Mitogen-activated protein kinases and retinal ischemia. INVEST OPHTHALMOL VIS SCI.. 2003;44(12):5383-95.

56. Altmann C, Schmidt M. The role of microglia in diabetic retinopathy: inflammation, microvasculature defects and neurodegeneration. INT J MOL SCI. 2018;19(1):110.

57. Cargnello M, Roux PP. Activation and function of the MAPKs and their substrates, the MAPK-activated protein kinases. MICROBIOL MOL BIOL REV. 2011;75(1):50-83.

58. Glotin A-L, Calipel A, Brossas J-Y, Faussat A-M, Tréton J, Mascarelli F. Sustained versus transient ERK1/2 signaling underlies the anti-and proapoptotic effects of oxidative stress in human RPE cells. INVEST OPHTHALMOL VIS SCI. 2006;47(10):4614-23.
59. Mielke K, Herdegen T. JNK and p38 stresskinases—degenerative effectors of signal-transduction-cascades in the nervous system. PROG NEUROBIOL. 2000;61(1):45-60.
60. Brecht S, Kirchhof R, Chromik A, Willesen M, Nicolaus T, Raivich G, et al. Specific pathophysiological functions of JNK isoforms in the brain. EUR J NEUROSCI. 2005;21(2):363-77.
61. Manabe S-i, Lipton SA. Divergent NMDA signals leading to proapoptotic and antiapoptotic pathways in the rat retina. INVEST OPHTHALMOL VIS SCI. 2003;44(1):385-92.
62. Mejía-García TA, Portugal CC, Encarnação TG, Prado MAM, Paes-de-Carvalho R. Nitric oxide regulates AKT phosphorylation and nuclear translocation in cultured retinal cells. CELLULAR SIGNAL. 2013;25(12):2424-39.
63. Asomugha CO, Linn DM, Linn CL. ACh receptors link two signaling pathways to neuroprotection against glutamate-induced excitotoxicity in isolated RGCs. J NEUROCHEM. 2010;112(1):214-26.
64. Swartz MM, Linn DM, Linn CL. Tropisetron as a neuroprotective agent against glutamate-induced excitotoxicity and mechanisms of action. NEUROPHARMACOLOGY. 2013;73:111-21.
65. Tsutsumi T, Iwao K, Hayashi H, Kirihara T, Kawaji T, Inoue T, et al. Potential neuroprotective effects of an LSD1 inhibitor in retinal ganglion cells via p38 MAPK activity. INVEST OPHTHALMOL VIS SCI. 2016;57(14):6461-73.
66. Lv B, Huo F, Dang X, Xu Z, Chen T, Zhang T, et al. Puerarin Attenuates N-Methyl-D-aspartic Acid–induced Apoptosis and Retinal Ganglion Cell Damage Through the JNK/p38 MAPK Pathway. J GLAUCOMA. 2016;25(9):e792-e801.
67. Zheng S, Yang H, Chen Z, Zheng C, Lei C, Lei B. Activation of liver X receptor protects inner retinal damage induced by N-methyl-D-aspartate. INVEST OPHTHALMOL VIS SCI. 2015;56(2):1168-80.
68. Zhang Z, Hu F, Liu Y, Ma B, Chen X, Zhu K, et al. Activation of type 5 metabotropic glutamate receptor promotes the proliferation of rat retinal progenitor cell via activation of the PI-3-K and MAPK signaling pathways. NEUROSCIENCE. 2016;322:138-51.

Chapter 4

Evaluate the protective effect of Compritol liposome-encapsulated betulinic acid derivatives in human Müller and retinal pigmented epithelium (RPE) cells

Abstract

Retinal pigmented epithelium (RPE) and Müller cells are important retinal cells essential in maintaining the physiological activities of retina and vision. Their dysfunction can lead to many irreversible retinal diseases. Oxidation is a leading cause of retinal cell damage. Our previous studies identified several betulinic acid derivatives that are potent in protecting human RPE and Müller cells from oxidative stress. However, it is highly desired that these compounds can be favorably delivered into retinal cells so as to avoid unnecessary toxicity with enhanced efficacy. In the current study, we encapsulated the active betulinic acid derivatives (H3, H5 and H7) into the Compritol 888 or Compritol HD5 ATO liposomes and molecularly evaluated the cytoprotective effect of each liposome-based formulations in human RPE and Müller cell models. We found that greatly reduced dosage is required to achieve the desired anti-oxidative effects in liposome-based formulations compared to their free drugs. Campritol 888 ATO liposome encapsulated with H5 is relatively most potent in protecting MIO-M1 cells from glutamate-induced oxidative damage; while both H5 loaded liposome formulations pronouncedly inhibited the ROS production induced by $CoCl_2$ in ARPE-19 cells. The anti-oxidative effects of H3 and H5 were greatly enhanced compare to their free drugs when delivered in liposome formulations in ARPE-19 cells. Furthermore, liposome-based formulations particularly the Compritol 888 ATO liposome enabled slow release of the betulinic acid derivatives and achieved prolonged effects. Overall, liposome-based nano-particles are promising drug delivery carriers for betulinic acid derivatives with an improved cellular protective effect against oxidative stress in human RPE and Müller cells.

4.1 Introduction

Retinal pigmented epithelium (RPE) and Müller cells are essential for retinal metabolism, homeostasis, visual signal transfer, vision maintenance and retinal neuron support (1-3). The dysfunction of either of these cells will lead to retinal diseases such as diabetic retinopathy (DR), age-related macular degeneration (AMD), choroidal neovascularization (CNV) and retinopathy of prematurity (ROP) (2). Although some of the pathologies can be managed by clinical treatments such as laser, surgery, anti-VEGF drugs, the therapeutic outcomes are unsatisfied and none of diseases can be cured. Nevertheless, it is emerged that cellular protective agents can be used to prevent retinal cell damage and reduce the risk of retinal disease progression.

As mentioned above in the our previously published studies (4, 5), we reported the anti-oxidative effects of betulinic acid and its derivatives on retinal cells and have confirmed the cytoprotective potentials of several candidates, in particular H3, H5 and H7. However, it was noticed that the effective concentrations of these compounds are no less than 5 μM. In practice, such plasma concentration is hard to achieve clinically in the retina; therefore it is expected that nano-technology could be adopted to improve drug delivery efficiency.

In the past decade, nanodrug systems have shown great potentials to delivery drugs by increasing efficacy, stability, bioavailability and solubility (6). Among all the nanoscale drug delivery systems, liposome is a more preferred route of compound delivery. Liposome is a sphere-shaped vesicle consisting of one or more phospholipid bilayers and can be used to encapsulate both hydrophilic and hydrophobic compounds (7, 8). It is a clinically preferred compound delivery carrier because it has relatively better biocompatibility and biodegradability, lower toxicity, and controlled release of the entrapped drug, improved pharmacokinetic and pharmacodynamic performance, enhanced therapeutic effects of drugs with minimum side effects (7-11), thus liposomes have risen widespread research interests in the past few decades and have already been marketed and used clinically. There have been many studies reporting betulinic acid and its derivatives delivered in liposomes (7, 12-17), but no previous literature studied the anti-oxidative activity of liposome-formulated betulinic acid and its derivatives in the retina. In this section, we prepared two types of liposomes (Compritol 888 ATO and Compritol HD5 ATO liposomes) loaded with the active betulinic derivatives identified in the our previous studies, and evaluated their protective effects on MIO-M1 and ARPE-19 cells against oxidative stress.

4.2 Materials and methods

4.2.1 Reagents and chemicals

Dulbecco's Modified Eagle Medium (DMEM), L-glutamine, AlamarBlue™ Cell Viability Reagent, Calcein-AM, CM-H_2DCFDA, 2-6 mL Pierce™ protein concentrator PES 100K MWCO and Fetal Bovine Serum (FBS) were purchased from Thermo Scientific (Lidcombe, NSW, Australia).Glutamic acid monosodium salt hydrate and cobalt chloride were purchased from Sigma-Aldrich (Castle Hill, NSW, Australia). Betulinic acid derivatives H3, H5 and H7 were synthesized in house. Compritol 888 ATO and Compritol HD5 ATO were purchased from Gattefossé S. A. (France), Pluronic F127 was purchased from BASF (Australia).

4.2.2 Liposome preparations

Liposomes were fabricated using micro-emulsion method. To make 50 mL formulation, 400 mg Compritol 888 ATO (lipid phase) was heated above the melting point (80 – 90°C).10 mL aqueous phase containing Pluronic F127 was heated to the same temperature. The aqueous phase was then dispersed in the melted lipid while the temperature was maintained at 80 °C. The mixture was next homogenized using homogenizer (D1000 Hand-Held Homogenizer, Benchmark Scientific; Edison, NJ, USA) in hot condition for 5 min at 5000 rpm to obtain hot oil in water (O/W) micro-emulsion. Next, the hot microemulsion was dispersed/diluted in water at the temperature of 2-4 °C under stirring conditions (6,000-8,000 rpm), which resulted in the formation of the liposome.

To encapsulate the drug, 0.0027 g H3 or 0.0023 g H5 or 0.0028 g H7 powder was mixed with the melted lipid phase before mixing with the aqueous phase.

Another type of lipid Compritol HD5 ATO was used for preparation of Compritol HD5 ATO liposome with the same procedure.

4.2.3 Particle size and concentration measurement

The size distribution and concentration of liposomes made from Compritol 888 ATO (named as 888 liposomes) and Compritol HD5 ATO (named as HD5 liposomes) were determined by using Nanosight NS300 system (Malvern Panalytical, Australia).

Liposomes were diluted 5,000 times with MilliQ water, 1 mL diluted sample was infused into the machine and the particle size was measured at 25 ℃. Three measurements were performed for each liposome, the mode value was used as the mean size of the liposomes.

4.2.4 Zeta potential measurement

The zeta potential values of two types of liposomes were determined with Zetasizer Nano ZS (Malvern Panalytical, Australia). 1 mL liposome sample was added into a polystyrene cuvette, then the zeta potential was measured. Measurements were repeated independently for twelve times. Then mean value was used as the mean zeta potential of liposomes.

4.2.5 Encapsulation efficiency (EE%) measurement

The amount of betulinic acid derivatives encapsulated in two types of liposomes was determined with ultra-high performance liquid chromatography (UPLC, shimadzu, Nexera X2, Australia). Liposomes were centrifuged with 100K centrifuge tubes at 4,400 rpm for 30 min, the supernatant sample was measured for free drugs with UPLC.

The liposome formulation was vortexed with 2 folds of methanol (v/v) for releasing the encapsulated drug, then centrifuged at 15,000 rpm for 20 min. Supernatant was collected and filtered with 0.45 μm membrane before UPLC detection.

The amount of betulinic acid derivatives was measured using a reverse C18 column (Phenomenex, 250×4.60 mm, 5 μm). The mobile phase consisted of acetonitrile and water (90:10 v/v, pH=2.5 with trifluoroacetate) with the flow rate of 1 mL/min. The injection volume was 20 μL and the detection wavelength was 210 nm. The encapsulation efficiency (EE%) was calculated according to the following equation:

$$EE\% = (W_{drug} \text{ in unprocessed formulation} - W_{drug} \text{ in supernatant}) / W_{drug} \text{ for preparation} \times 100\%$$

The H compound concentration in the liposome formulation was calculated according to the following equation:

$$C_{drug} = W_{drug} \text{ for preparation} / (\text{Molecular weight} \times V_{formulation}) \times EE\%$$

4.2.6 Cell culture

MIO-M1 and ARPE-19 cells were cultured in 37 ℃ and 5% CO_2 with DMEM plus 10% FBS (v/v) and 1% L-glutamine (v/v).

4.2.7 Anti-oxidative assays on MIO-M1 cells

MIO-M1 cells were seeded into 96-well plates (1×10^4 cells/well) and maintained overnight, cells were then treated with 888 and HD5 liposomes with and without betulinic acid derivatives (diluted for 100 and 200 times) in DMEM containing 1% FBS (v/v) for 24 h, 48 h and 72 h. Blank liposomes with the same dilution were served as negative control. Cell were further treated with 300 mM glutamate for 4 h (4) before Alamar blue assay. Cell viability was evaluated according to the manufacturer's manual. AlamarBlue^{TM} Cell Viability Reagent was diluted 10 times with DMEM and incubated with cells in dark for 2 h. The plate was measured at Ex/Em: 550/590 nm with PerkinElmer Victor^{TM} X4 Multimode plate reader (PerkinElmer, Melbourne, VIC, Australia).

Cell viabilities was also verified with Calcein-AM assay after glutamate incubation. Cells were washed with PBS once and then incubated in dark with 2 μM Calcein-AM for 30 min. The fluorescence was measured at Ex/Em: 485/535 nm, readings were corrected by subtraction of that in Calcein-AM free cells.

4.2.8 Anti-oxidative assays on ARPE-19 cells

ARPE-19 cells were seeded into 96-well plates (2×10^4 cells/well) and maintained overnight, cells were then treated with 888 and HD5 liposomes with and without betulinic acid derivatives (diluted for 100 and 200 times) in DMEM containing 1% FBS (v/v) for 24 h, 48 h and 72 h. Blank liposomes with the same dilution were served as negative control. Cell were further treated with 8 mM $CoCl_2$ for 4 h before MTT assay (5): Cells were incubated with 0.5 mg/mL MTT solution for 2 h in dark and washed with PBS. 100 μL DMSO was then added into each well and shake at room temperature for 10 min. The absorbance was measured at 550 nm with the BioRad Model 680 microplate reader (Bio-rad, Gladesville, NSW, Australia).

4.2.9 Measurement of reactive oxygen species (ROS) on ARPE-19 cells

ARPE-19 cells were seeded in 96-well plates (2×10^4 cells/well) and cultured overnight, cells were then treated with 888 and HD5 liposomes with and without betulinic acid derivatives (diluted for 100 and 200 times) in DMEM containing 1% FBS (v/v) for 24 h, 48 h and 72 h. Blank liposome and PEGylated liposome were served as negative control. Cell were further treated with 8 mM $CoCl_2$ for 4 h (5), then incubated with 1 μM CM-H_2DCFDA reagent for 40 min in dark at 37℃. Afterwards, cells were washed with PBS for three times and measured at Ex/Em: 485/535 nm. The ROS ratio was calculated as the fold of corresponding liposome control.

4.2.10 Statistics

All the data are shown as mean ± standard deviation (SD). Two-way ANOVA was used to compare liposome treated groups vs. corresponding liposome control group. $p<0.05$ was considered as significant.

4.3 Results

4.3.1 Characterization of Compritol 888 ATO and Compritol HD5 ATO liposome encapsulated with betulinic acid derivatives

The size, particle concentration, zeta potential, polydispersity index (PDI) value and encapsulation efficiency (EE%) of Compritol 888 ATO and Compritol HD5 ATO liposomes loaded with H3, H5, H7 or vehicle are listed in Table 4.1 and Table 4.2.

The size of the two types of compound-loaded liposomes are similar and narrowly distributed between 50-70 nm. PDI values are below 0.3, suggesting that all types of liposomes are uniformly distributed with minimal aggregation.

In general, zeta potentials are all negative and higher than -30 mV, which indicated the good stability of all the liposome preparations. For the Compritol 888 ATO liposomes, H3 encapsulation didn't change the zeta potential; while the entrapment of H5 and H7 both decreased the charge. The Compritol HD5 ATO control liposome possesses relatively higher zeta potential compared to that of Compritol 888 ATO formulation. H7 encapsulation didn't change the zeta potential in this type of liposome,

but the charge dramatically increased when H3 and H5 were loaded. As zeta potential is determined by liposome surface chemistry and medium properties such as pH and ionic strength, such changes may be due to compound characteristics.

In this study, Pluronic F127 (Poloxamer 407) was used as surfactant for both types of liposomes. Surfactants can not only assist the formation of solid liposome nanoparticles but also stabilize the nano-structure and prevent coagulation (18). In Compritol 888 ATO liposome formulation, surfactants can also help to prevent liposome polymorphic transition (19).

All the drug-loaded liposomes showed relatively high EE% compared to parental liposome preparations, which indicated that the betulinic derivatives used in this study are suitable for liposome preparation with Compritol 888 ATO and Compritol HD5 ATO. And the different EE% values among the three betulinic acid derivative formulations may be due to the diverse physiochemical properties of lipids and compounds.

Table 4.1 Physicochemical properties of 888 ATO and HD5 ATO liposomes loaded with H3, H5 and H7

Sample	Size(nm)	Particle concentration (particles/mL)	Zeta potential (mV)	PDI
888 liposome Control	53.6±9.3	$9.50\times10^{11}\pm1.86\times10^{11}$	-17.60±6.31	0.294
888 with H3	58.4±10.2	$1.70\times10^{12}\pm2.13\times10^{11}$	-17.90±5.70	0.262
888 with H5	58.5±9.8	$1.57\times10^{12}\pm4.70\times10^{11}$	-6.45±5.58	0.246
888 with H7	58.7±6.1	$2.34\times10^{12}\pm1.81\times10^{11}$	-9.84±3.40	0.222
HD5 liposome Control	52.5±3.4	$2.26\times10^{12}\pm2.39\times10^{11}$	-7.51±5.76	0.231
HD5 with H3	66.6±8.7	$1.94\times10^{12}\pm2.69\times10^{11}$	-20.90±6.40	0.288
HD5 with H5	56.4±1.7	$2.60\times10^{12}\pm2.22\times10^{11}$	-12.40±4.80	0.231

HD5 with H7	50.2±7.7	$1.52\times10^{12}\pm1.23\times10^{11}$	-9.71±4.09	0.256

Table 4.2 Encapsulation efficiency (EE%) and H compound concentration of 888 ATO and HD5 ATO liposomes loaded with H3, H5 and H7

Sample	EE%	H compound concentration in the liposome formulation (μM)
888 liposome Control		
888 with H3	78.55	78.55
888 with H5	75.10	75.10
888 with H7	55.27	55.27
HD5 liposome Control		
HD5 with H3	76.23	76.23
HD5 with H5	58.92	58.92
HD5 with H7	48.30	48.30

4.3.2 Protective effects of liposomes encapsulated with betulinic acid derivatives in the MIO-M1 cells against glutamate-induced oxidative stress

In accordance with our previous study (4), we used glutamate to mimic the excitotoxicity in MIO-M1 cells. Alamar blue and Calcein-AM assays were applied to test the cytoprotective effect of the two types of liposomes loaded with betulinic acid derivatives. The viability of cells exposed to liposome treatment are listed in Table 4.3-Table 4.7. In our previous study (4), H3, H5 and H7 showed potent antioxidative effects

on MIO-M1 cells from 24 h to 72 h in Calcein-AM assay (Fig. 3.3); therefore we selected 24 h, 48 h and 72 h as the time points to evaluate the cytoprotective effect of liposome preparations. Considering the accumulative toxicity with repetitive dosages (data now shown), we only applied single treatment on cells and incubated for 24 h, 48 h or 72 h.

In Alamar blue assay (Table 4.3 and Table 4.4), both dilutions (×100 and ×200) for all the liposomes didn't show significant cytotoxicity at any time points. The control 888 ATO and HD5 ATO liposomes had no effect on cells against $CoCl_2$-induced oxidative stress (data not shown). No liposomes loaded with drugs exhibited cytoprotective effects at 24 h. However, significant cellular protective effect was observed upon the treatment of H5 888 ATO liposome with ×100 dilution at 48 h, H3 888 ATO liposome with ×100 dilution, H5 888 ATO liposome with ×100 and ×200 dilutions at 72 h. In contrast, for HD5 ATO liposomes, only the one loaded with H5 with ×200 dilution had moderate cellular protective effect at 48 h.

Next, the liposome formulations and experimental conditions shown cytoprotective activities in Alamar blue assay were selected to be assessed using Calcein-AM assay (Table 4.5 and Table 4.6). We only observed that H5 888 ATO liposome with ×100 dilution restored cell viability significantly compared to the corresponding liposome control (91.8±8.6 % of H5 888 ATO liposome *vs*. 62.3±12.0% of control) at 48 h. However, none of the liposome formulations showed anti-oxidative activity at 72 h.

The pronounced effect of liposome-based formulations was also compared to the corresponding free drugs. Noteworthy, the concentration of free drugs to be used were calculated as to EE% and drug amounts added when preparing the liposome-based compound formulations. As listed in Table 4.2, H3 has the highest concentration (nearly 80 μM in both formulations), thus it is estimated that the actual concentration of encapsulated compounds should be no more than 0.8 μM (×100 dilution) and 0.4 μM (×200 dilution) in all the liposome formulations, these two concentrations was chosen for free drugs to compare the cyto-protective effect with their liposomal forms.

MIO-M1 cells were treated with 0.8 μM or 0.4 μM of H3 or H5 in the form of free drugs. The viability of cells exposed to free drugs was evaluated using the Calcein-AM assay (Table 4.7). In Chapter 3 (4), we performed the concentration and time dependent assay of H3, H5 and H7, all the compounds showed anti-oxidative effect at minimum of 5 μM. As we expected, compared to their liposome formulations, the free drugs didn't show any cellular protective effects under the current treatment condition.

Table 4.3 Cell viability of 888 ATO liposomes with or without glutamate in MIO-M1 cells (Alamar blue assay)

MIO-M1 cells were treated with 888 ATO liposomes loaded with H3, H5 and H7 (×100 and ×200 dilution), then incubated for 24 h, 48 h and 72 h, followed by 300 mM glutamate for additional 4 h. Cell viability was evaluated with Alamar blue assay. Data was presented as the percentage of cell viability to that of cells treated with liposome with the same dilution. #p<0.05, ##p<0.01, ###p<0.001, two-way ANOVA.

Treatment	24h viability (%)	48h viability (%)	72h viability (%)
888 lipoosme Control ×100	100.0±6.5	100.0±6.7	100.0±2.5
888 liposome Control ×100 +glutamate	65.3±4.5	65.2±5.8	51.2±1.5
888 with H3 ×100	106.6±8.4	105.1±7.7	99.6±6.2
888 with H3 ×100 +glutamate	74.8±5.9	78.5±5.7	60.7±3.4##
888 with H5×100	103.3±1.3	103.5±5.6	103.6±4.5
888 with H5 ×100 +glutamate	70.5±4.5	81.2±4.6#	67.8±4.0###
888 with H7 ×100	99.1±6.2	97.6±10.4	98.4±1.4
888 with H7×100 +glutamate	69.1±8.5	61.2±1.7	56.8±0.9
888 liposome Control ×200	100.0±0.9	100.0±7.5	100.0±2.8
888 liposome Control ×200+glutamate	75.7±0.4	68.4±9.5	56.0±2.7
888 with H3 ×200	108.0±3.6	112.6±6.2	103.0±3.5
888 with H3×200 +glutamate	76.9±3.8	79.0±9.0	64.0±6.5
888 with H5 ×200	91.2±4.2	104.5±8.6	105.6±6.1
888 with H5×200 +glutamate	74.8±4.4	84.3±5.4	69.6±4.3#
888 with H7 ×200	85.6±1.2	102.4±7.4	96.7±3.8
888 with H7×200 +glutamate	68.8±2.9	73.1±2.8	58.5±3.4

Table 4.4 Cell viability of HD5 ATO liposomes with or without glutamate in MIO-M1 cells (Alamar blue assay)

MIO-M1 cells were treated with HD5 liposomes loaded with H3, H5 and H7 (×100 and ×200 dilution), then incubated for 24 h, 48 h and 72 h, followed by 300 mM glutamate for additional 4 h. Cell viability was evaluated with Alamar blue assay. Data was presented as the percentage of cell viability to that of cells treated with liposome with the same dilution. #p<0.05, two-way ANOVA.

Treatment	24h viability (%)	48h viability (%)	72h viability (%)
HD5 liposome Control ×100	100.0±6.5	100.0±8.2	100.0±7.3
HD5 liposome Control ×100+glutamate	65.3±4.5	68.2±3.8	54.5±5.7
HD5 with H3 ×100	106.4±3.6	111.9±9.8	105.3±1.9
HD5 with H3 ×100 +glutamate	81.9±6.6	84.0±5.5	66.7±5.3
HD5 with H5×100	90.9±7.0	106.0±9.1	104.6±8.0
HD5 with H5 ×100 +glutamate	71.5±2.4	79.6±5.9	67.8±9.1
HD5 with H7 ×100	91.0±5.6	99.6±5.3	100.9±2.3
HD5 with H7×100 +glutamate	71.7±4.2	61.4±2.6	57.4±5.6
HD5 liposome Control ×200	100.0±5.6	100.0±5.7	100.0±6.1
HD5 liposome Control ×200+glutamate	65.2±2.3	60.5±4.8	58.5±3.1
HD5 with H3 ×200	99.6±1.7	107.0±8.2	104.6±2.9
HD5 with H3×200 +glutamate	71.5±3.5	77.0±4.6	66.3±6.5
HD5 with H5 ×200	90.1±6.4	109.0±5.1	106.4±3.5
HD5 with H5×200 +glutamate	59.7±6.2	84.4±7.3#	67.0±7.6
HD5 with H7 ×200	87.0±4.7	97.5±8.7	101.2±2.2
HD5 with H7×200 +glutamate	60.3±5.8	65.6±0.6	58.4±1.2

Table 4.5 Cell viability of 888 ATO liposomes with or without glutamate in MIO-M1 cells (Calcein-AM assay)

MIO-M1 cells were treated with 888 ATO liposomes loaded with H3 and H5 (×100 dilution), then incubated for 48 h and 72 h, followed by 300 mM glutamate for additional 4 h. Cell viability was evaluated with Calcein-AM assay. Data was presented as the percentage of cell viability to that of cells treated with liposome with the same dilution. ##p<0.01, two-way ANOVA.

Treatment	48h viability (%)	72h viability (%)
888 liposome Control ×100	100.0±9.7	100.0±5.0
888 liposome Control ×100+glutamate	62.3±12.0	35.9±9.1
888 with H3×100		102.0±6.7
888 with H3×100 +glutamate		36.6±6.4
888 with H5×100	106.0±1.7	102.0±6.7
888 with H5 ×100 +glutamate	91.8±8.6##	36.6±6.4
888 with Control ×200		100.0±6.4
888 with Control ×200 +glutamate		32.7±3.3
888 with H5 ×200		103.1±12.3
888 with H5 ×200 +glutamate		43.5±8.8

Table 4.6 Cell viability of HD5 ATO liposomes with or without glutamate in MIO-M1 cells (Calcein-AM assay)

MIO-M1 cells were treated with HD5 ATO liposomes loaded with H5 (×200 dilution), then incubated for 48 h, followed by 300 mM glutamate for additional 4 h. Cell viability was evaluated with Calcein-AM assay. Data was presented as the percentage of cell viability to that of cells treated with liposome with the same dilution.

Treatment	48h viability (%)
HD5 liposome Control ×200	100.0±7.5
HD5 liposome Control×200 +glutamate	51.1±7.2
HD5 with H5 ×200	114.8±8.5
HD5 with H5×200 +glutamate	51.5±8.9

Table 4.7 Cell viability of free H3 and H5 with or without glutamate in MIO-M1 cells (Calcein-AM assay)

MIO-M1 cells were treated with 0.8 μM H3, 0.8 μM H5 and 0.4 μM H5, then incubated for 48 h and 72 h, followed by 300 mM glutamate for additional 4 h. Cell viability was evaluated with Calcein-AM assay. Data was presented as the percentage of cell viability to that of cells treated with medium.

Treatment	48h viability (%)	72h viability (%)
Control	100.0±4.3	100.0±3.0
Control+glutamate	69.7±2.8	51.7±8.0
H3 0.8 μM		106.2±9.4
H3 0.8 μM+glutamate		39.3±4.9
H5 0.8 μM	115.8±8.2	106.8±1.5
H5 0.8 μM+glutamate	56.0±4.7	60.2±2.7
H5 0.4 μM	117.8±7.7	98.8±6.1
H5 0.4 μM+glutamate	53.2±5.1	52.9±3.4

4.3.3 888 ATO and HD5 ATO liposomes loaded with betulinic acid derivatives showed no antioxidative effect in ARPE-19 cells stressed with $CoCl_2$

As we previously reported (5), $CoCl_2$ could lead to hypoxia in ARPE-19 cells with inducing oxidative stress. We treated ARPE-19 cells with all the liposome formulations as to the same experimental conditions adopted in MIO-M1 cells above and applied MTT method to further explore the toxicity and cytoprotective potential of liposome-based formulations. The viabilities of two types of liposomes were shown in Table 4.8 and Table 4.9. However, we didn't observe anti-oxidative effects in any types of

liposomes in ARPE-19 cells.

Table 4.8 Cell viability of 888 ATO liposomes with or without $CoCl_2$ in ARPE-19 cells (MTT assay)

ARPE-19 cells were treated with 888 ATO liposomes loaded with H3, H5 and H7 (×100 and ×200 dilution), then incubated for 24 h, 48 h and 72 h, followed by 8 mM $CoCl_2$ for additional 4 h. Cell viability was evaluated with MTT assay. Data was presented as the percentage of cell viability to that of cells treated with liposome with the same dilution.

Treatment	24h viability (%)	48h viability (%)	72h viability (%)
888 lipoosme Control ×100	100.1±2.2	100.0±4.2	100.0±7.7
888 liposome Control ×100 +$CoCl_2$	47.4±1.7	41.3±1.5	36.3±0.1
888 with H3 ×100	97.8±3.2	109.7±3.6	90.7±1.6
888 with H3 ×100 + $CoCl_2$	48.5±0.5	41.1±1.3	36.5±0.9
888 with H5×100	100.1±2.3	103.7±4.8	84.6±4.6
888 with H5 ×100 + $CoCl_2$	48.3±3.0	38.3±2.3	32.7±1.4
888 with H7 ×100	102.3±3.9	97.3±4.3	101.2±3.0
888 with H7×100 + $CoCl_2$	47.4±1.7	37.3±2.1	34.3±0.8
888 liposome Control ×200	99.9±5.3	99.9±5.0	100.0±3.2
888 liposome Control ×200+ $CoCl_2$	50.9±2.8	38.5±0.8	32.7±1.4
888 with H3 ×200	94.4±6.8	105.9±8.6	98.5±3.3
888 with H3×200 + $CoCl_2$	51.6±2.4	42.4±0.7	36.3±4.7
888 with H5 ×200	100.4±8.9	105.7±5.7	86.3±1.2
888 with H5×200 + $CoCl_2$	49.1±2.5	43.3±2.1	35.8±2.6
888 with H7 ×200	90.8±2.7	97.3±4.0	89.8±2.1

888 with H7×200 + $CoCl_2$	49.9±3.6	41.9±1.0	33.8±1.0

Table 4.9 Cell viability of HD5 liposomes with or without $CoCl_2$ in ARPE-19 cells (MTT assay)

ARPE-19 cells were treated with HD5 liposomes loaded with H3, H5 and H7 (×100 and ×200 dilution), then incubated for 24 h, 48 h and 72 h, followed by 8 mM $CoCl_2$ for additional 4 h. Cell viability was evaluated with MTT assay. Data was presented as the percentage of cell viability to that of cells treated with liposome with the same dilution.

Treatment	24h viability (%)	48h viability (%)	72h viability (%)
HD5 liposome Control ×100	100.0±3.0	100.0±4.3	100.0±2.0
HD5 liposome Control ×100+ $CoCl_2$	42.0±0.9	44.3±2.1	35.6±0.2
HD5 with H3 ×100	104.2±2.5	96.7±11.4	96.6±2.3
HD5 with H3 ×100 + $CoCl_2$	42.8±2.8	44.6±0.4	37.9±0.7
HD5 with H5×100	93.9±5.2	97.7±2.0	92.7±2.8
HD5 with H5 ×100 + $CoCl_2$	36.6±1.5	37.5±1.1	31.3±0.4
HD5 with H7 ×100	95.7±2.8	112.0±6.9	111.8±2.0
HD5 with H7×100 + $CoCl_2$	36.6±1.1	39.5±1.0	31.4±1.5
HD5 liposome Control ×200	100.0±3.5	99.9±2.7	100.0±3.3
HD5 liposome Control ×200+ $CoCl_2$	40.4±2.6	52.0±1.9	38.9±1.0
HD5 with H3 ×200	101.6±9.6	125.6±8.5	110.6±8.7
HD5 with H3×200 + $CoCl_2$	43.2±5.7	58.5±2.4	42.1±1.6
HD5 with H5 ×200	107.5±8.2	131.8±4.5	94.5±4.7
HD5 with H5×200 + $CoCl_2$	43.1±0.5	51.2±3.7	38.2±0.6
HD5 with H7 ×200	110.0±9.4	133.2±15.4	116.9±6.2

HD5 with H7×200 + $CoCl_2$	40.6±2.2	55.8±1.9	38.8±1.5

4.3.4 888 ATO and HD5 ATO liposomes loaded with betulinic acid derivatives suppressed ROS production induced by $CoCl_2$ in ARPE-19 cells

$CoCl_2$ was reported to increase ROS production in the previous study (5). As presented in Table 4.10 and Table 4.11, we observed that the ROS production induced by $CoCl_2$ were significantly attenuated with the treatment of 888 ATO H5 formulation at ×200 dilution for 24 h; 888 ATO H5 formulation at ×100 dilution, 888 ATO H5 formulation at ×200 dilution for 48 h and 888 ATO H5 formulation at ×100 dilution at 72 h. In the case of HD5 ATO liposome (Table 4.11), HD5 ATO H3 formulation at ×100 dilution, HD5 ATO H5 formulation at ×100 dilution and HD5 ATO H7 formulation at ×100 dilution for 24 h, HD5 ATO H5 formulation at ×200 dilution and HD5 ATO H7 formulation at ×200 dilution for 48 h significantly inhibited ROS production upon $CoCl_2$ exposure. Our earlier study showed H7 was more potent in inhibiting $CoCl_2$-induced oxidative stress in ARPE-19 cells than H3 and H5 (5); with liposome embedded formulations, H3 and H5 had more pronounced anti-oxidative effect on ARPE-19 cells than H7. Furthermore, H5 in both liposome formulations showed consistent anti-oxidative effect, which indicated that the two liposome formulations used in this study may be favorable for H5 encapsulation with enhanced anti-oxidative effects.

Table 4.10 888 ATO liposomes loaded with betulinic acid derivatives suppressed ROS production induced by $CoCl_2$ in ARPE-19 cells

ARPE-19 cells were treated with 888 ATO liposomes loaded with H3, H5 and H7 (×100 and ×200 dilution), then incubated for 24 h, 48 h and 72 h, followed by 8 mM $CoCl_2$ for additional 4 h. ROS level was measured with CM-H_2DCFDA. Data was presented as folds of liposome control with the same dilution. #p<0.05, ##p<0.01, two-way ANOVA.

Treatment	24h ROS level	48h ROS level	72h ROS level
888 liposome Control ×100	1.00±0.03	1.00±0.07	1.00±0.04
888 liposome Control	2.06 ±0.19	4.22±0.09	4.82±0.09

×100+$CoCl_2$			
888 with H3 ×100	1.00±0.07	1.05±0.07	0.94±0.08
888 with H3 ×100 + $CoCl_2$	1.94±0.01	4.12±0.25	4.90±0.66
888 with H5×100	0.98±0.02	1.03±0.04	1.00±0.06
888 with H5 ×100 + $CoCl_2$	1.87±0.13	3.83±0.28#	4.40±0.12##
888 with H7 ×100	0.90±0.03	1.05±0.07	1.02±0.06
888 with H7×100 + $CoCl_2$	1.99±0.40	4.05±0.39	4.33±0.46
888 liposome Control ×200	1.00±0.04	1.00±0.01	1.00±0.03
888 liposome Control ×200+ $CoCl_2$	2.07±0.05	4.19±0.23	4.94±0.44
888 with H3 ×200	1.02±0.11	1.00±0.01	1.03±0.00
888 with H3×200 + $CoCl_2$	2.08±0.07	4.24±0.20	5.66±0.02
888 with H5 ×200	0.96±0.05	0.99±0.03	1.07±0.09
888 with H5×200 + $CoCl_2$	1.68±0.12##	3.67±0.05#	4.36±0.13
888 with H7 ×200	0.98±0.12	1.02±0.05	1.03±0.04
888 with H7×200 + $CoCl_2$	1.84±0.12	4.05±0.46	5.29±0.49

Table 4.11 HD5 ATO liposomes loaded with betulinic acid derivatives suppressed ROS production induced by $CoCl_2$ in ARPE-19 cells

ARPE-19 cells were treated with HD5 ATO liposomes loaded with H3, H5 and H7 (100 and 200 times dilution), then incubated for 24 h, 48 h and 72 h, followed by 8 mM $CoCl_2$ for additional 4 h. ROS level was measured with CM-H_2DCFDA. Data was presented as folds of liposome control with the same dilution. #p<0.05, ##p<0.01, ###p<0.001, two-way ANOVA.

Treatment	24h ROS level	48h ROS level	72h ROS level
HD5 liposome Control ×100	1.00±0.13	1.00±0.04	1.00±0.03
HD5 liposome Control	2.49±0.22	4.42±0.23	5.24±0.36

×100+ $CoCl_2$			
HD5 with H3 ×100	1.19±0.07	1.08±0.14	1.01±0.00
HD5 with H3 ×100 + $CoCl_2$	1.72±0.14###	4.29±0.28	5.58±0.49
HD5 with H5×100	0.81±0.04	1.01±0.01	0.97±0.10
HD5 with H5 ×100 + $CoCl_2$	1.60±0.27#	4.30±0.21	4.78±0.44
HD5 with H7 ×100	0.79±0.05	0.98±0.03	1.02±0.06
HD5 with H7×100 + $CoCl_2$	1.35±0.22##	4.36±0.47	5.33±0.82
HD5 liposome Control ×200	1.00±0.24	1.00±0.08	1.00±0.08
HD5 liposome Control ×200+ $CoCl_2$	1.47±0.19	5.64±0.51	6.57±0.57
HD5 with H3 ×200	0.71±0.05	1.03±0.04	1.20±0.17
HD5 with H3×200 + $CoCl_2$	1.33±0.17	5.20±0.07	6.79±0.32
HD5 with H5 ×200	1.30±0.00	0.99±0.04	1.08±0.02
HD5 with H5×200 + $CoCl_2$	1.67±0.24	4.20±0.26#	5.57±0.38
HD5 with H7 ×200	0.78±0.04	0.97±0.08	1.06±0.07
HD5 with H7×200 + $CoCl_2$	1.33±0.01	4.50±0.35#	7.02±2.17

4.4 Discussion

In this study, we prepared betulinic derivatives in liposome dosage formulations and examined their cytoprotective and antioxidative activities in MIO-M1 and ARPE-19 cells. We found several compound-loaded liposomes showed improved protective effects in both cell lines with sustained drug-releasing ability to some extent.

The Compritol 888 ATO liposome is a hydrophobic mixture of mono- (12-18% w/w), di- (45-54% w/w) and tri- (28-32% w/w) esters of behenic acid (C22) (19, 20). In pharmaceutical research, there are several types of liposomes potentially applicable for drug delivery including solid lipid microparticles (SLMs), solid lipid nanoparticles (SLNs) and nanostructured lipid carriers (NLCs). Among them, Compritol 888 ATO is the most commonly used lipid material (19). The complex composition and long carbon chain favorably improve drug entrapment efficiency (19). The Compritol HD5 ATO

liposome consists of mono, di-and triglycerides and PEG-8 mono-and di- esters of (C22) behenic acid (20). It is more hydrophilic than Compritol 888 ATO (19). Both Compritol 888 ATO and HD5 ATO have been utilized in ophthalmic drug delivery (21-26).

As to our previous report (4, 5), the betulinic acid derivatives H3, H5 and H7 are clinically relevant and were then encapsulated into liposomes. In the MIO-M1 cells, we used two cell viability assays to evaluate the cellular protective effects of liposomes against glutamate-induced oxidative stress. Alamar blue assay takes effect on the oxidation-reduction process while Calcein-AM analysis measures the activity of intracellular esterase. None of the liposome formulations was potent at 24 h (Table 4.3 -4.6). However, both liposomes entrapped with H5 showed significant anti-oxidative effects at 48 h, similarly in the case of 888 liposome with H3 and H5 at 72 h. 888 liposome loaded with H5 also showed significant cellular protective effects in Calcein-AM assay (Table 4.5). 888 liposome with H5 was considered to be the most potent anti-oxidative formulation as it consistently showed significant cellular protective effect in both assays, this might be explained by the prolonged drug release profile of Compritol 888 ATO (27-30).

Moreover, although H7 free drug showed relatively more potent anti-oxidative effect in the previous study (4), when it was encapsulated in these two types of liposome formulations, it didn't show enhanced anti-oxidative effect, which is likely related to its physiochemical property and its interactions with the two liposomes. H7 has the lowest EE%, which may because it has the lowest hydrophobicity in three compounds, and the low EE% further prohibits the releasing of H7 and consequently, impacts on its pharmacological performance in cells. Future study will need to evaluate the effectiveness of other types of liposome preparations in delivering H7.

In Chapter 3 (4), anti-oxidative evaluations of three compounds proved H5 has superior efficacy than H3, as H5 could suppress the activation of Akt, Erk and JNK pathways while H3 could only inhibit the activation of Erk, which may explain its potent effect.

In ARPE-19 cells, both 888 ATO and HD5 ATO liposomes showed no protective effect in MTT assay, but liposomes loaded with H3 and H5 significantly decreased ROS production in $CoCl_2$-treated cells at the estimated absolute compound concentrations of 0.8 μM and 0.4 μM (Table 4.10 and Table 4.11). Interestingly, as reported before (5), $CoCl_2$ can cause hypoxia in RPE and lead to ROS increase, and H7 was more effective in reducing ROS production compared to H3 and H5, which was different from that when they were applied as free drugs. This observation suggested that liposome encapsulation may have greatly improved the cellular delivery of H3 and H5 and enhanced their antioxidative potencies.

In addition, it was also noticed that the liposome-based betulinic acid derivatives especially those embed in 888 ATO liposomes had a trend of delayed response (effective at 48 or 72 h) in the current study; while the free drug was shown to be onset at 24 h (4, 5). This might be explained by the prolonged drug release profile of Compritol 888 ATO and HD5 ATO liposomes (27-30). It is expected that such liposome-based formations could be clinically beneficial with significantly lower dosages applied and extended drug half-lives achieved.

4.5 Conclusions

We assessed the anti-oxidative effect of the Compritol 888 and HD5 ATO liposome-based formulations of active betulinic acid derivatives H3, H5 and H7 in MIO-M1 and ARPE-19 cell lines. The cytoprotective and antioxidative effects of specific derivatives have been greatly enhanced in liposome-based formulations. Compritol 888 ATO liposome encapsulated with H5 is relatively the most potent formulation that significantly increase the viability of MIO-M1 cells exposed to glutamate; while both H5 loaded liposome formulations could potently inhibit the ROS production induced by $CoCl_2$ in ARPE-19 cells. And H3 and H5 had greatly improved pharmacologically effect compared to their free drugs against oxidative stress in ARPE-19 cells. Liposome-based formulations generally showed a prolonged drug release and delayed cellular effects, which can be clinically favorable. Overall, liposome-based nano-technology is a promising approach to improve cellular delivery of betulinic acid derivatives and enhance the efficacy of their antioxidative effect. Such formulations are desired to optimize delivery and improve pharmacology effects of agents that can prevent/treat retinal diseases.

References

1. Telegina D, Kozhevnikova O, Kolosova N. Changes in retinal glial cells with age and during development of age-related macular degeneration. BIOCHEMISTRY (MOSCOW). 2018;83(9):1009-17.
2. Araújo RS, Santos DF, Silva GA. The role of the retinal pigment epithelium and Müller cells secretome in neovascular retinal pathologies. BIOCHIMIE. 2018;155:104-8.
3. Hu D-N, Savage HE, Roberts JE. Uveal melanocytes, ocular pigment epithelium, and Müller cells in culture: in vitro toxicology. INT J TOXICOL. 2002;21(6):465-72.
4. Cheng Z, Zhang T, Zheng J, Ding W, Wang Y, Li Y, et al. Betulinic acid derivatives can protect human Müller cells from glutamate-induced oxidative stress. EXP CELL RES. 2019;383(1):111509.
5. Cheng Z, Yao W, Zheng J, Ding W, Wang Y, Zhang T, et al. A derivative of betulinic acid protects human Retinal Pigment Epithelial (RPE) cells from cobalt chloride-induced acute hypoxic stress. EXP EYE RES. 2019;180:92-101.
6. Merisko-Liversidge EM, Liversidge GG. Drug nanoparticles: formulating poorly water-soluble compounds. TOXICOL PATHOL. 2008;36(1):43-8.
7. Liu Y, Gao D, Zhang X, Liu Z, Dai K, Ji B, et al. Antitumor drug effect of betulinic acid mediated by polyethylene glycol modified liposomes. MATER SCI ENG C MATER BIOL APPL. 2016;64:124-32.
8. Akbarzadeh A, Rezaei-Sadabady R, Davaran S, Joo SW, Zarghami N, Hanifehpour Y, et al. Liposome: classification, preparation, and applications. NANOSCALE RES LETT. 2013;8(1):102.
9. Bulbake U, Doppalapudi S, Kommineni N, Khan W. Liposomal formulations in clinical use: an updated review. PHARMACEUTICS. 2017;9(2):12.
10. Yadav D, Sandeep K, Pandey D, Dutta R. Liposomes for drug delivery. J BIOTECHNOL BIOMATER. 2017;7:276.
11. Al-Jamal WT, Kostarelos K. Liposomes: from a clinically established drug delivery system to a nanoparticle platform for theranostic nanomedicine. ACC CHEM RES. 2011;44(10):1094-104.
12. Mullauer FB, van Bloois L, Daalhuisen JB, Ten Brink MS, Storm G, Medema JP, et al. Betulinic acid delivered in liposomes reduces growth of human lung and colon cancers in mice without causing systemic toxicity. ANTICANCER DRUGS. 2011;22(3):223-33.
13. Jin X, Yang Q, Cai N, Zhang Z. A cocktail of betulinic acid, parthenolide, honokiol and ginsenoside Rh2 in liposome systems for lung cancer treatment. NANOMEDICINE. 2019;15(1):41-54.
14. Liu Y, Zhang X, Liu Z, Wang L, Luo L, Wang M, et al. Gold nanoshell-based betulinic acid liposomes for synergistic chemo-photothermal therapy. NANOMED NANOTECHNOL BIOL MED. 2017;13(6):1891-900.

15. Csuk R, Barthel A, Kluge R, Ströhl D. Synthesis, cytotoxicity and liposome preparation of 28-acetylenic betulin derivatives. BIORG MED CHEM. 2010;18(20):7252-9.
16. Csuk R, Barthel A, Sczepek R, Siewert B, Schwarz S. Synthesis, encapsulation and antitumor activity of new betulin derivatives. ARCH PHARM. 2011;344(1):37-49.
17. Saneja A, Arora D, Kumar R, Dubey RD, Panda AK, Gupta PN. Therapeutic applications of betulinic acid nanoformulations. ANN N Y ACAD SCI. 2018;1421(1):5-18.
18. Kuo Y-C, Chung C-Y. Solid lipid nanoparticles comprising internal Compritol 888 ATO, tripalmitin and cacao butter for encapsulating and releasing stavudine, delavirdine and saquinavir. COLLOIDS SURF B BIOINTERFACES. 2011;88(2):682-90.
19. Aburahma MH, Badr-Eldin SM. Compritol 888 ATO: a multifunctional lipid excipient in drug delivery systems and nanopharmaceuticals. EXPERT OPIN DRUG DELIV. 2014;11(12):1865-83.
20. https://www.gattefosse.com.
21. Saettone M, Torracca M, Pagano A, Giannaccini B, Rodriguez L, Cini M. Controlled release of pilocarpine from coated polymeric ophthalmic inserts prepared by extrusion. INT J PHARM. 1992;86(2-3):159-66.
22. Gokce EH, Sandri G, Bonferoni MC, Rossi S, Ferrari F, Güneri T, et al. Cyclosporine A loaded SLNs: evaluation of cellular uptake and corneal cytotoxicity. INT J PHARM. 2008;364(1):76-86.
23. Gonzalez-Mira E, Nikolić S, Calpena AC, Egea MA, Souto EB, García ML. Improved and safe transcorneal delivery of flurbiprofen by NLC and NLC-based hydrogels. J PHARM SCI. 2012;101(2):707-25.
24. Hippalgaonkar K, Adelli GR, Hippalgaonkar K, Repka MA, Majumdar S. Indomethacin-loaded solid lipid nanoparticles for ocular delivery: development, characterization, and in vitro evaluation. J OCUL PHARMACOL THER. 2013;29(2):216-28.
25. Üstündağ-Okur N, Gökçe EH, Bozbıyık DI, Eğrilmez S, Özer Ö, Ertan G. Preparation and in vitro–in vivo evaluation of ofloxacin loaded ophthalmic nano structured lipid carriers modified with chitosan oligosaccharide lactate for the treatment of bacterial keratitis. EUR J PHARM SCI. 2014;63:204-15.
26. Niu M, Shi K, Sun Y, Wang J, Cui F. Preparation of CyA-loaded solid lipid nanoparticles and application on ocular preparations. J DRUG DELIV SCI TECHNOL. 2008;18(4):293-7.
27. Fini A, Cavallari C, Ospitali F, Gonzalez-Rodriguez ML. Theophylline-loaded compritol microspheres prepared by ultrasound-assisted atomization. J PHARM SCI. 2011;100(2):743-57.
28. Kuo Y-C, Chen H-H. Entrapment and release of saquinavir using novel cationic solid lipid nanoparticles. INT J PHARM. 2009;365(1-2):206-13.
29. Patlolla RR, Chougule M, Patel AR, Jackson T, Tata PN, Singh M. Formulation, characterization and pulmonary deposition of nebulized celecoxib encapsulated nanostructured lipid carriers. J CONTROLLED RELEASE. 2010;144(2):233-41.
30. Yan X, He H, Meng J, Zhang C, Hong M, Tang X. Preparation of lipid aspirin sustained-release

pellets by solvent-free extrusion/spheronization and an investigation of their stability. DRUG DEV IND PHARM. 2012;38(10):1221-9.

Chapter 5

Conclusions and future directions

5.1 Conclusions

As mentioned in Chapter 1, chemical modifications and formulation optimisation are two approaches to enhance drug therapeutic efficacy. In this thesis, we adopted both approaches to improve the clinical applications of betulinic acid in treating retinal pathologies.

In Chapter 2, we screened 20 betulinic analogues in ARPE-19 cells as to their anti-oxidative effect and found H7 is the most potent candidate compound. It can inhibit ROS induction, increase cell viability, prevent cellular apoptosis and necrosis. Furthermore, we reported that such cellular protective effect of H7 was mediated through the deactivation of Akt, Erk1/2 and JNK pathways upon oxidative stress. The observation was further consolidated with the confirmatory experiments on human primary RPE cells.

In Chapter 3, we found the betulinic acid derivatives H3, H5 and H7 can protect MIO-M1 from glutamate-triggered excitotoxicity. These compounds were all effective in reducing cellular necrosis. They could alleviate ROS production. The anti-oxidative effect of H5 and H7 were likely involved with the decreased phosphorylation of Akt, Erk1/2 and JNK signaling; while H3 mainly inhibited the activation of Erk1/2.

Overall, specific betulinic acid derivatives have more pronounced anti-oxidative effects than the parental compounds. Such effect was achieved via downregulating the Akt/MAPK pathways in both cell lines, which signaling may serve as therapeutic targets for treating/preventing retinal diseases. In Chapter 2 and Chapter 3, we identified specific betulinic acid derivatives that are promising candidates for protecting retinal cells from oxidative stress.

The accessibility of agents in the retina is a problem in practice. Therefore, we proved our concept that nano-technology is a solution to this in the Chapter 4. We prepared liposome-based formations of H3, H5 and H7 (Compritol 888 ATO and Compritol HD5 ATO) to increase their drug delivery efficacy. According to our molecular evaluations,

we observed greatly improved cellular anti-oxidative effects in specific liposome-compound formulations in both retinal cell models. We noticed that H3 and H5 liposome formulations obtained greatly improved anti-oxidative effect in ARPE-19 cells. In general, significantly reduced dosage is required for all three compounds when encapsulated in liposomes, to exert the desired pharmacological effects (more than 10 folds reduction). Moreover, prolonged drug release and extended half-lives were achieved in these compounds when embedded in liposomes. All these improved characteristics are favorable in clinical applications. Therefore, nano-technology is a feasible way to optimize drug performance.

5.2 Future directions

Although we have initially proved that nano-technology can potentially improve pharmacological performances of betulinic acid derivatives, further study is highly desired in the following aspects:

1. Further *in vitro* studies (eg. cell cycle, apoptosis/necrosis level) are needed to explore the protective and anti-oxidative effects of Compritol 888 ATO and Compritol HD5 ATO liposomes in ARPE-19 and MIO-M1 cells.
2. The drug efficacy, PK and PD profiles of Compritol 888 ATO and Compritol HD5 ATO liposomes are to be studied *in vivo*.
3. Optimization of liposome preparation and trials of other nano-particles will be required.
4. We used chemical stimulus ($CoCl_2$ and glutamate) to establish the acute oxidative retinal cell models in Chapter 2 and Chapter 3. Since retinal cells are also susceptible to other factors such as light exposure ischemia, inflammation, and more likely in a long-term exposure mode, it would be desirable to comprehensively elucidate the pharmacological potentials of betulinic acid derivatives on retinal cells upon chronically exposure to light or other stimulus.

Appendix Supplementary data for Chapter 3

Supplementary Table 1 Time dependence of the anti-oxidative effect of H3, H5 and H7 against glutamate-induced toxicity in MIO-M1 cells

(A) MIO-M1 cells were pre-treated with DMSO for 24 to 72 h, followed with or without 300 mM glutamate incubation for 4 h. Cell viability was then assessed with Calcein-AM assay. Data are presented as percentages of cell viability relative to the control without glutamate treatment.

Treatment	Cell viability (%) (AVG ± SD)
Control 24 h	100.0±7.6
Control 24 h+glutamate	48.0±2.5
Control 40 h	100.0±3.4
Control 40 h+glutamate	50.6±3.4
Control 48 h	100.0±2.1
Control 48 h+glutamate	45.3±4.6
Control 64 h	100.0±2.3
Control 64 h+glutamate	52.6±0.4
Control 72 h	100.0±7.6
Control 72 h+glutamate	54.4±3.0

(B) The anti-oxidative effect of the control group at different time points (a re-analysis of data in the Supplementary Table 1A). Data was calculated as the viability of cells treated with glutamate divided by that of cells treated without glutamate.

Treatment	Anti-oxidative effect (%) (AVG± SD)
Control 24 h	48.0±2.5
Control 40 h	50.6±3.4
Control 48 h	45.3±4.6
Control 64 h	52.6±0.4
Control 72 h	54.4±3.0

(C) MIO-M1 cells were pre-treated with 10 μM H3 for 24 to 72 h, followed with or without 300 mM glutamate incubation for 4 h. Cell viability was then assessed with Calcein-AM assay. Data are presented as percentages of cell viability relative to the control (DMSO treated only) without glutamate treatment.

Treatment	Cell viability (%) (AVG ± SD)
H3 24 h	112.0±6.5
H3 24 h+glutamate	67.9±1.4
H3 40 h	108.0±11.3
H3 40 h+glutamate	61.5±6.8
H3 48 h	115.7±4.4
H3 48 h+glutamate	79.8±6.5
H3 64 h	119.8±2.6
H3 64 h+glutamate	84.0±10.3
H3 72 h	118.9±9.9
H3 72 h+glutamate	75.5±8.5

(D) The anti-oxidative effect of the H3 group at different time points (a re-analysis of data in the Supplementary Table 1C). Data was calculated as the viability of cells treated with glutamate divided by that of cells treated without glutamate.

Treatment	Anti-oxidative effect (%) (AVG ± SD)
H3 24 h	60.6±1.2
H3 40 h	56.9±3.6
H3 48 h	69.0±5.6
H3 64 h	70.1±8.6
H3 72 h	65.9±7.2

(E) MIO-M1 cells were pre-treated with 10 μM H5 for 24 to 72 h, followed with or without 300 mM glutamate incubation for 4 h. Cell viability was then assessed with Calcein-AM assay. Data are presented as percentages of cell viability relative to the control (DMSO treated only) without glutamate treatment.

Treatment	Cell viability (%) (AVG± SD)
H5 24h	105.3±2.3
H5 24 h+glutamate	67.9±1.4
H5 40 h	108.0±11.3
H5 40 h+glutamate	61.5±6.8

H5 48 h	115.7±4.4
H5 48 h+glutamate	79.8±6.5
H5 64 h	119.8±2.6
H5 64 h+glutamate	84.0±10.3
H5 72 h	118.9±9.9
H5 72 h+glutamate	75.5±8.5

(F) The anti-oxidative effect of the H5 group at different time points (a re-analysis of data in the Supplementary Table 1E). Data was calculated as the viability of cells treated with glutamate divided by that of cells treated without glutamate.

Treatment	**Anti-oxidative effect (%) (AVG ± SD)**
H5 24 h	66.2±5.4
H5 40 h	70.0±10.3
H5 48 h	67.7±2.0
H5 64 h	83.5±9.3
H5 72 h	87.6±4.4

(G) MIO-M1 cells were pre-treated with 10 μM H7 for 24 to 72 h, followed with or without 300 mM glutamate incubation for 4 h. Cell viability was then assessed with Calcein-AM assay. Data are presented as percentages of cell viability relative to the control (DMSO treated only) without glutamate treatment.

Treatment	**Cell viability (%) (AVG ± SD)**
H7 24 h	136.9±2.2
H7 24 h+glutamate	98.5±13.2
H7 40 h	116.4±12.0
H7 40 h+glutamate	99.9±5.6
H7 48 h	129.4±6.6
H7 48 h+glutamate	107.4±15.3
H7 64 h	118.1±15.1
H7 64 h+glutamate	104.0±8.4
H7 72 h	125.8±9.6
H7 72 h+glutamate	115.9±5.9

(H) The anti-oxidative effect of the H7 group at different time points (a re-analysis of data in the Supplementary Table 1G). Data was calculated as the viability of cells treated with glutamate divided by that of cells treated without glutamate.

Treatment	Anti-oxidative effect (%) (AVG ± SD)
H7 24 h	71.9±9.6
H7 40 h	85.8±4.8
H7 48 h	86.5±9.1
H7 64 h	88.0±7.1
H7 72 h	92.1±4.7

Supplementary Table 2 Concentration dependence of the anti-oxidative effect of H3, H5 and H7 against glutamate-induced toxicity in MIO-M1 cells

(A) MIO-M1 cells were pre-treated with 0.5-20 μM H3 for 24 h, followed with or without 300 mM glutamate incubation for 4 h. DMSO was used as vehicle control. Cell viability was then assessed with Calcein-AM assay. Data was presented as the percentage of cell viability to that of DMSO treated cells.

Treatment	Cell viability (%) (AVG ± SD)
Control	100.0±5.5
Control + glutamate	49.3±10.6
H3 0.5 μM	103.8±8.7
H3 0.5 μM+glutamate	61.1±5.6
H3 1 μM	110.0±3.7
H3 1 μM+glutamate	61.1±4.1
H3 5 μM	108.6±2.8
H3 5 μM+glutamate	74.4±5.0
H3 10 μM	107.9±4.2
H3 10 μM+glutamate	73.5±2.7
H3 15 μM	121.5±3.8
H3 15 μM+glutamate	79.7±7.1
H3 20 μM	107.1±1.0
H3 20 μM+glutamate	77.8±7.4

(B) The anti-oxidative effect of the H3 group at different concentrations (a re-analysis of data in the Supplementary Table 2A). Data was calculated as the viability of cells treated with glutamate divided by that of cells treated without glutamate.

Treatment	Anti-oxidative effect (%) (AVG ± SD)
Control	49.3±10.6
H3 0.5 μM	58.9±5.4
H3 1 μM	55.6±3.8
H3 5 μM	68.5±4.6 ***
H3 10 μM	68.2±2.5 ***
H3 15 μM	65.7±5.8 *
H3 20 μM	72.7±6.9 *

p < 0.01,p<0.01, ***p < 0.001 vs. control, t-test.

(C) MIO-M1 cells were pre-treated with 0.5-20 μM H5 for 24 h, followed with or without 300 mM glutamate incubation for 4 h. DMSO was used as vehicle control. Cell viability was then assessed with Calcein-AM assay. Data was presented as the percentage of cell viability to that of DMSO treated cells.

Treatment	Cell viability (%) (AVG ± SD)
Control	100.0±7.7
Control + glutamate	43.3±9.0
H5 0.5 μM	102.5±7.3
H5 0.5 μM+glutamate	50.2±5.4
H5 1 μM	117.5±8.5
H5 1 μM+glutamate	46.0±7.6
H5 5 μM	99.2±10.8
H5 5 μM+glutamate	56.7±11.0
H5 10 μM	98.4±10.5
H5 10 μM+glutamate	61.6±11.9
H5 15 μM	100.1±8.8
H5 15 μM+glutamate	71.2±10.1
H5 20 μM	92.2±7.4
H5 20 μM+glutamate	71.5±8.1

(D) The anti-oxidative effect of the H5 group at different concentrations (a re-analysis of data in the Supplementary Table 2C). Data was calculated as the viability of cells treated with glutamate divided by that of cells treated without glutamate.

Treatment	Anti-oxidative effect (%) (AVG ± SD)
Control	43.3±8.8
H5 0.5 μM	49.0±5.3
H5 1 μM	43.3±0.2
H5 5 μM	57.2±11.1 **
H5 10 μM	58.4±7.1 **
H5 15 μM	71.1±10.1 ***
H5 20 μM	77.6±8.8 ***

p < 0.01,p<0.01, ***p < 0.001 vs. control, t-test.

(E) MIO-M1 cells were pre-treated with 0.5-20 μM H7 for 24 h, followed with or without 300 mM glutamate incubation for 4 h. DMSO was used as vehicle control. Cell viability was then assessed with Calcein-AM assay. Data was presented as the percentage of cell viability to that of DMSO treated cells.

Treatment	Cell viability (%) (AVG ± SD)
Control	100.0±7.0
Control + glutamate	44.4±7.7
H7 0.5 μM	109.1±8.0
H7 0.5 μM+glutamate	52.2±7.1
H7 1 μM	109.6±7.3
H7 1 μM+glutamate	48.1±7.6
H7 5 μM	113.4±10.9
H7 5 μM+glutamate	67.3±5.2
H7 10 μM	98.3±6.4
H7 10 μM+glutamate	66.9±8.2
H7 15 μM	104.6±8.2
H7 15 μM+glutamate	71.9±10.7
H7 20 μM	107.0±4.6
H7 20 μM+glutamate	73.6±7.1

(F) The anti-oxidative effect of the H7 group at different concentrations (a re-analysis of data in the Supplementary Table 2E). Data was calculated as the viability of cells treated with glutamate divided by that of cells treated without glutamate.

Treatment	Anti-oxidative effect (%) (AVG ± SD)
Control	44.4±7.7
H7 0.5 μM	47.8±6.5
H7 1 μM	43.9±6.9
H7 5 μM	59.4±4.5 ***
H7 10 μM	68.1±8.4 ***
H7 15 μM	68.8±10.3 ***
H7 20 μM	68.8±6.6 ***

p < 0.01,p<0.01, ***p < 0.001 vs. control, t-test.